



INVESTIGATION OF THE GEOMETRY OF INTERACTION
OF PLANAR DYES WITH DNA
BY LINEAR DICHROIC ABSORPTION SPECTROSCOPY

GREGORY RAYMUND KELLY, B.Sc. (Hons.)

Department of Physical and Inorganic Chemistry,
University of Adelaide.

Thesis presented for the degree of
Doctor of Philosophy

October, 1974

To the best of my knowledge and belief, this thesis contains no material previously published or written by another person, nor any material previously submitted for a degree or diploma at any University, except where due reference is made in the text.

ACKNOWLEDGEMENTS

I wish to thank Dr. T. Kurucsev for his encouragement during the course of this project.

I wish to thank Mrs. H. Brereton for the Calf Thymus DNA preparation and also the technical staff, in particular Mr. K. Shepherdson and Mr. R. Byrne for their help in the construction of the apparatus required for this project.

My appreciation is expressed to Miss J. Newport and Mrs. H. Christiani for the typing of this thesis and to Mr. I. Graham for his help in the preparation of the diagrams for photo-copying.

A Commonwealth Postgraduate Award is also acknowledged.

G. R. Kelly

Department of Physical and
Inorganic Chemistry,
The University of Adelaide,
South Australia.

October, 1974.

SUMMARY

Anisotropic deoxyribonucleic acid (DNA) films suitable for polarised absorption spectroscopy were prepared. The isotropic DNA film was supported as a thin layer on the surface of a poly(vinyl alcohol) (PVA) film. Subsequent orientation was achieved by a motor driven mechanical stretching device. The properties of the films were investigated and although "full" hyperchromicity was not attained it was concluded that the DNA structure was native at high and denatured at low relative humidity. The DNA-PVA film method produced homogeneous and reproducible highly oriented samples.

Anisotropic dye/DNA films suitable for polarised absorption spectroscopy were prepared by modification of the DNA-PVA film method. The isotropic dye/DNA film was prepared independently and then oriented on the surface of a thick DNA layer cast separately on a PVA film support. The intermediate DNA layer was necessary to eliminate dye penetration into the polymer matrix. An attachment to a Zeiss PMQII Spectrophotometer was designed which effectively eliminated the need for scatter corrections to the measured spectra of the two film preparations.

Aqueous and DNA solution spectra were recorded for three acridine and four reporter molecules in the visible and near ultra-violet region. The theoretically calculated transition moment vectors of the dye molecules were correlated with the experimental spectra.

The polarised absorption and dichroic spectra for the anisotropic dye/DNA films of the seven dyes were determined at high relative humidity under identical conditions of orientation and relative humidity equilibration time. The degree of orientation of the films was evaluated in terms of the fraction of oriented DNA chains. The dichroism associated with each observable electronic transition of the dye in the DNA complex was interpreted in terms of tilt and twist angles. These angles relate the plane of the dye moiety to the DNA helix axis.

CONTENTS

Page

CHAPTER ONE

INTRODUCTION

1.1 Binding Models for the Acridine/DNA Complex	2
1.2 Interpretation of Linear Dichroism in terms of Orientation and Molecular Structure	4
1.2.1 General	4
1.2.2 Model for Perfect Alignment	6
1.2.3 Model for Partial Alignment	8
1.3 Linear Dichroism in Solution and in the Solid State	10

CHAPTER TWO

PHYSICAL AND SOLUTION PROPERTIES OF THE DYES

AND THEIR DNA COMPLEXES

2.1 Materials	16
2.1.1 Aminoacridines	16
2.1.2 Reporter Molecules	18
2.1.3 DNA	19
2.1.4 Water	19
2.2 Reagent Solutions	19
2.2.1 DNA Solutions	19
2.2.2 Dye and Dye/DNA Solutions	20
2.3 Isotropic Solution Absorption Spectroscopy	20
2.4 Degree of Intercalation	24
2.5 Transition Moment Directions	28
2.5.1 Experimental Classification	28
2.5.2 Theoretical Calculation	30

CHAPTER THREEINSTRUMENTATION

3.1 General	35
3.2 Spectrophotometric Arrangements Investigated	36
3.2.1 Zeiss PMQII Spectrophotometer with Wide-window Photomultiplier Detector	37
(a) Construction	37
(b) Light Path	40
3.2.2 Zeiss PMQII Spectrophotometer with Integrating Sphere (KA) Attachment	41
3.2.3 Comparison of the Two Spectrophotometric Arrangements	42
3.3 Comparison of Absorbance Measurements Obtained with Different Spectrophotometers	43
3.3.1 DNA-PVA Films	45
3.3.2 Dye/DNA-PVA Films	46
3.4 Measurement and Correction of Film Spectra	48
3.4.1 DNA-PVA Films	48
3.4.2 Dye/DNA-PVA Films	49
3.5 Spectrophotometric Calibration	54
3.6 Conclusion	55

CHAPTER FOURPREPARATION AND PROPERTIES OF ANISOTROPIC DNA FILM SAMPLES

4.1 Current Preparative Methods	56
4.2 The Selected Preparative Method	57
4.3 The Stretching Process	58
4.4 Preparation of the Isotropic Films Required for the Preparative Method	59
4.4.1 PVA Films	59

	Page
4.4.2 DNA Films	60
4.4.3 DNA Film Cast on the PVA Film Surface	
- A Cast DNA-PVA Film	60
4.5 Preparation of the Anisotropic DNA Films	61
4.5.1 From a Cast DNA-PVA Film	61
4.5.2 From a Combined DNA-PVA Film	61
4.6 Mounting of the Anisotropic DNA-PVA Film	
for Spectroscopy	62
4.7 Comparison of the Two DNA-PVA Film Preparations	64
4.8 Relative Humidity Equilibration Time	65
4.9 Properties of the Cast DNA-PVA Film	65
4.9.1 Absorption and Dichroic Spectra	66
4.9.2 Hyperchromicity and Dichroic Ratio as a	
Function of Relative Humidity	68
4.9.3 Dichroic Ratio as a Function of	
Extension Ratio	71
4.10 Conclusion	72

CHAPTER FIVE

PREPARATION AND PROPERTIES OF ANISOTROPIC DYE/DNA FILMS

5.1 The Preparation in Principle	73
5.2 The Initial Preparative Method	73
5.2.1 Preparation of the Isotropic Dye/DNA Films	74
5.2.2 Preparation of the Anisotropic	
Dye/DNA Film	74
5.2.3 Dye Penetration into the PVA Matrix	75
5.3 The Preparative Method	77
5.3.1 The Elimination of Dye Penetration into	
the PVA Matrix	77
5.3.2 Fraction of Oriented DNA Chains	80

	Page
5.4 The Polarised Absorption and Dichroic Spectra of the Dye/DNA Complexes	81
5.4.1 The Acridine/DNA Complex	82
5.4.2 The Reporter/DNA Complex	84
5.5 Relative Humidity Equilibration Time	85
5.5.1 The Acridine/DNA Complex	86
5.5.2 The Reporter/DNA Complex	86
5.6 Quality of the Anisotropic Dye/DNA Films	87

CHAPTER SIX

INTERPRETATION OF LINEAR DICHROISM FOR THE DYE/DNA COMPLEX

6.1 Estimation of the Fraction of Oriented DNA Chains	90
6.2 Determination of the Angle between the Transition Moment Vector of the Dye and the DNA Helix Axis	95
6.3 Geometry of the Dye Molecule in the Dye/DNA Complex	100
6.4 Conclusion	104

APPENDIX

BIBLIOGRAPHY



CHAPTER ONE

INTRODUCTION

For some time, much interest has been focussed on the interaction of various dyes with DNA. In particular, acridine dyes have been used as histological stains on account of their high affinity for biological macromolecules and it was not until their antibacterial activity was discovered that they were extensively studied (Albert, 1966). More recently, considerable interest in the interaction of acridines with DNA has been aroused because of their ability to cause mutations by the insertion or deletion of a single nucleotide in DNA, thus providing convincing evidence for the existence of the triplet genetic code (Brenner et al, 1961; Crick et al, 1961) and furthermore because structurally they resemble the powerful polycyclic aromatic carcinogens.

In spite of the intensive study of these systems, many aspects of the interaction, for example, the geometry or the specificity, are either not known or controversial. The principal justification for undertaking the work presented here has been to attempt a remedy for the above situation. In particular, this work describes the development of a technique that can provide definite answers to at least some of the geometric aspects of the interaction between DNA and biologically active or potentially active dye molecules.

1.1 Binding Models for the Acridine/DNA Complex

The interaction of acridines and DNA has been the subject of many reviews and discussions (Blake and Peacocke, 1968; Lober, 1969 and 1971; Peacocke, 1970). As early as 1956, two different modes of binding for the acridine dye proflavine were recognised (Peacocke and Skerrett, 1956). The binding at low ratios of dye to DNA phosphate (maximum ratio, 0.20-0.25) was denoted the "strong" binding process while that at high ratios of dye to DNA phosphate was denoted the "weak" binding process. The weak process, limited by electrical neutrality of the complex, has an upper limit of one dye molecule per DNA phosphate. It has been little studied.

Lerman (1961 and 1964) described the strong process in terms of an intercalation model where the planar dye molecule was presumed to fit between and lie centrally over successive base pairs in the double helix of the DNA. Such a process is accompanied by local untwisting and extension of the double helix and observations indicating an increase in the molecular dimensions of the DNA helix have served as the basis for the evidence of the intercalation model. The techniques employed have included low shear viscometry (Lerman, 1964; Drummond et al, 1966), autoradiography (Cairns, 1962), low angle X-Ray scattering (Luzzati et al, 1961), sedimentation in the ultracentrifuge (Lerman, 1961; Lloyd et al, 1968) and X-Ray diffraction (Lerman, 1961; Neville and Davies, 1966).

However, the interpretation of the data referred above has been controversial for some time. According to the Watson and Crick model, the local structure of DNA is rod-

like while according to the Kratky and Porod (1949) model, its macromolecular structure is "worm-like", i.e. sufficiently flexible to coil back on itself. The difficulty in the interpretation, and this has led to possible alternative models (Mason and McCaffery, 1964; Gurskii, 1966; Rigler, 1969), is whether the noted changes to the DNA hydrodynamic properties have been caused by intercalation which would directly affect the local rod-like structure or alternatively by some form of external binding which would affect the overall flexibility of the DNA coil. Recent determinations on sonic degraded DNA by light scattering (Mauss et al, 1967), sedimentation in the ultra-centrifuge and low shear viscometry (Cohen and Eisenberg, 1969) may be regarded as conclusive confirmation that for these rod shaped molecules the decrease in the mass per unit length and the enhanced viscosity is due to alteration of the local structure and cannot be explained by an external binding model.

As the binding of various acridines to heat denatured DNA is similar to native DNA (Blake and Peacocke, 1968) and moreover, as bulky substituents added to the 9-amino position of the parent acridine do not inhibit binding (Drummond et al, 1965), a modified intercalation model has been proposed in which the acridine is inserted between the flat base rings of one of the polynucleotide chains in DNA (Pritchard et al, 1966). This model together with Lerman's original model (Lerman, 1961 and 1964) may represent but the limiting cases for a whole series of positions for the intercalated molecule relative to the central axis and the nucleotide bases (Lober and Achttert, 1969; Peacocke, 1970).

In this respect, co-operative changes to the circular dichroism spectra of 3-aminoacridine, 3,6-diaminoacridine (proflavine) and ethidium bromide with dye concentration, combined with the steric binding limitations of the bulky ethidium bromide cation, have allowed similar intermediate binding positions to be inferred for the two acridines. On the other hand, 9-aminoacridine and substituted derivatives which do not exhibit this co-operative behaviour were considered to be more representative of the binding position as formally presented by the Lerman model (Dalglish et al, 1969 and 1971).

1.2 Interpretation of Linear Dichroism in terms of Orientation and Molecular Structure

Although considerable evaluation of the binding site of the intercalated dye has been made through various models, there is still relative uncertainty as to the more subtle details of the intercalation geometry. This work concerns the geometry of certain intercalating planar dye molecules with DNA as evaluated from the dichroic spectra of the anisotropic dye/DNA complex. The mathematical model used for this interpretation is presented below.

1.2.1 General

Visible and ultra-violet absorption spectroscopy is characterised by the interaction of the electric vector of light with the transition moment vector of the molecule. Interaction with the magnetic vector is negligible. The probability, P_{i0} , that a molecule in its ground state will absorb light of energy $h\nu_i$ to an higher electronic state is given by the product of the Einstein coefficient of absorption,

B_{i0} , and the density radiation function, $\rho(\nu_i)$.

$$P_{i0} = B_{i0}\rho(\nu_i) \quad (1.1)$$

The Einstein coefficient of absorption is proportional to the square of the transition moment vector, T_{i0}

$$B_{i0} \propto T_{i0}^2 \quad (1.2)$$

where

$$T_{i0} = \int \psi_0 M_{i0} \psi_i d\tau \quad (1.3)$$

and where ψ_0 , ψ_i are the time independent eigenfunctions and M_{i0} is the transition dipole.

For linearly polarised light, a factor relating the angle σ between the transition moment vector and the electric vector of the light must be introduced. The effective radiation density in the direction T_{i0} is proportional to the average of the square of the component of the electric field strength, E_T , parallel to T_{i0} .

$$\rho(\nu_i) \propto \overline{E_T^2} \quad (1.4)$$

As the electric field, E , may be represented by

$$E = E_0 \cos 2\pi \overline{\nu_i} t \quad (1.5)$$

where t is the time, then

$$\overline{E_T^2} = \frac{1}{2} E_0^2 \cos^2 \sigma \quad (1.6)$$

and so

$$\rho(v_i) \propto E_0^2 \cos^2 \sigma \quad (1.7)$$

Thus, from the combination of equations 1.1, 1.2 and 1.7, it is found that the rate of absorption of polarised light per molecule or per absorbing centre of a macromolecule for a particular transition moment vector is proportional to $(\underline{T}_{0i} \cdot \underline{E}_0)^2$. It therefore follows that the molar absorptivity, ϵ , for a particular direction of E_0 , may be written as

$$\epsilon = NT^2 \cos^2 \sigma \quad (1.8)$$

where N is the number of molecules or absorbing centres of a macromolecule per unit volume, σ is the angle as previously defined and T is the magnitude of a vector T , proportional to the transition moment vector, T_{i0} (Fraser, 1960).

1.2.2 Model for Perfect Alignment

Consider the co-ordinate system OABC in Fig.1.1 where the helix axis of the DNA molecule is perfectly aligned along OC. The orientation of a particular transition moment vector of the purine and pyrimidine bases in DNA or that of an intercalated dye molecule is represented by the vector T , which is described by the polar co-ordinates δ and θ . Light is propagated in the direction OA. Absorbance measurements are made with light polarised in the direction OC parallel to the DNA helix axis (A_{11}) and with light polarised in the direction OB perpendicular to the DNA helix axis (A_1). The dichroic ratio R is defined as

$$R = A_{11}/A_1 \quad (1.9)$$

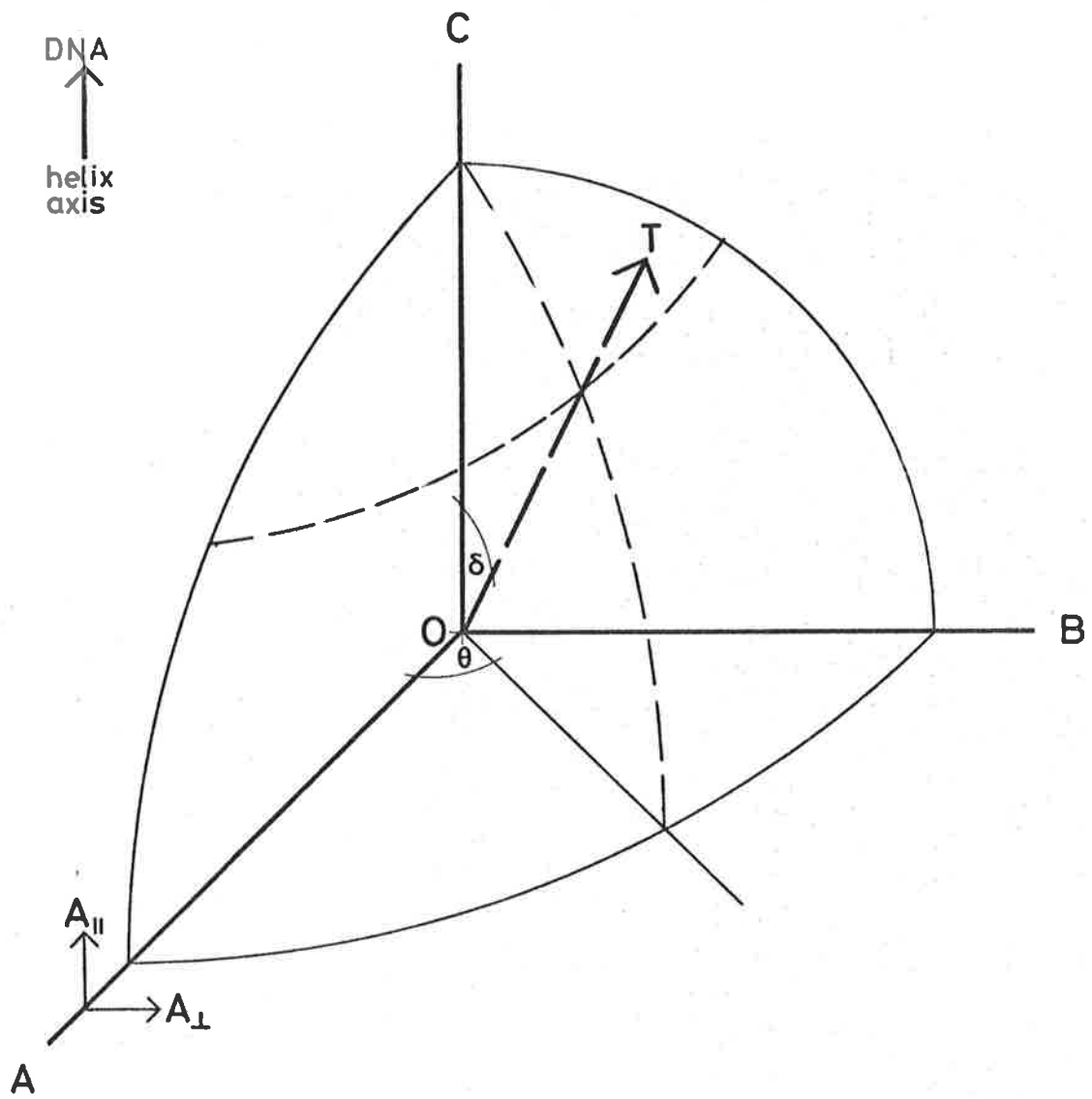


FIG 1.1 THE CO-ORDINATE SYSTEM OABC

and is equal to $\epsilon_{11}/\epsilon_{\perp}$. Another commonly used alternative is the dichroism, Δr , where

$$\Delta r = A_{11} - A_{\perp} \quad (1.10)$$

All orientations of the DNA molecules around OC are equally probable and so the transition moment vectors will be uniformly distributed on a right circular cone of semi-angle, $\delta = \omega$, with OC as axis, where ω is the angle between the transition moment vector and the DNA helix axis. For polarised radiation parallel to OC, $\delta = \omega$ and therefore

$$\epsilon_{11} = NT^2 \cos^2 \omega \quad (1.11)$$

For polarised radiation parallel to OB,

$$\cos^2 \theta = \sin^2 \omega \sin^2 \theta \quad (1.12)$$

and the number of transition moment vectors per unit volume between θ and $\theta + d\theta$ is $Nd\theta/2\pi$, therefore,

$$\epsilon_{\perp} = \frac{NT^2}{2\pi} \int_0^{2\pi} \sin^2 \omega \sin^2 \theta \, d\theta \quad (1.13)$$

$$= \frac{1}{2} NT^2 \sin^2 \omega \quad (1.14)$$

For perfect alignment of the DNA molecules along OC, the dichroic ratio, R_0 , becomes

$$R_0 = \epsilon_{11}/\epsilon_{\perp} \quad (1.15)$$

$$= 2 \cot^2 \omega \quad (1.16)$$

and relates the inclination of the transition moment vector to the DNA helix axis (Fraser, 1953).

1.2.3 Model for Partial Alignment

For this model, Fraser (1953) proposed that a fraction, f , of the molecules are perfectly aligned parallel to the OC axis and the remaining fraction, $(1 - f)$, are perfectly random. From equations 1.11, 1.14 and 1.16, it follows that

$$\epsilon_{11} = NT^2 \{f \cos^2 \omega + (1 - f)/3\} \quad (1.17)$$

and

$$\epsilon_{\perp} = NT^2 \{\frac{1}{2}f \sin^2 \omega + (1 - f)/3\} \quad (1.18)$$

and in terms of the dichroic ratio for perfect alignment, R_0 , and f , the dichroic ratio for this model (Fraser, 1956) is

$$R = \frac{\{1 + (R_0 - 1)(1 + 2f)/3\}}{\{1 + (R_0 - 1)(1 - f)/3\}} \quad (1.19)$$

and solving for f (Fraser, 1956)

$$f = \frac{\{(R - 1)(R_0 + 2)\}}{\{(R_0 - 1)(R + 2)\}} \quad (1.20)$$

For DNA, which aligns with its helix axis parallel to the direction of the orienting force, the measured dichroic ratio of an absorption band of an intercalated dye molecule (or of the DNA bases) together with a knowledge of the fraction of oriented DNA chains will determine R_0 and the orientation of that transition moment vector relative to the DNA helix axis.

Although the angle between the transition moment vector of the dye and the DNA helix axis may be readily calculated, it does not directly indicate the relationship between the plane of the dye molecule and the DNA helix axis. For this type of interpretation, use has been made of the following expression

$$R_{11} = K_1 \cos^2 \phi + 2K_{12} \sin \phi \cos \phi + K_2 \sin^2 \phi \quad (1.21)$$

which has been previously derived for in-plane (π^* , π) transitions for molecules embedded in an anisotropic matrix (Bott and Kurucsev, 1974), where

$$R_{11} = R_0 / (R_0 + 2) \quad (1.22)$$

and where ϕ is the angle between the transition moment vector and the molecular z axis, and K_1 , K_{12} and K_2 are molecular orientation parameters to be defined below.

Of the three Eulerian angles α , β , and γ used to specify the relationship between the laboratory-fixed, OXYZ, and the molecular-fixed, Oxyz, co-ordinate systems (Fig.1.2), α is uniformly occupied (Michl et al, 1970; Bott and Kurucsev, 1974) by the molecules so that the expressions for the molecular orientation parameters involve β and γ only:

$$K_1 = \langle \cos^2 \beta \rangle_{av} \quad (1.23)$$

$$K_{12} = \langle \sin \beta \cos \beta \cos \gamma \rangle_{av} \quad (1.24)$$

$$K_2 = \langle \sin^2 \beta \cos^2 \gamma \rangle_{av} \quad (1.25)$$

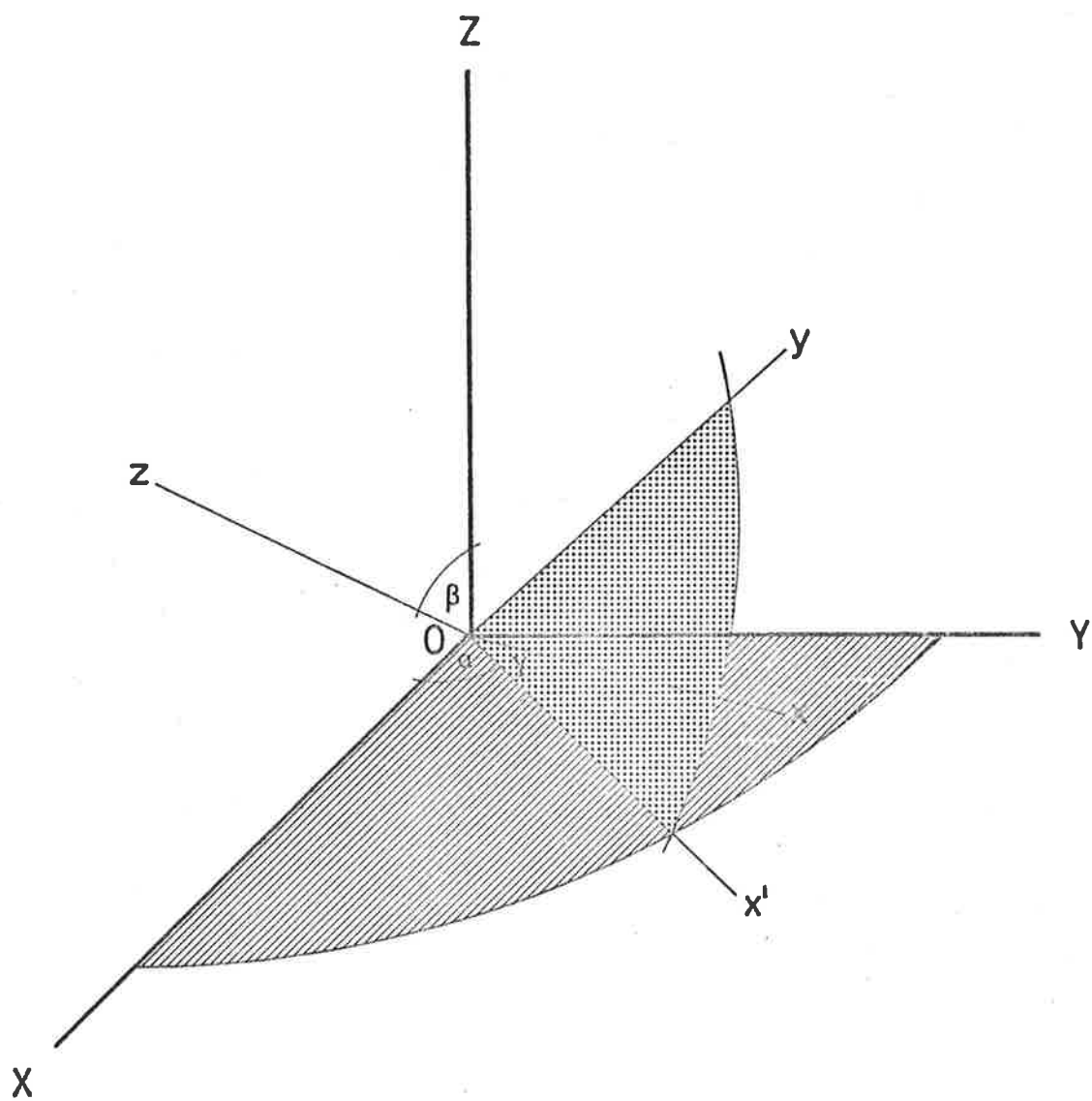


FIG 1.2 THE RELATION BETWEEN THE LABORATORY-FIXED, OXYZ, AND THE MOLECULAR-FIXED, Oxyz, CO-ORDINATE SYSTEMS

It has been assumed that in the case of the dye/DNA system the distribution of molecular orientations about β and γ is very narrow and therefore single angles may be used instead of averages to define the molecular tilt and twist angles, β and γ , respectively. These angles are shown in Fig.1.2, where β is the angle between the Z axis (the DNA helix axis) and the dye z molecular axis and γ is the angle between the x molecular axis (the normal to the dye molecular yz plane) and its projection x' into the XY plane (the plane perpendicular to the DNA helix axis) as formed by the line of intersection of the xy and XY planes. Thus, R_{11} is given by

$$R_{11} = \cos^2\beta \cos^2\phi + 2\sin\beta \cos\beta \cos\gamma \sin\phi \cos\phi + \sin^2\beta \cos^2\gamma \sin^2\phi \quad (1.26)$$

1.3 Linear Dichroism in Solution and in the Solid State

Two methods have been used to measure the linear dichroism of the dye/DNA complex in solution. The orientation of the DNA complex has either been obtained under the influence of an electric field (Houssier, 1965; Houssier and Fredericq, 1966) or achieved through streaming solutions (Lerman, 1963; Nagata et al, 1966; Jackson and Mason, 1971). The interpretation of the data has been restricted firstly, by the small orientation of the complex produced and secondly, by contributions from non-intercalated dye species, either free or externally bound dye. This latter factor becomes more important at low ionic strengths and high dye to DNA phosphate ratios. It has been shown that there is a loss in the negative dichroism of the bound dye at 10^{-3} M ionic strength as

D/P, the dye to DNA phosphate ratio increases above 0.1 and this has been interpreted as an increase in the weak binding process (Houssier and Fredericq, 1966). Lerman (1963) desired saturation of binding sites and so used a dye (quinacrine) to DNA concentration (as nucleotide) of 0.37 where the concentration of free dye was considerable. He concluded from the close similarity of the dichroism values for quinacrine and DNA that the plane of the purine and pyrimidine base pairs were parallel to the direction of the long wavelength transition of quinacrine and from further considerations that the planes of both were parallel. A similar conclusion has been reached for various intercalating polynuclear aromatic hydrocarbons, 4-nitroquinoline-1-oxides and various dyes (Nagata et al, 1966). More recently, Jackson and Mason (1971) determined from measurements at $10^{-3}M$ ionic strength and D/P ratio between 0.04 to 0.22, that the longer in-plane axis of 3- and 9-aminoacridine is oriented in the DNA complex at an angle approximately 20° to the plane normal to the helix axis and that the shorter in-plane axis of these molecules together with 1-, 2- and 4-aminoacridine lies at a somewhat greater angle. For this interpretation, it was assumed that the molecular plane of 9-aminobenz[a]acridine and the base pair were parallel in the DNA complex. This allowed the calculation of the amount of orientation of the DNA complex which was considered to be the same for the other DNA complexes under the same conditions. The problems associated with linear dichroism measurements from solution may be listed therefore, as:-

- (i) the preparation of dye/DNA samples of only limited orientation,

- (ii) the assessment of the amount of orientation of the dye/DNA complex (the fraction of oriented DNA chains),
- (iii) the possible contribution to the measured dichroic ratio from free dye, and
- (iv) the possible contribution to the measured dichroic ratio from externally bound dye.

The difficulties associated with solution dichroism measurements on the other hand, are more readily overcome in the solid state. Better orientations, allowing a more accurate assessment of the total fraction of orientation may be achieved. In addition, suitable dye absorbances may be maintained at very low ratios of dye to DNA phosphate, simply by increasing the thickness (light path) of the sample. However, it is also important to examine the factors which affect the secondary structure of DNA so that it may be maintained in its native form. This will ensure not only reproducible experimental conditions but will also allow the geometry of the dye in the complex to be related to the in vivo system where DNA probably occurs in the gel like state; and further, will complement current knowledge of DNA behaviour in vitro.

The structure of DNA in the solid state has been investigated by X-Ray diffraction and has been shown to be highly dependent on relative humidity (Franklin and Gosling, 1953). At least four diffraction patterns have been found and these have been interpreted as distinct molecular configurations, each stable over a limited relative humidity range (Feughelman et al, 1955; Langridge et al, 1957, 1960a, 1960b; Marvin et al, 1961). Of these configurations, the native B form existed at 92% relative humidity, with the plane of the

purine and pyrimidine bases approximately perpendicular to the helix axis whereas the A form occurred at 75% relative humidity, with the plane of the bases tilted by 20° from the perpendicular to the helix axis.

In addition, salt content is important in determining the secondary structure of DNA. For samples with salt contents in excess of 9% (weight of salt to dry weight of DNA), the B form only is observed at relative humidities above 75%. On the other hand, at salt contents less than 0.5%, the A form was present at 75% and 98% relative humidities. Further, some samples of 5% salt content did not reveal the B form at 92% relative humidity while others with salt contents in the range 0.6 - 4.0% did show the A \rightarrow B transition. Clearly, this suggested that other factors were involved (Cooper and Hamilton, 1966). More recently, it has been observed that the conformational change was not only a function of the relative humidity and the salt content but also of the DNA base composition (Bram, 1971; Pilet and Brahms, 1973). The reported changes in the infra-red spectrum of solid DNA films as a function of relative humidity, first observed by Sutherland and Tsuboi (1957) and later confirmed and extended by Falk and co-workers (1963a), indicated that the observed structural changes were analogous to the denaturation of DNA in aqueous solution. Similar changes in the ultra-violet spectrum of solid DNA films have also been reported (Falk, 1964).

Linear dichroism has not been a widely used technique in the solid state and the few reported measurements of the dye/DNA complex are not well documented. Lerman (1961) inferred from oriented fibres of the proflavine/DNA complex

that the normal to the plane of the proflavine molecule was less than 55° from the fibre axis. From a visual observation, a considerably smaller angle was estimated. Neville and Davies (1966) observed dichroisms for the oriented acridine-orange and proflavine/DNA complexes at both room and 100% relative humidities, with the maximum light absorption occurring with the radiation vector perpendicular to the direction of orientation. They measured a dichroic ratio for the proflavine/DNA complex, $D/P = 0.17$ at 50% relative humidity at both 460 and 440 nm of 0.6. Rupprecht and co-workers (1969) have reported from a single measurement at the maximum dye absorption for one wet-spun sample each of acridine-orange/DNA and proflavine/DNA at 66% relative humidity, dichroic ratios of 0.415 and 0.317, respectively. The minimum angle of inclination of the absorption vector of the dye molecule to the DNA helix axis was calculated at 65° and 67° , respectively. Kurucsev and Zdysiewicz (1971) have recorded the dichroism in the visible region of the spectrum, of an acridine-orange/DNA film stretched to 1.4 times its original length at 100% relative humidity. A minimum dichroic ratio of 0.6 was obtained which they concluded supported the generally accepted intercalation model with the dye molecule more or less parallel to the plane of the bases.

The difficulties that arise for the quantitative interpretation of the dye/DNA geometry from solid state dichroism studies may be summarised as:-

- (i) the development of an experimentally reproducible method capable of preparing highly oriented DNA samples,
- (ii) the elimination of, or correction for, the light scattering properties of the samples and,

(iii) the assessment of the amount of orientation of the samples.

The ideal situation is to overcome the scattering problem and then to improve the quality of the samples. This is not possible, since the measured dichroism reflects the capability of the measuring instrument together with the quality of the sample. In practice therefore, the development of a suitable measuring instrument is accompanied by advances in the quality of the samples. For convenience, Chapter Three is devoted to the instrumentation problem of light scattering from DNA film samples, whilst Chapter Four describes a method suitable for the preparation of highly oriented DNA films. This method is later modified in Chapter Five to include the dye/DNA complex.

CHAPTER TWO

PHYSICAL AND SOLUTION PROPERTIES OF THE DYES AND THEIR DNA COMPLEXES

Two classes of dyes have been investigated throughout this work, aminoacridines and reporter molecules. Proflavine, acriflavine and 9-aminoacridine have been selected as representative of the first group, with the first two mentioned dyes being used mainly to substantiate the preparative method (refer to Chapter Five). The second group is of interest because they have been synthesised specifically to interact strongly with polyanions, in particular, DNA (Gabbay, 1968; Gabbay and Mitschele, 1969). A variety of reporter molecules, $R(CH_2)_nN^+(CH_3)_2(CH_2)_3N^+(CH_3)_3 \cdot 2Br^-$ where R represents a chromophore absorbing in the 300 - 500nm region, have been reported (Gabbay, 1969). These molecules may be particularly useful in the analysis of the structure of the dye/DNA complex since the R chromophore may be conveniently manipulated. Four such reporter molecules have been investigated.

2.1 Materials

2.1.1 Aminoacridines

Proflavine (3,6-diaminoacridine hemisulphate hemihydrate from B.D.H., England) was purified as the free base (Weill and Calvin, 1963; Ellerton and Isenberg, 1969) and subsequently converted to the hydrochloride by the method previously outlined for acridine-orange (Armstrong et al, 1970). The microanalysis (C.S.I.R.O., Melbourne) carried

out on both the hemisulphate and the purified hydrochloride is shown in Table 2.1. The analysis indicates that the purity of the proflavine hydrochloride has been increased to greater than 98%.

Table 2.1
Proflavine Microanalysis

Element	Proflavine Hemisulphate $(C_{13}H_{11}N_3)_2 \cdot H_2SO_4$		Proflavine Hydrochloride $C_{13}H_{11}N_3 \cdot HCl$	
	Calculated(%)	Found(%)	Calculated(%)	Found(%)
Carbon	60.45	57.76	63.54	61.83
Hydrogen	4.68	4.89	4.92	5.17
Nitrogen	16.27	15.35	17.11	16.95
Sulphur	6.21	7.5	-	-
Chlorine	-	-	14.43	14.6
"Sulphated Ash"	-	0.3	-	0.2

Acriflavine (3,6-diamino-N-methylacridinium chloride), free of proflavine, was obtained from commercial acriflavine hydrochloride (B.D.H. Acriflavina B.P.C.) by the method of Albert (1966). The microanalysis (C.S.I.R.O., Melbourne) for the commercial and the purified sample is shown in Table 2.2. The analysis indicates that the purified acriflavine is of very high purity.

Table 2.2

Acriflavine Microanalysis

Acriflavine Hydrochloride; $C_{13}^{14}H_{14}^{14}N_3.HCl$			
Element	Calculated (%)	Commercial Found (%)	Purified Found (%)
Carbon	64.74	60.93	64.48
Hydrogen	5.43	5.40	5.57
Nitrogen	16.18	15.77	16.40
Chlorine	13.65	13.1	13.7
"Sulphated Ash"	-	0.3	0.5

9-Aminoacridine hydrochloride (A.G. Fluka) was recrystallised twice from ethanol and dried under vacuum. It was a sample kindly supplied by Dr. L.N. Sansom.

2.1.2 Reporter Molecules

N,N,N-Trimethyl-N',N'-dimethyl-N'-(β -2,4-dinitroanilinoethyl)-1,3-diammoniumpropane dibromide (to be called 2,4-dinitroaniline reporter), N,N,N-trimethyl-N',N'-dimethyl-N'-(β -4-nitroanilinoethyl)-1,3-diammoniumpropane dibromide (to be called paranitroaniline reporter), N,N,N-trimethyl-N',N'-dimethyl-N'-(γ -2-nitroanilinopropyl)-1,3-diammoniumpropane dibromide (to be called orthonitroaniline reporter) and N,N,N-trimethyl-N',N'-dimethyl-N'-(γ -4-nitronaphthylaminopropyl)-1,3-diammoniumpropane dibromide (to be called 4-nitro-1-naphthylamine reporter)

were kindly provided by Dr. E.J. Gabbay (Department of Chemistry, University of Florida, Gainesville, Florida).

2.1.3 DNA

Herring Sperm DNA was supplied by the Sigma Chemical Company as the "Type V, Sodium Salt, Highly Polymerised" form. Calf Thymus DNA may be prepared by two main methods. In one case, the basic proteins with which DNA occurs in combination are removed by anionic detergent treatment (Kay et al, 1952) and in the other, by the chloroform-gel method (Jordan, 1960). A comparison of the different methods of preparation resulted in the conclusion that the chloroform-gel method gives a lower molecular weight product with marked fractionation occurring as compared to the anionic detergent procedure (Jordan, 1960). Throughout this work, Calf Thymus DNA was prepared by the anionic detergent procedure as outlined by Steiner and Beers (1961). The DNA samples were stored dry at 0°C.

2.1.4 Water

The water used for all preparative work was obtained by the distillation of deionized water through a 35cm fractionating column. The conductivity of the water did not exceed 3.5×10^{-6} ohm cm^{-1} .

2.2 Reagent Solutions

2.2.1 DNA Solutions

Aqueous DNA solutions in 0.1mM EDTA (disodium salt) were prepared by dissolving the DNA directly in aqueous EDTA in the cold (0°C - 4°C) with continual shaking over a seven day period. In the concentration range employed, 0.1% to 1.0%, the DNA retains its native configuration (Kurucsev, 1963).

The DNA solutions were centrifuged at 12,000 RPM for forty-five minutes in a Sorvall Superspeed RC-B automatic refrigerated centrifuge. The solutions were maintained at 4°C throughout and autoclavable polycarbonate centrifuge tubes (steam cleaned) were used. The DNA solutions were stored in the frozen state and were degassed prior to use. The method used for degassing was to freeze the solution in liquid nitrogen, evacuate the containing vessel and thaw the frozen solution under vacuo. This process was repeated several times. It has been reported that the double helical structure of DNA is not broken down by freezing DNA solutions to -192°C, followed by thawing (Shikama, 1965). The pH of the DNA solutions was 5.0 ± 0.3 .

2.2.2 Dye and Dye/DNA Solutions

The dye and dye/DNA solutions were prepared as outlined in Chapter Five, Section 5.2.1. A fifteen-fold dilution of the dye and the dye/DNA solutions listed in Table 5.1 gave absorbances that were conveniently measured in 1cm optical path-length cells. The pH of all solutions was 5.0 ± 0.3 .

2.3 Isotropic Solution Absorption Spectroscopy

A Zeiss PMQII manual spectrophotometer equipped with an automatic slit control unit was used to measure aqueous solution spectra while the basic instrument with wide-window PM attachment (Chapter Three) was used to measure dye/DNA solution spectra. The solution spectra were measured at $20 \pm 1^\circ\text{C}$ using silica cells of optical path length 1cm. The calibration of the spectrophotometer is described in Chapter Three, Section 3.5.

The visible absorption spectra of proflavine and acriflavine, in aqueous and in DNA solution at pH5 (no buffer), are presented in Figs.2.1 and 2.2, for each dye respectively. The dyes' absorption maxima in water and in the presence of DNA have been normalised to demonstrate clearly the red shift of the spectrum in the nucleic acid environment relative to the aqueous environment. Fig.2.3 shows similar spectra for 9-aminoacridine in the visible and near ultra-violet region where an isotropic film spectrum of the 9-aminoacridine/DNA complex at 93% relative humidity has been substituted for the equivalent solution spectrum (refer to Chapter Five, Fig.5.6). The relevant details are summarised in Table 2.3 together with previously determined data that has been converted to the wavenumber scale to facilitate a comparison. The precision of the wavenumber maxima determined for this work is 50cm^{-1} and although not listed, would be expected to be of the same magnitude for the other reference work. Thus, the very close agreement between this and other work indicates that at the very low dye to DNA phosphate, D/P, ratios used, both pH (provided the DNA is native) and ionic strength, μ , effects are not important in the determination of the spectrum of the DNA bound dye monomer. This is consistent with the pK_a values for these acridine dyes being in excess of 9.65 (Albert, 1966).

Figs.2.4 to 2.7 show the visible and near ultra-violet absorption spectra of paranitroaniline, orthonitroaniline, 2,4-dinitroaniline and 4-nitro-1-naphthylamine reporters respectively, in aqueous and in DNA solution at pH5 (no buffer) (maxima have been normalised).

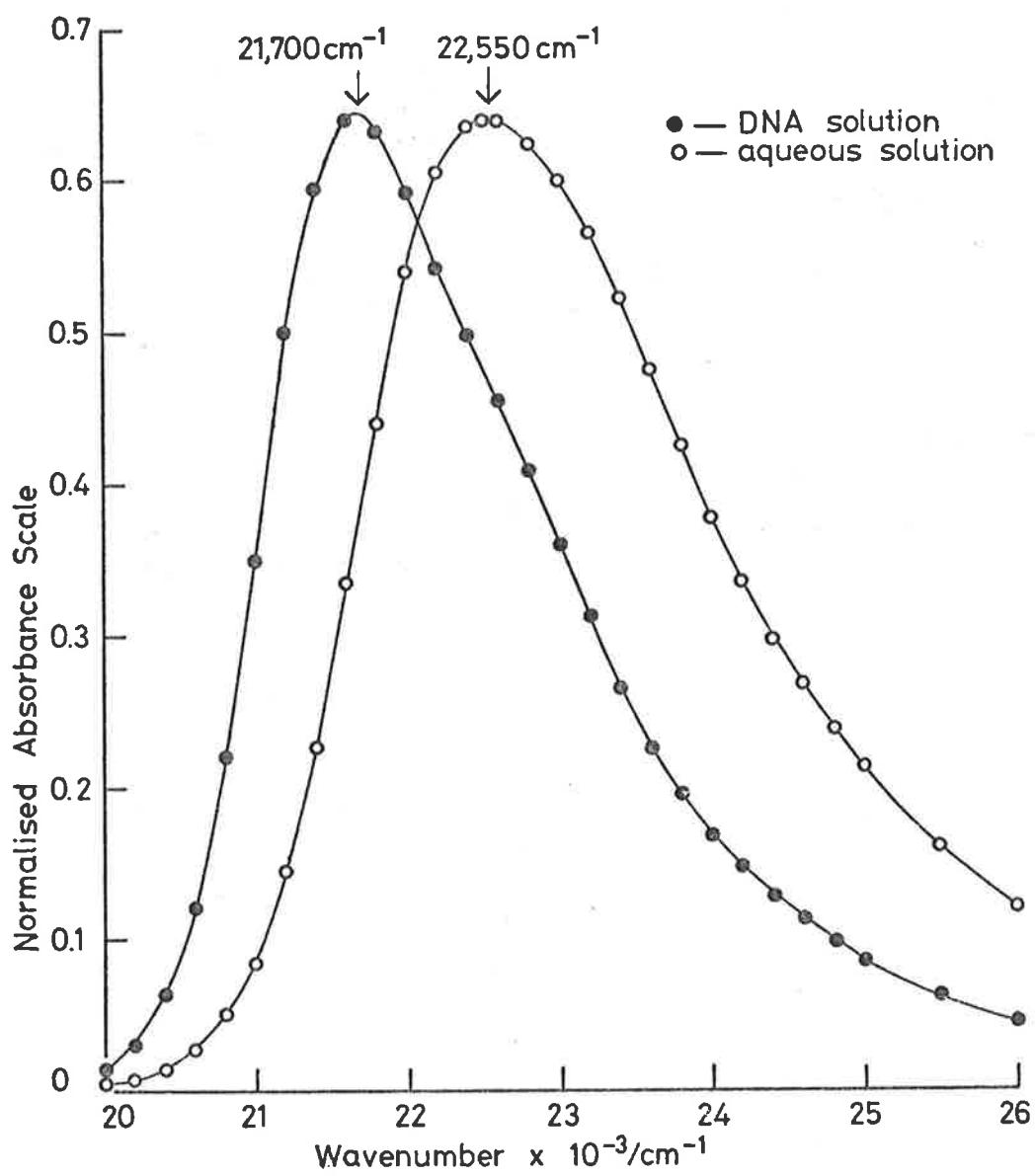


FIG 2.1 VISIBLE SPECTRA OF PROFLAVINE IN AQUEOUS AND IN DNA SOLUTION AT pH 5.0
NORMALISED MAXIMA

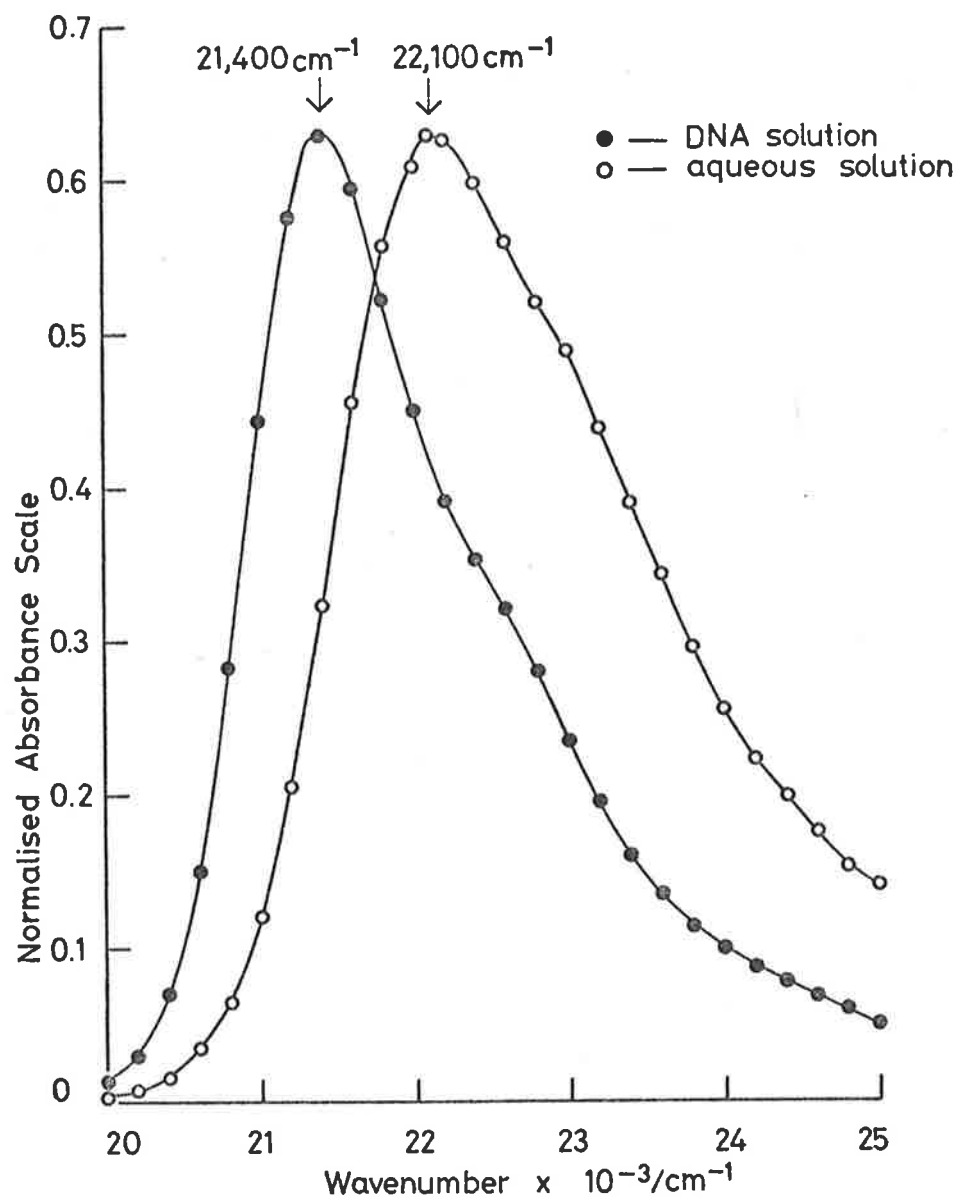


FIG 2.2 VISIBLE SPECTRA OF ACRIFLAVINE IN AQUEOUS AND IN DNA SOLUTION AT pH 5.0
NORMALISED MAXIMA

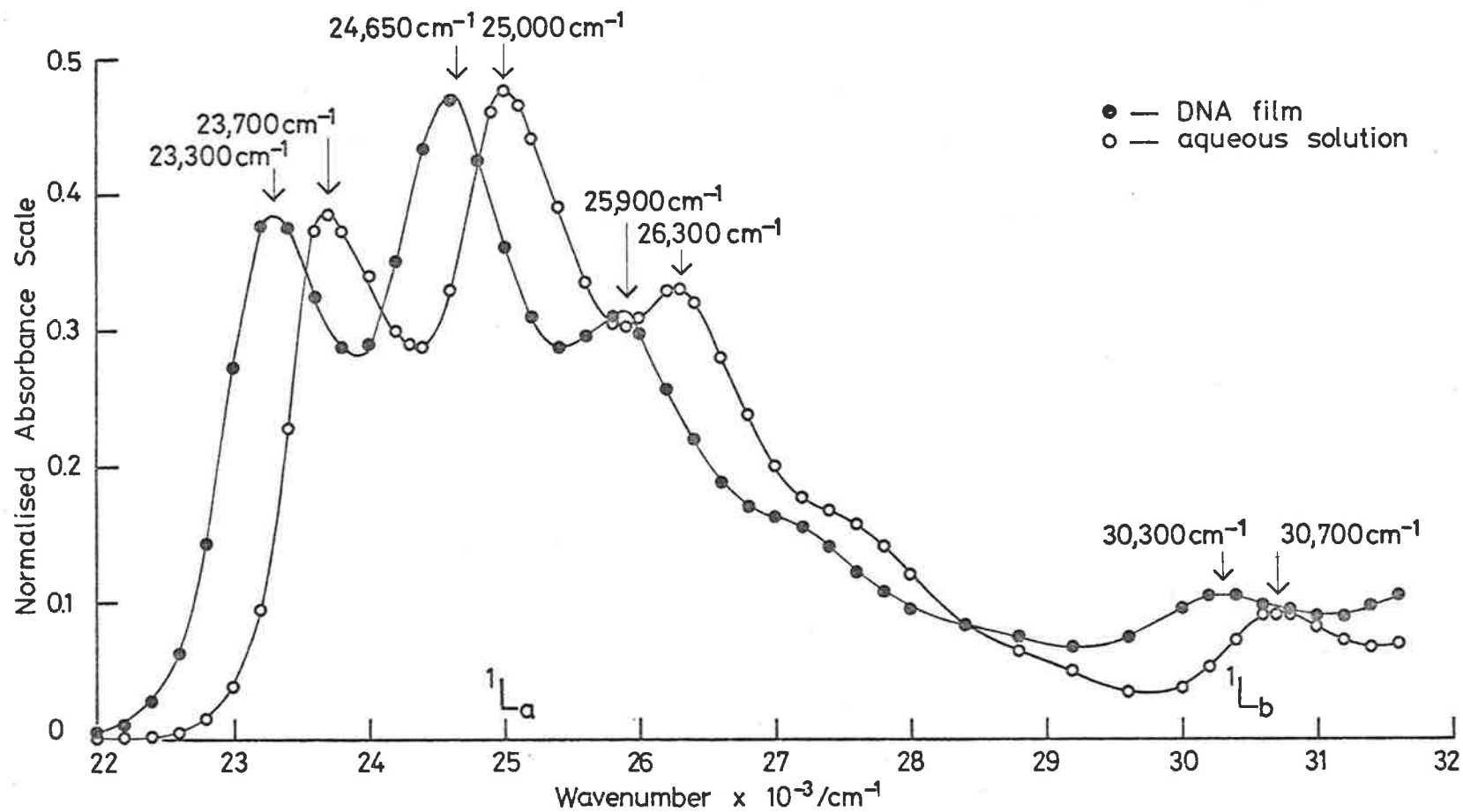


FIG 23 VISIBLE AND NEAR ULTRA-VIOLET SPECTRA OF 9-AMINOACRIDINE IN AQUEOUS SOLUTION AND IN DNA FILM (93% RELATIVE HUMIDITY) AT pH 5.0
 NORMALISED MAXIMA

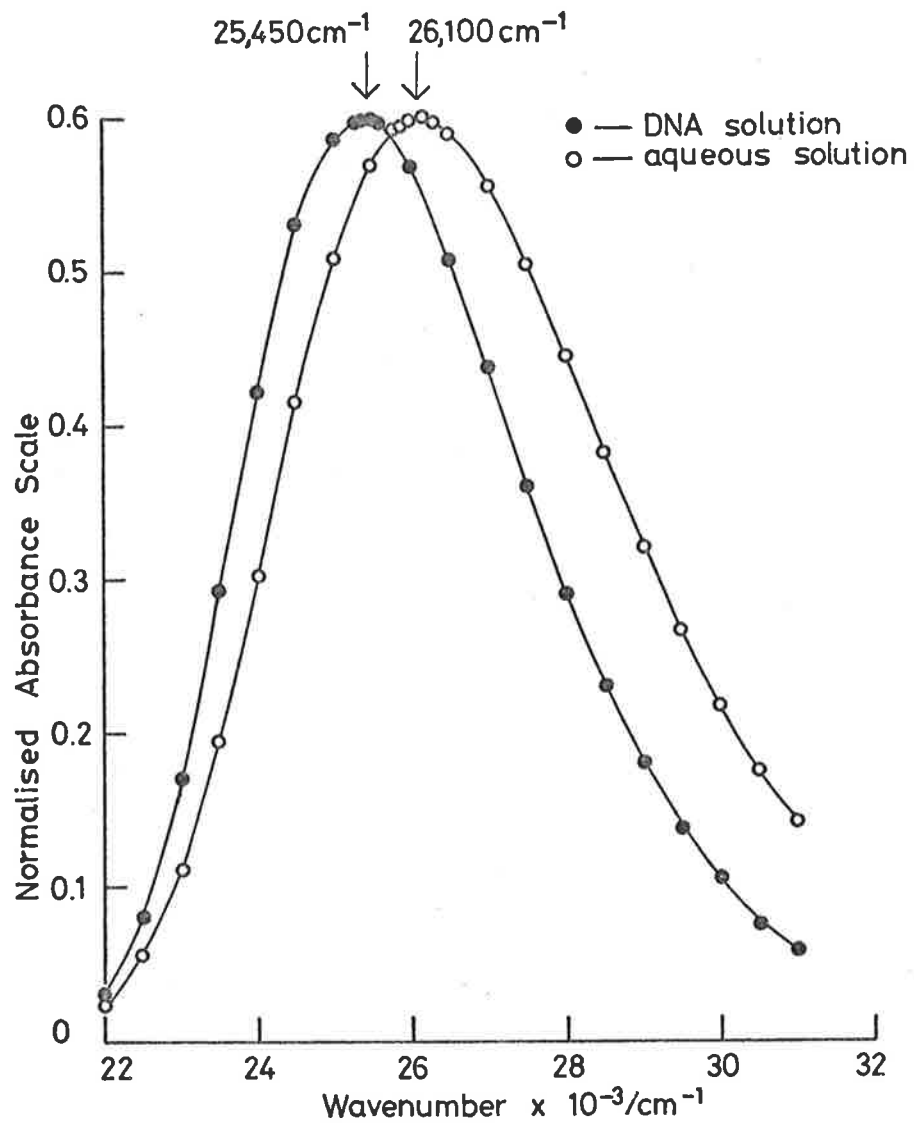


FIG 24 VISIBLE AND NEAR ULTRA-VIOLET SPECTRA OF PARANITRO-ANILINE REPORTER IN AQUEOUS AND IN DNA SOLUTION AT pH 5.0
NORMALISED MAXIMA

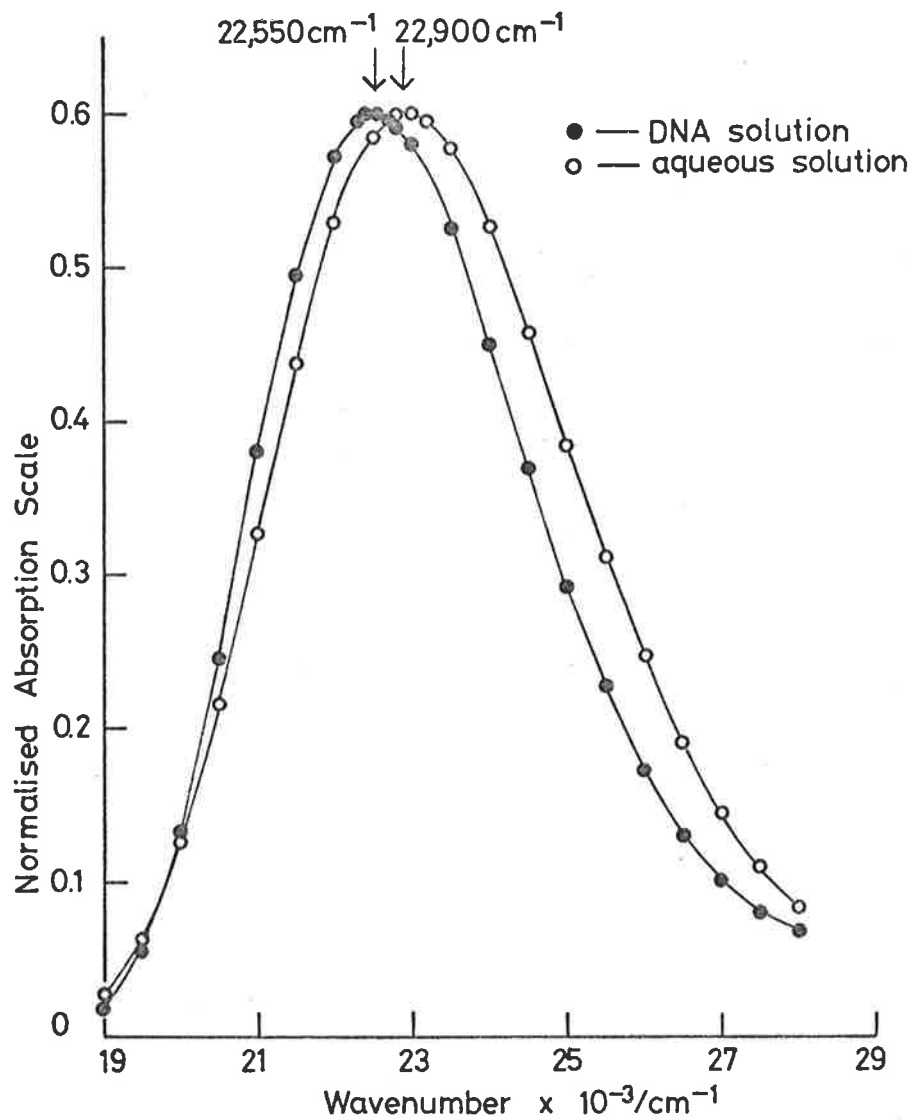


FIG 25 VISIBLE AND NEAR ULTRA-VIOLET SPECTRA OF ORTHONITROANILINE REPORTER IN AQUEOUS AND IN DNA SOLUTION AT pH 5.0 NORMALISED MAXIMA

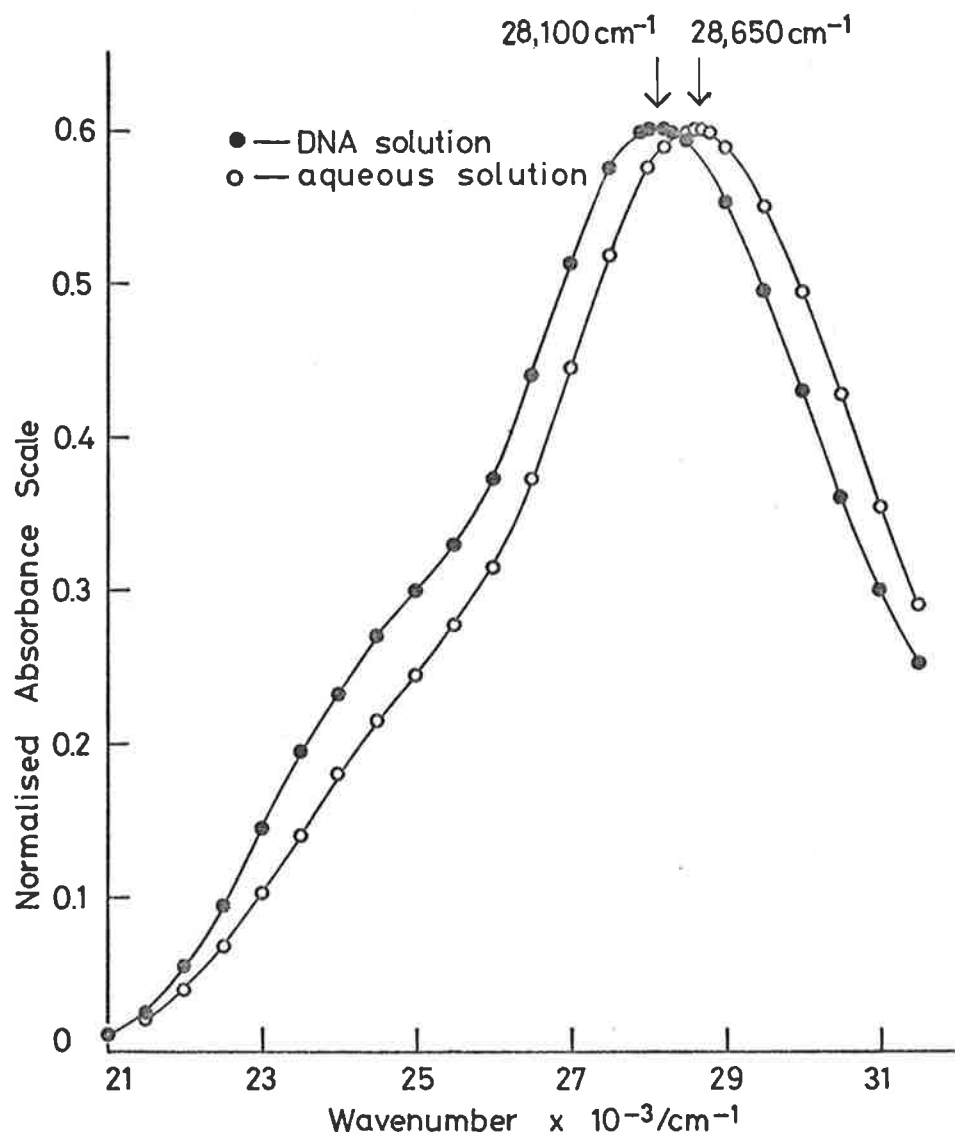


FIG 2.6 VISIBLE AND NEAR ULTRA-VIOLET SPECTRA OF 2,4-DINITROANILINE REPORTER IN AQUEOUS AND IN DNA SOLUTION AT pH 5.0
NORMALISED MAXIMA

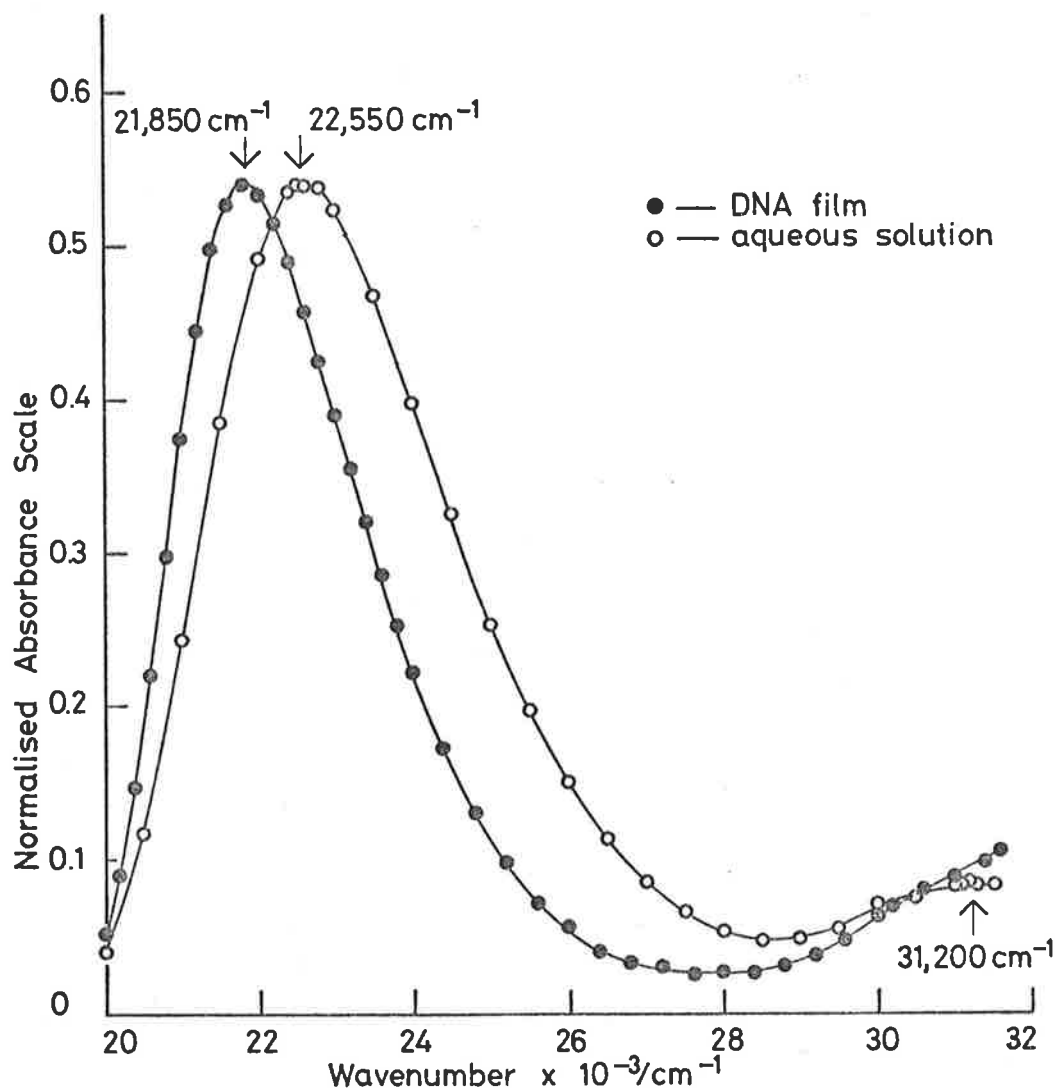


FIG 2.7 VISIBLE AND NEAR ULTRA-VIOLET SPECTRA OF 4-NITRO-1-NAPHTHYLAMINE REPORTER IN AQUEOUS SOLUTION AND IN DNA FILM (93% RELATIVE HUMIDITY) AT pH 5.0
NORMALISED MAXIMA

Table 2.3

Absorption Maxima of Aminoacridines in Aqueous
and in DNA Solution

Acridine and Environment	$\bar{\nu}_{\max}$ cm ⁻¹	Molarity or D/P	μ	pH	Reference
Proflavine	22,520	< 5 x 10 ⁻⁵	0.01	4.0	Haugen & Melhuish 1964
Aqueous	22,550	2 x 10 ⁻⁵	-	5	This work
Proflavine	21,690	0.026	0.10	6.9	Peacocke & Skerrett, 1956
DNA	21,650	extrap. to zero	0.002	6.5	Armstrong et al, 1970
	21,700	0.002-0.003	-	5	This work
Acridine	22,120		0.10	6.8	Tubbs et al, 1964
Aqueous	22,100	1.5 x 10 ⁻⁵	-	5	This work
Acridine	21,450	fully bound	0.10	6.8	Tubbs et al, 1964
DNA	21,400	0.002-0.003	-	5	This work
9-Aminoacridine	23,640				
	24,940				
Aqueous	26,250		-	6	Albert, 1966
	30,670				
	23,700				
	25,000				
	26,300	3.5 x 10 ⁻⁵	-	5	This work
	30,700				
9-Aminoacridine	23,310				
	24,630				
DNA	25,910	0.04 ₅	0.1	6.9	Peacocke & Skerrett, 1956; Fig.8
	30,210				
	23,300				
	24,650				
	25,900	0.004-0.008	-	5	This work
	30,300				

An isotropic film spectrum of the 4-nitro-1-naphthylamine reporter/DNA complex at 93% relative humidity (Chapter Five, Fig.5.10) has been used in place of the solution spectrum. The spectral behaviour of the reporter molecules is very similar to the aminoacridines with all the dyes exhibiting a red shift in the nucleic acid medium relative to the aqueous medium. Table 2.4 presents a summary of data similar to Table 2.3. Once again, the very close agreement between this and other work indicates that pH and ionic strength effects are not important in the determination of the spectrum of the DNA bound reporter molecule at the D/P ratios used here. As the reporter molecules do not associate, the bound dye is the monomer species (Gabbay, 1969).

A summary of the red shift of the absorption maximum(a) for both the aminoacridines and the reporter molecules is presented in Table 2.5. The red shift varies between 350cm^{-1} and 850cm^{-1} , with the fully intercalated dyes (Section 2.4) exhibiting a much larger red shift than the non fully intercalated dyes. The fully intercalated dye, 9-aminoacridine, appears to be an exception.

2.4 Degree of Intercalation

The fact that certain planar molecules may intercalate between DNA base pairs has been discussed in Chapter One. Moreover, the resultant change in the dimensions of the DNA helix has been well substantiated by viscosity data (Lerman, 1961; Drummond et al, 1966; Muller and Crothers, 1968; Cohen and Eisenberg, 1969; Armstrong et al, 1971). Similarly, the increased viscosity of DNA in the presence of reporter molecules strongly indicates that these molecules also are

Table 2.4
Absorption Maxima of Reporter Molecules in Aqueous
and in DNA Solution

Reporter and Environment	$\bar{\nu}_{\max}$ cm ⁻¹	D/P	μ	pH	Reference
Paranitroaniline Aqueous	26,110		0.01	6.5	Gabbay,1969
	26,100		-	5	This work
Paranitroaniline DNA	25,450	.012-.014	0.01	6.5	Gabbay,1969
	25,450	0.007	-	5	This work
Orthonitroaniline Aqueous	22,880		0.01	6.5	Gabbay,1969
	22,900		-	5	This work
Orthonitroaniline DNA	22,570	0.08	0.01	6.5	Gabbay,1969
	22,550	.018-.019	-	5	This work
2,4-Dinitroaniline Aqueous	28,570		0.01	6.5	Gabbay,1969
	28,650		-	5	This work
2,4-Dinitroaniline DNA	28,170	.012-.014	0.01	6.5	Gabbay,1969
	28,100	.007-.010	-	5	This work
4-Nitro-1- naphthylamine Aqueous	22,570		0.01	6.5	Gabbay,1969
	31,060				
	22,550		-	5	This work
	31,200				
4-nitro-1- naphthylamine DNA	21,930	.012-.014	0.01	6.5	Gabbay,1969
	21,850		-	5	This work
	30,600(s)	0.007			

(s) denotes shoulder

Table 2.5

Red Shift of Dye Absorption Maximum in DNA
Relative to Aqueous Environment

Dye	Red Shift of Absorption Maximum (cm^{-1})
Proflavine	850 ± 100
Acridine	700 ± 100
9-Aminoacridine	400 ± 100 (a) 350 ± 100 400 ± 100 400 ± 100
Paranitroaniline reporter	350 ± 100
Orthonitroaniline reporter	350 ± 100
2,4-Dinitroaniline reporter	550 ± 100
4-Nitro-1-naphthylamine reporter	700 ± 100 (a) 600 ± 200

(a) where more than one maximum, maxima are shown in order of increasing wavenumbers.

intercalated (Kurucsev, 1969; Passero et al, 1970; Gabbay et al, 1970; Gabbay and DePaolis, 1971). In addition, further supporting evidence has been obtained from visible and ultra-violet spectroscopy, circular dichroism, pmr and hypochromicity measurements (Gabbay, 1969; Gabbay and Gaffney, 1970; Gabbay et al, 1972; plus above references pertaining to reporters).

The intrinsic viscosities of the proflavine and reporter/DNA complexes measured relative to pure DNA, $[\eta]/[\eta_0]$, and obtained under identical experimental conditions, are shown in Table 2.6. The percentage of intercalated to total dye (intercalated, free and externally bound) has been calculated from the ratio of the relative intrinsic viscosity of the respective dye relative to that of the proflavine determined value. At the D/P ratio of 0.09 and the ionic strength of 0.03, the amount of free proflavine is very small and the amount of externally bound dye is negligible (Armstrong et al, 1970). Proflavine is therefore a good comparative standard for full intercalation. It has been assumed* that each intercalated dye molecule produces the same increase in the length of the DNA double helix so that the relative intrinsic viscosity increments for the complexes are a measure of the equilibrium between the intercalated and the externally bound dye (Passero et al, 1970).

It follows from Table 2.6 that not all the reporter molecules are intercalated to the same extent under identical conditions. Moreover, provided that the binding constants for the intercalation process and the externally bound process remain the same at the much lower D/P ratios

Table 2.6

Intrinsic Viscosity of the Dye/DNA Complex Relative to Pure DNA (a)

Dye	$[\eta]/[\eta_0]$	Percent Intercalated	Ionic Strength	D/P	Reference
Proflavine	1.35(b)	100(fully)	0.03	0.09	Armstrong et al, 1970
Paranitroaniline reporter	1.14	40	(d)	0.09	Kurucsev, 1969
Orthonitroaniline reporter	1.13	40	(d)	0.09	(c)
2,4-Dinitroaniline reporter	1.39	100(fully)	(d)	0.09	Passero et al, 1969
4-Nitro-1-naphthylamine reporter	1.36	100(fully)	(d)	0.09	Kurucsev, 1969

(a) all viscosity measurements were carried out with the same Zimm low shear viscometer by Dr. T. Kurucsev (1969).

(b) obtained by interpolation of data in Fig.4 of reference.

(c) obtained from a correlation of hypochromicity data (Gabbay, 1969) with intrinsic viscosity data (Kurucsev, 1969).

(d) viscosity measurements were carried out in 0.025M sodium phosphate buffer (pH 6.50), 0.025M in Na^+ ions of ionic strength 0.028.

(0.007 - 0.019) used throughout this work, then it would be expected that Table 2.6 presents a reliable estimate of the percentage of the intercalated dye in as much as the 2,4-dinitroaniline and 4-nitro-1-naphthylamine reporters are fully intercalated while the paranitroaniline and ortho-nitroaniline reporters are not fully intercalated.

The viscosities of the 9-aminoacridine and proflavine/DNA complexes have been reported to be the same at an ionic strength of 0.005 for a D/P ratio less than 0.14 (Drummond et al, 1966). Thus, 9-aminoacridine may also be taken to be fully intercalated at the low D/P ratio (0.004 - 0.008) used throughout this work. There is no viscosity data available for acriflavine. However, in the D/P range less than 0.08, intercalation is the only kind of significant binding (Chan and Van Winkle, 1969). At the very small D/P ratios (0.002 - 0.003) used throughout this work, this dye is also considered to be fully intercalated.

2.5 Transition Moment Directions

2.5.1 Experimental Classification

Zanker (1954) has classified the absorption bands for acridine as $\pi^* \leftarrow \pi$ according to the Platt electron model for aromatic hydrocarbons (Platt, 1949; Platt and Klevens, 1949) where the polarisation of the L_a , B_a and L_b , B_b bands is perpendicular and parallel to the long axis of the acridine molecule respectively. The classification has further been extended to include mono- and diaminoacridines, by studying the effect of NH_2 - substitution on the absorption and the polarised fluorescence of the parent acridine at low temperatures (Wittwer and Zanker, 1959). It was concluded,

that the visible (lowest wavenumber) absorption band of the proflavine cation is a composite band where the low intensity 1L_a band is completely overlapped by the very intense 1L_b band. A further low intensity band, noticeable as an inflexion ($32,000\text{ cm}^{-1}$ at -183°C in ethanol) prior to intense ultra-violet absorption, is clearly indicated by the strong decrease in the degree of the polarised fluorescence. This band is polarised perpendicular to the 1L_b band and has been tentatively classified as a 1B_a band. A similar classification for the absorption bands of acriflavine to those of proflavine can be made since the methyl group substituted on the ring nitrogen has little effect on the absorption spectrum (compare Figs.2.1 and 2.2). The spectra are almost superimposable but for the slight red shift of the acriflavine spectrum.

Finally, the Platt classification for the low wavenumber absorption bands of 9-aminoacridine measured at -183°C in Ether/Ethanol has been carried out, where the relative position of the 1L_a and 1L_b bands is similar to acridine, but where the intensity of the bands is reversed. The 1L_a band has gained intensity relative to acridine and is now many times more intense than the 1L_b band which has lost intensity relative to acridine (Zanker and Schiefele, 1958). The two absorption bands shown in Fig.2.3 have been labelled accordingly. A summary of the transition moment directions associated with the observed absorption maxima of the dye/DNA complex is shown with respect to the molecular axes in Fig.2.8 for the acridine molecules. The position of the (0,0) absorption maximum for the 1L_a band of the 9-aminoacridine/DNA complex has been recorded in the figure.

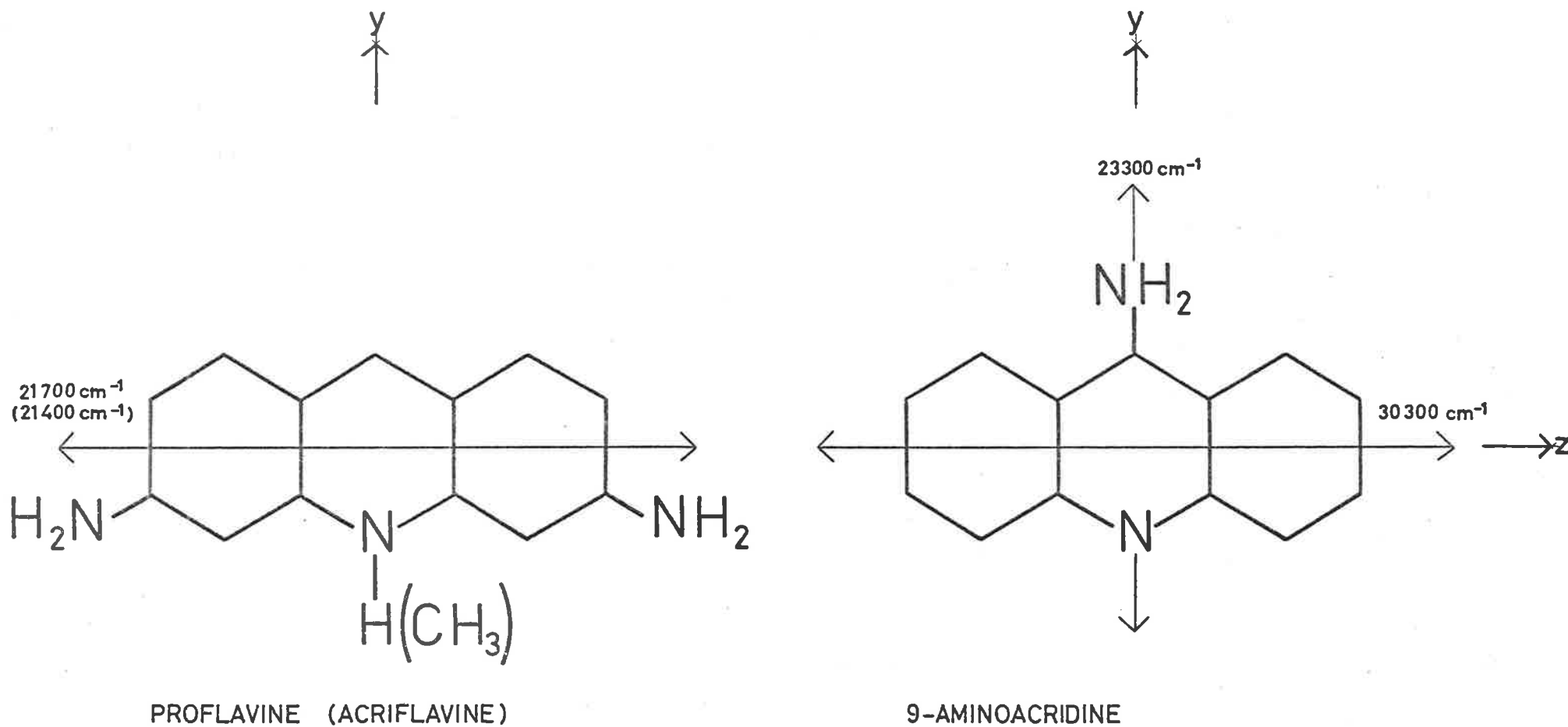


FIG 2.8 TRANSITION MOMENT VECTORS IN THE ACRIDINE MOLECULES

The visible and near ultra-violet absorption bands of the reporter molecules, assigned to $\pi^*\leftarrow\pi$ transitions (Gabbay, 1969), may be classified as 1L_a , 1L_b according to the Platt notation. However, because the planar benzene or naphthalene rings are assymmetrically substituted with NO_2 - and $-\text{NH}$ - groups, a loss of C_{2v} symmetry has occurred so that no conclusions concerning the transition moment direction(s) associated with particular absorption band(s) can be made.

2.5.2 Theoretical Calculation

Theoretical calculations have been carried out using the Pariser-Pople-Parr self-consistent-field molecular orbital method (SCF-CI-PPP) for π -electron systems (Parr, 1963) in the form described by Bailey (1969). This method has been shown to give good agreement between theoretical and experimental data for a number of heterocyclic purine and pyrimidine derivatives (Bailey, 1970). More recently, it has been emphasised with relatively large conjugated molecules, that the SCF-CI-PPP method, with CI (configuration interactions) limited to singly excited configurations, is sufficient to predict transition moment directions within a few degrees for strong transitions, although oscillator strengths are rather poorly predicted. For weak transitions (oscillator strengths near 0.01), acceptable transition moment directions require at least some doubly excited configurations (Downing and Michl, 1972).

The geometry of the reporter molecules (the N,N,N -trimethyl- N',N' -dimethyl- N' -ethyl(or propyl)-1,3-diammoniumpropane moiety has been ignored) has been based on the atomic co-ordinates of paranitroaniline (Sutton, 1965).

Both Clementi double zeta orbitals (CO) (Clementi, 1963) and Slater orbitals (SO) have been used and the calculations have included all possible singly excited configuration interactions. Oscillator strengths have been determined by the method of Hansen (1967) which employs a mixed dipole length-dipole velocity expression. The π electron calculations carried out on the aniline nucleus of the reporter molecules are indistinguishable from those of the reporter molecules themselves.

The mean energies, oscillator strengths and the angles between the transition moment vectors and the z axis of the reporter molecules (refer to Fig.2.9) are shown in Tables 2.7 to 2.10 for the lowest energy transitions and are correlated with the observed maxima of the transitions. The absolute values of the energies of the calculated (π^* , π) transitions are too large when compared with the corresponding experimental values. This may be a reflection to some extent on the environment of the dye. Nevertheless, the correspondence between theory and experiment is satisfactory. The number of transitions and the oscillator strengths of the paranitroaniline, orthonitroaniline and 2,4-dinitroaniline reporters in the visible and near ultra-violet region (Figs.2.4 to 2.6) is correctly predicted. The calculated energies of following bands correctly indicate that there is no overlap from higher energy bands. The first calculated transition of the 4-nitro-1-naphthylamine reporter can be correlated to the first absorption band (Fig.2.7) because of its high predicted oscillator strength. The second transition may be ignored due to its negligible oscillator strength. Thus, either calculated transition three or four

Table 2.7

Calculated (π^* , π) Transitions in Paranitroaniline/Reporter

No.	Energy (cm^{-1})		Oscillator Strength		Angle of Moment with z axis		Experimental Maximum (cm^{-1})
	CO	SO	CO	SO	CO	SO	
1	28,630	27,510	0.340	0.360	90°	90°	25,450
2	32,900	32,480	~0	0.001	0°	0°	
3	39,010	38,470	0.026	0.012	0°	0°	

Table 2.8

Calculated (π^* , π) Transitions in Orthonitroaniline/Reporter

No.	Energy (cm^{-1})		Oscillator Strength		Angle of Moment with z axis		Experimental Maximum (cm^{-1})
	CO	SO	CO	SO	CO	SO	
1	25,600	24,830	0.096	0.102	8°	7°	22,550
2	35,650	35,080	0.087	0.107	41°	42°	

Table 2.9
Calculated (π^* , π) Transitions in
2,4-Dinitroaniline/Reporter

No.	Energy (cm^{-1})		Oscillator Strength		Angle of Moment with z axis		Experimental Maximum (cm^{-1})
	CO	SO	CO	SO	CO	SO	
1	26,860	26,090	0.086	0.102	13°	20°	inflexion of shoulder
2	29,980	28,890	0.278	0.289	~90°	88°	28,100
3	35,720	35,120	0.065	0.056	27°	25°	

Table 2.10
Calculated (π^* , π) Transitions in
4-Nitro-1-naphthylamine/Reporter

No.	Energy (cm^{-1})		Oscillator Strength		Angle of Moment with z axis		Experimental Maximum (cm^{-1})
	CO	SO	CO	SO	CO	SO	
1	24,920	24,060	0.286	0.306	84°	84°	21,850
2	30,760	30,820	0.001	0.002	68°	63°	
3	34,870	34,820	0.017	0.018	56°	69°	shoulder at
4	36,980	36,360	0.051	0.067	67°	66°	

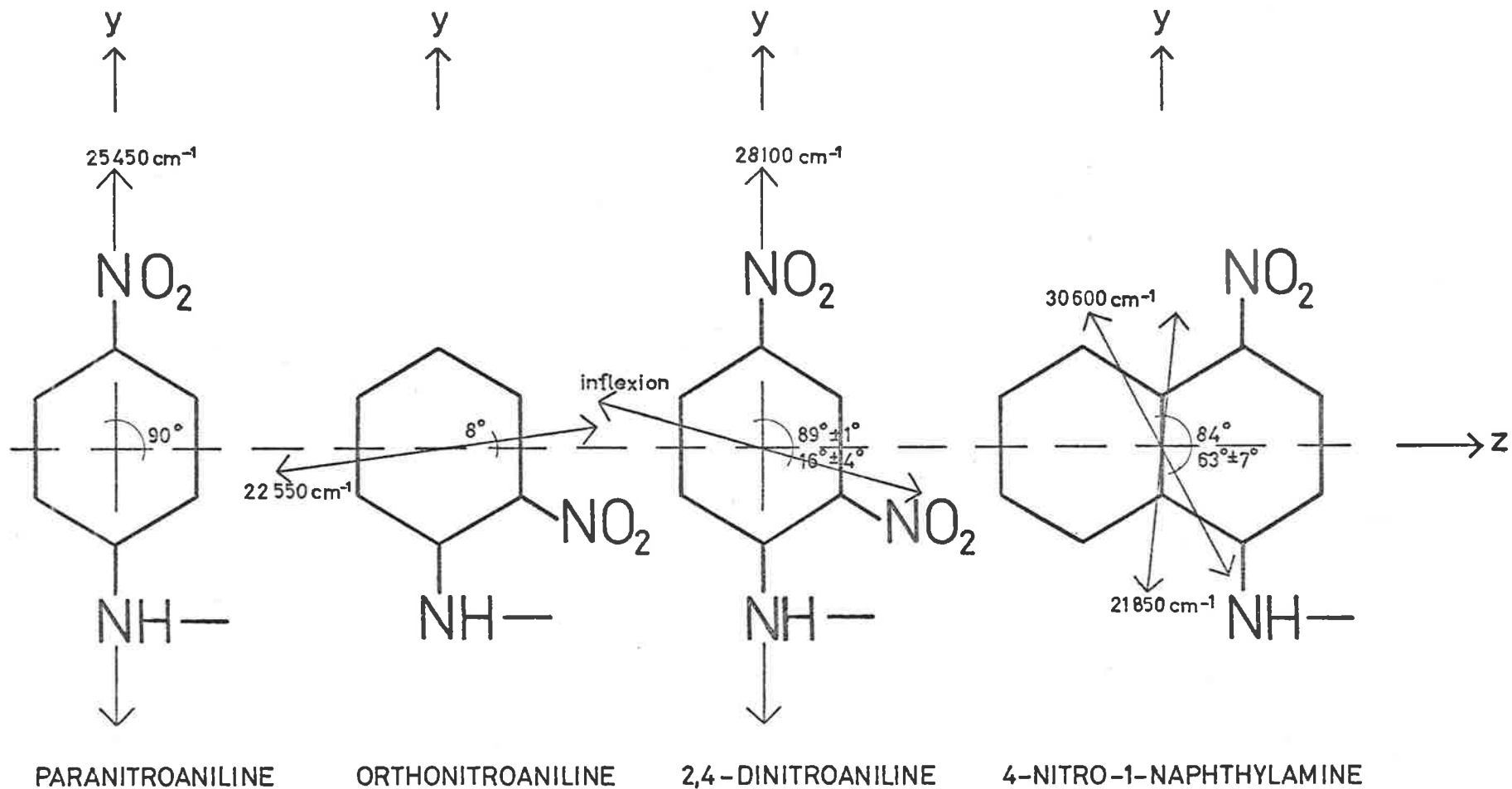


FIG 2.9 TRANSITION MOMENT VECTORS IN THE REPORTER MOLECULES

may be correlated to the observed shoulder at $30,600 \text{ cm}^{-1}$. This is probably a composite band and for further interpretation no assignment need be made since the polarisation directions of the two transitions are the same within the variations of the CO and SO methods used here.

A summary of the transition moment directions associated with the observed absorption maxima of the dye/DNA complex is shown with respect to the molecular axes in Fig.2.9 for the reporter molecules.

CHAPTER THREE

INSTRUMENTATION

3.1 General

Currently available commercial spectrophotometers are designed primarily for absorption spectroscopy of dilute homogeneous solutions where light scattering may be neglected. In contrast, the problem of light scattering contribution to the measured absorption spectrum of solid samples, in particular of DNA film samples, cannot be overlooked. Some workers have ignored it (Rich and Kasha, 1960; Wetzel et al, 1969), while others have assumed that it is negligible because of the similarity between the solution and film spectra (Falk, 1964; Zdysiewicz, 1969). Gellert (1961) and Brunner and Maestre (1974) have assumed that the DNA absorbance at 320 and 350nm respectively was zero and subtracted this amount as a constant correction at all wavelengths. Yet in another case, a reference DNA film has been used to correct for the measured absorbance, where the spectrum (in the non-absorbing DNA region) of a dye associated with DNA was of interest (Rupprecht et al, 1969).

Rayleigh scattering is known to have an inverse fourth power dependence upon wavelength while scattering from long rods or coils (to which DNA may be compared) is less wavelength dependent (Oster, 1955). To estimate the functional dependence of the scatter contribution to the measured absorbance, log-log plots of absorbance versus wavenumber from $13,500\text{cm}^{-1}$ to $31,000\text{cm}^{-1}$ have been used

and such plots extrapolated to obtain the corrected absorbance at the required wavelengths (Englander and Epstein, 1957; Gray and Rubenstein, 1968; Kurucsev and Zdysiewicz, 1971). Some workers felt compelled to assume a gradient of four for such a plot (Kurucsev and Zdysiewicz, 1971) since the measured absorbance in the DNA non-absorption region varied only slightly with wavenumber making an accurate extrapolation difficult. It should also be mentioned that there is no exact correction for scattering caused by the inhomogeneity of the sample (Fraser, 1960). In view of the questionable merits and effectiveness of the above methods, it was decided to investigate in some detail the scatter contribution to the measured absorbance of DNA film samples prepared for this work (for preparation of samples, see Chapters Four and Five).

◆ 3.2 Spectrophotometric Arrangements Investigated

Two parts of a spectrophotometer are of particular importance in measurements of the light scattering ability of a sample:-

- (a) the sample compartment; because it determines the distance between the sample (the source of the scattered light) and the detector, and
- (b) the detector; since its size and shape will determine to what extent the scattered light is gathered and recorded.

Of the two spectrophotometric arrangements to be described, the Zeiss PMQII spectrophotometer mounted on a 1.25 metre triangular bar has been used as the basic unit. In both these arrangements, only the sample compartment and

detector unit have been altered.

3.2.1 Zeiss PMQII Spectrophotometer with Wide-window Photomultiplier Detector

(a) Construction

The sample compartment and detector housing, shown schematically in Fig.3.1, were constructed from the Tubular Cell Equipment supplied by Carl Zeiss Pty. Ltd. (refer to pamphlet No.1). The interior cell carriage was removed but both the fixed platform (N) and pull platform (K) support rods were left intact. The tubular holder (P) with its two lenses (only one lens (O) is shown) was also left undisturbed at the side of the sample compartment. The exit hole for the light beam, originally 48mm diameter, was enlarged to form a 50mm square. A further 5mm was removed from the upper wall section of the sample compartment to form a final exit hole of 50mm base, by 55mm height. The two original holes that had been made to support the standard photomultiplier housing were plugged.

A cell carriage with sample and reference holders was designed. Each holder could be centralised (horizontally) in the light beam by moving the pull platform support rod which passed through the platform (J) (thickness, 5mm; width, 34mm; length, 220mm) of the cell carriage. The other end of the platform rested on and slid over the fixed platform support rod. The platform protruded into the exit hole and was flush with the outer wall of the sample compartment where it fractionally cleared the bottom of the exit hole. The walls of the cell carriage, formed from three pieces of brass (thickness, 3mm; height, 23mm; length, 70mm), were attached to the surface of the platform at that

Fig.3.1

Film Transmittance Attachment - Horizontal Section through the Optic Axis

Key to Letters

Detector Housing

- A. Circular brass plate
- B. Space for resistor chain and connectors(not shown)
- C. Moveable support for photomultiplier tube
- D. Tube socket
- E. Fixed support for tube
- F. EMI 6255S photomultiplier
- G. Photomultiplier window
- H. Cylindrical collar

Sample Compartment

- I. Film sample
- J. Platform for sample holders
- K. Pull platform support rod
- L. Polarising prism (mounting not shown)
- M. Optic axis
- N. Fixed platform support rod
- O. Lens
- P. Tubular lens holder

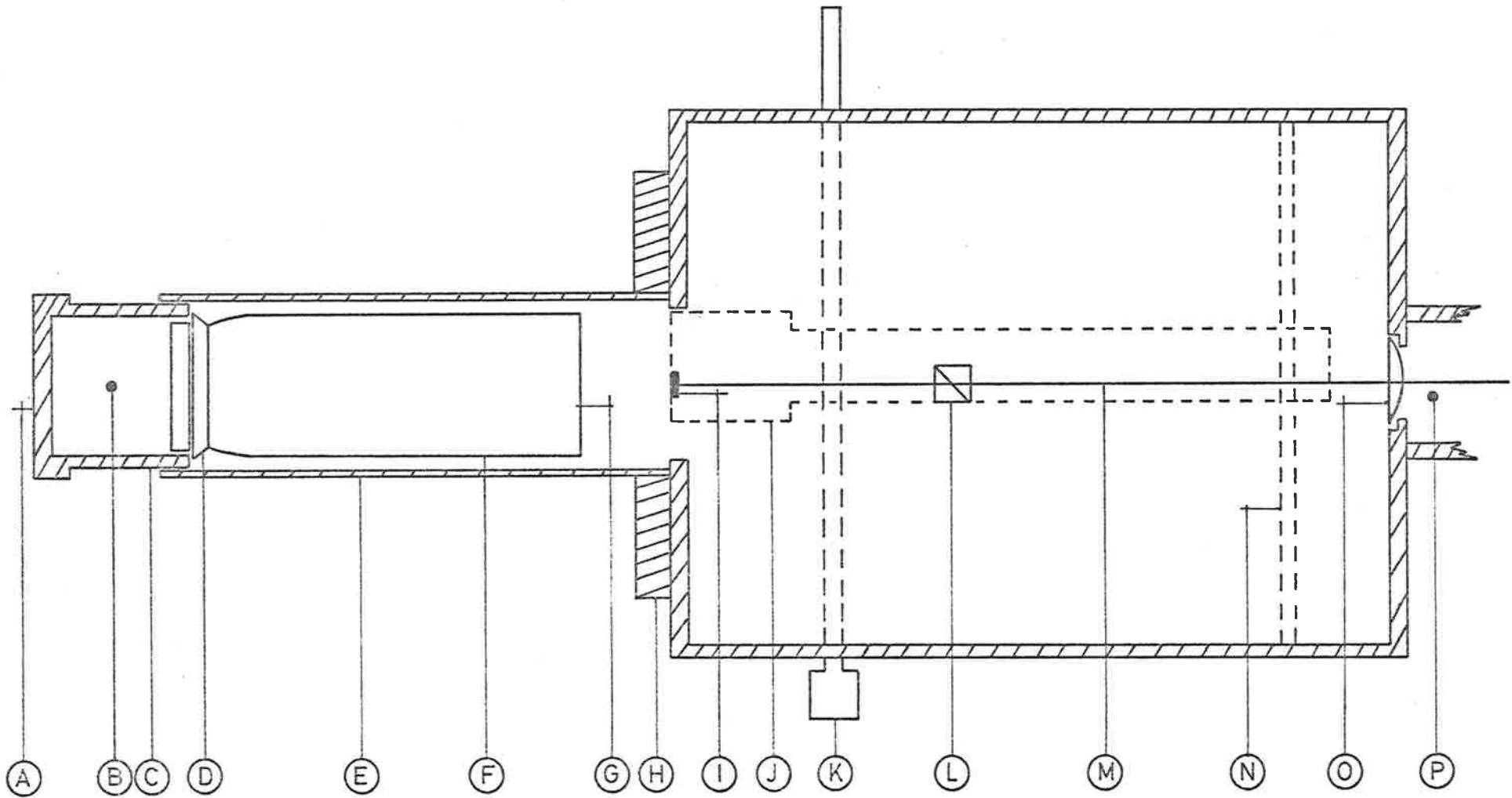


FIG 3.1 FILM TRANSMITTANCE ATTACHMENT — HORIZONTAL SECTION THROUGH OPTIC AXIS — HALF FULL SIZE

end nearest the light exit hole. They were spaced 12.5mm apart.

The photomultiplier electron tube (F) (EMI, type 6255S, front window 50mm outer diameter) was supported in a fifteen pin socket (D) which in turn was mounted on the front face of a cylindrical brass sleeve (C) (outer diameter, 58mm; length, 54mm) which contained the chain of resistors and connectors (B). A circular brass plate (A) of slightly greater external diameter (63mm) than the sleeve enclosed the other face. (Both the sleeve and the plate were cut as a single unit from a solid brass cylinder.) Two cables passed from the sleeve through the circular plate. One cable connected the photomultiplier to a stabilised variable high voltage supply (EILCO, Norwood, South Australia; High Voltage Power Supply, type 6324 No.1; output range, 500-2500 Volt), whilst the other carried the signal from the photomultiplier to input socket B (hole No.2) of the Zeiss Amplifier. The earth wire was connected to socket C (bottom hole) for convenience, instead of the central earth hole of socket B.

The photomultiplier with supporting socket and sleeve was centrally housed in a further cylindrical sleeve (E) (internal diameter, 58mm; length 173mm) which was attached by means of a cylindrical collar (H) to the outside wall of the sample compartment. This arrangement allowed the outer sleeve to be located centrally relative to the exit hole. The length of the outer sleeve was 1mm greater than the total length of the photomultiplier with supporting socket and sleeve. Thus, with the inner sleeve acting as a movable slide, the front window of the photomultiplier could be

positioned at any predetermined distance up to a closest approach distance of 1mm from the outside wall of the sample compartment. When a sample humidity cell (Chapter Four; Section 4.6) was placed in the cell carriage the sample film mounted inside the cell could be as close as 3mm from the outside wall. Thus, the overall closest approach distance between film sample and front window of the photomultiplier was 4mm. The 1mm separation between photomultiplier window and sample cell was a safety margin to protect the photomultiplier from damage.

Provision was made to mount a Glan-Taylor calcite polarising prism (L) (Archard-Taylor modification of a Glan-Foucault polariser) in the sample compartment. A circular collar which had a small projection (3mm x 3mm) at one point was attached to the prism (12mm square, mounted in a 20mm diameter tube). A cylinder, with a small section removed from one quarter (plus 3mm) of its circumference, supported the prism and enabled it to be rotated through 90° . A metal rod was attached at one end to the prism support. The other slotted end was screwed to an overhead, horizontally positioned T-shaped rod which slid inside a brass tube supported by the side walls of the sample compartment. With this arrangement, the movement of the T-shaped rod allowed the prism to be moved horizontally while movement of the metal rod (attached to the prism support) enabled it to be moved vertically. The screw type arrangement (between the metal rod and the T-shaped rod) allowed an angle adjustment of the front face of the prism relative to the vertical plane. The prism, when in position, was 90mm from the exit hole of the sample compartment. All metal components inside

the sample compartment and detector housing had a non-reflecting dull black finish.

(b) Light Path

The light path through the sample compartment is controlled by two lenses in the tubular holder, the image of the monochromator slit being so adjusted by lens two that it is focussed fractionally before the aperture formed by the exit hole of the sample compartment. A 3.5mm diaphragm was positioned in the entrance aperture to the monochromator to attenuate the height of the incident radiation. When linear polarised light was required, the polarising prism was centralised horizontally and vertically with respect to the light beam. It was further positioned with its entrance and exit faces perpendicular to it. The light beam impinged centrally on the front face of the photomultiplier (25mm from both sides) in the horizontal direction. In the vertical direction, it was positioned 28mm from the top and 16mm from the bottom. The dimensions of the light beam in the sample compartment, shown in Table 3.1 for two slit widths, are important when the position and polarising ability of the prism are to be considered.

Firstly, it can be seen that the light beam is not vignetted as it passes through the prism (12mm square). Secondly, the calculated angular field of the light path with the prism is less than two degrees. This falls well within the specified limits of the useable angular polarised field of from seven to nine degrees in the wavelength range 2300nm to 214nm (Karl Lambrecht, pamphlet). The direction of the optic axis for the Glan-Taylor polarising prism is the plane of polarisation. Consequently, linear parallel

Table 3.1
Dimensions of Light Beam in Sample Compartment

	Beam Dimensions of Light at					
	Entrance (zero)		Prism Position (150mm)		Exit (240mm)	
	height (mm)	width (mm)	height (mm)	width (mm)	height (mm)	width (mm)
0.3mm Slit Width	13	8	8	4	6	1
>2mm Slit Width (fully open)	13	12	8	7	6	4.5

(plane) polarised light was obtained with the direction of the optic axis positioned horizontally while linear perpendicular (plane) polarised light was obtained by rotating the prism (i.e. the optic axis) through 90° .

3.2.2 Zeiss PMQII Spectrophotometer with Integrating Sphere (KA) Attachment

The sphere attachment was placed next to the outer wall of the sample compartment and was set up to measure spectral transmittance (Carl Zeiss, refer to pamphlet No.2). The sample compartment is that described in Section 3.2.1, with detector housing removed.

The principle of the integrating sphere is to trap all the scattered light within the totally reflecting surface of the sphere. It is necessary therefore, to place all scattering samples directly in the plane of the sampling aperture of the sphere, if all the transmitted light is to

be measured.

3.2.3 Comparison of the Two Spectrophotometric Arrangements

The two arrangements were compared for bandwidth and for amplifier noise. In the case of the sphere attachment, a small bandwidth could only be obtained with a high voltage setting on the amplifier unit. This necessitated increasing the response time of the unit to decrease the correspondingly large statistical fluctuations of the reading. For the wide-window photomultiplier (PM) arrangement, the high voltage supply was maintained at 620 Volt throughout all wavenumber settings of the monochromator. At the response time of one second, the amplifier noise was low.

Fig.3.2 sets out the relationship between bandwidth and wavenumber for the two arrangements at workable noise levels. The various amplifications and response times are shown; no samples have been used. Whereas the sphere attachment may be useful in the visible range, it was impractical in the ultra-violet for the maximum workable amplification (40 times) at the response time of one second (curve three). Further, when a diaphragm and polarising prism were introduced into the optics the bandwidths became too large for the measured spectrum to be significant (curve one). Curves one, two and four show the change in bandwidth at various amplifications, at the appropriate response time, for acceptable noise with the sphere attachment. It can be seen that for comparable bandwidths, a much higher amplification and therefore a longer response time is needed with the sphere attachment when compared to the wide-window photomultiplier arrangement (curves four and six). Even at the

	Attachment	Amplification	Response Time (sec)	Diaphragm (mm)	Prism Setting
●	sphere	10	1	3.5	⊥
○	sphere	300	5	3.5	⊥
⊙	sphere	40	1	—	—
○	sphere	3000	15	3.5	⊥
△	PM	—	1	3.5	⊥
▲	PM	—	1	3.5	⊥

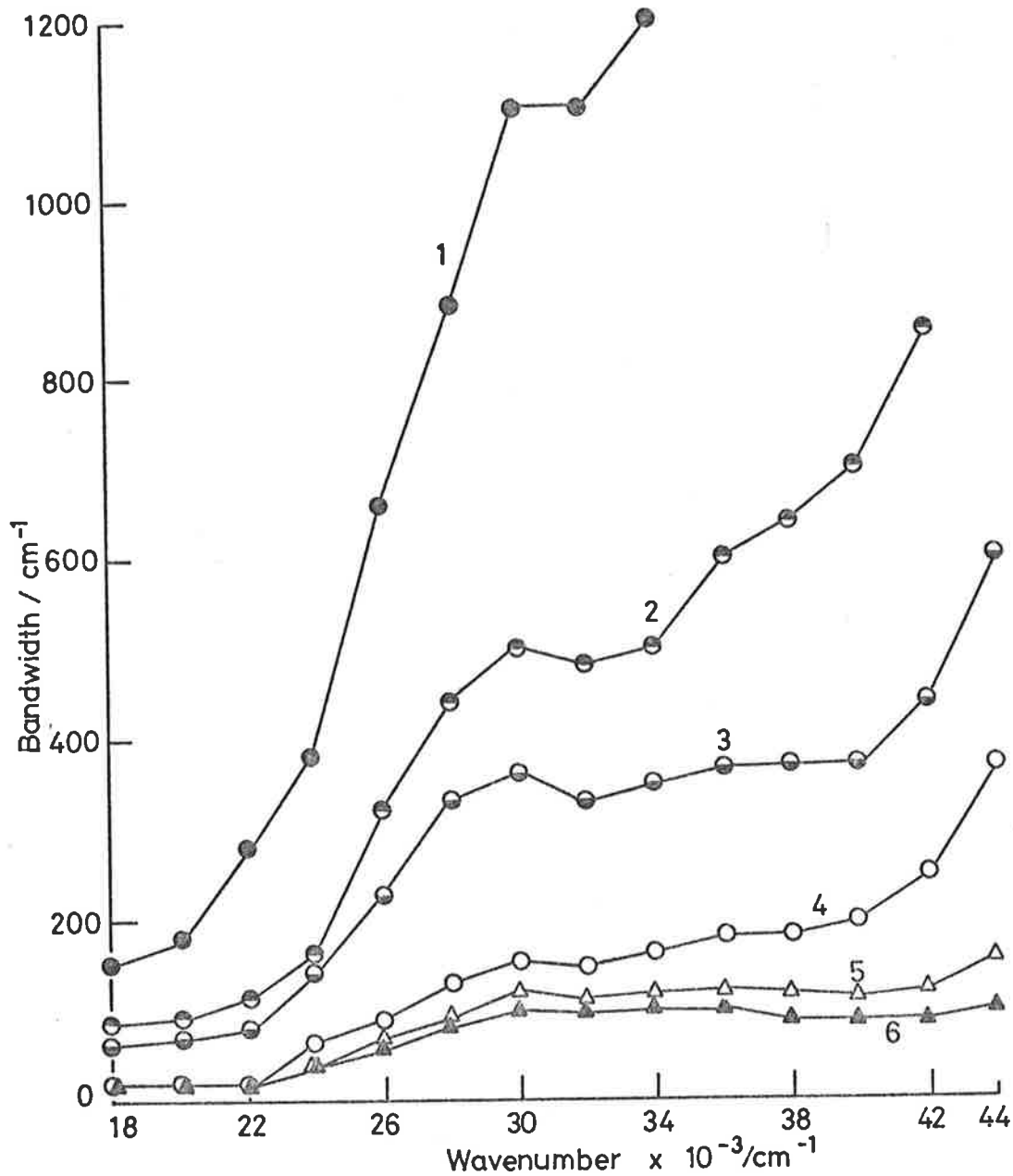


FIG 3.2 VARIATION OF BANDWIDTH WITH WAVENUMBER FOR THE TWO ATTACHMENTS TO THE ZEISS PMQII SPECTROPHOTOMETER

maximum workable amplification (3,000 times), at the response time of 15 seconds, the bandwidths were excessive in the range $40,000\text{cm}^{-1}$ to $44,000\text{cm}^{-1}$. At these high amplifications and longer response times, the measurement of a spectrum was inconvenient. In any case, the bandwidths obtained with the wide-window photomultiplier attachment were much smaller; they were obtained at a lower amplification and at a faster response time. Consequently, this arrangement was used in preference to the sphere attachment to record the absorption spectra of suspected light scattering samples.

3.3 Comparison of Absorbance Measurements Obtained with Different Spectrophotometers

For the comparison of the absorbance measurements, two types of film samples were investigated:-

- (i) DNA-PVA films; a single layer of DNA on the surface of a poly(vinyl alcohol)(PVA) film (for preparation see Chapter Four). The absorption spectrum of DNA was recorded in the ultra-violet region and,
- (ii) dye/DNA-PVA films; two layers of DNA on the surface of a PVA film with the outer DNA layer containing the dye (for preparation see Chapter Five). The absorption spectrum of the dye was recorded in the visible and near ultra-violet region (region prior to DNA absorption).

Absorbance measurements have been recorded at 93% relative humidity (unless otherwise indicated) against a reference that consisted of a complete humidity cell without any film. The spectrophotometers that were used for the comparison are listed in Table 3.2, along with their relevant optics. The Zeiss and Unicam SP700 spectrophotometers were

Table 3.2

Relevant Optics of Investigated Spectrophotometers

Spectrophotometer	Attachment	Distance between Film and Detector (mm)	Detector Surface Area (sq.cm)	Light Beam Dimensions at Film Surface (mm)	
				for slit widths 0.3mm	0.05mm
Zeiss PMQII	-	140	1	7 x 3	7 x 1
Zeiss PMQII	Microcell	110	1	6 x 1	6 x 0.1
Zeiss PMQII	Wide-window PM	variable, 4-	20	6 x 1	6 x 0.1
Unicam SP700	-	420	20	10 x 2	-
Cary 14	Scatter Transmission	variable, 12-	20	6 x 4 (maximum slit-width)	

freely accessible. The Cary 14 spectrophotometer with Scatter Transmission Accessory which was kindly made available by Dr. N.K. Boardman, Division of Plant Industry, C.S.I.R.O., Canberra, A.C.T. was situated in Canberra.

3.3.1 DNA-PVA Films

Although the DNA-PVA films appeared clear and homogenous they scattered light (Table 3.3). The absorption relative to the empty humidity cell has been recorded at various distances between the film and the photomultiplier detector, by moving the detector not the film for the Zeiss PMQII spectrophotometer with wide-window photomultiplier attachment. It can be seen at the three wavenumbers selected (DNA maximum absorption and two non-absorption wavenumbers) that scattering is negligible at the 4mm setting.

A scattering contribution to the absorbance increases with increasing distance between detector and film as seen by the first six entries in the Table. The major significance of the photocathode dimensions is emphasized by the last three entries in Table 3.3: the greater collecting area of the photomultiplier in the Unicam SP700 spectrophotometer more than compensates for the much greater distance between the film and the detector compared with the Zeiss standard and microcell arrangements.

Finally, a comparison between the results obtained on the Zeiss standard and the Zeiss with microcell attachment indicate an effect associated with the dimensions of the light beam. The variation in the distance between the film and the detector in the two set-ups is unlikely to account for the total difference in the measured absorbance; it is more in keeping with the assumption that the greater the

Table 3.3
Absorbance Measurements of a DNA-PVA Film

Spectrophotometer	Distance between Film and Detector (mm)	Absorbance at Selected Wavenumbers (cm ⁻¹)		
		28,000	31,500	38,600
Zeiss, wide-window PM	4	0.044	0.047	0.565
	9	0.044	0.048	0.567
	14	0.044	0.049	0.568
	19	0.046	0.051	0.569
	24	0.048	0.053	0.570
	34	0.050	0.056	0.572
Zeiss, standard	140	0.173	0.191	0.759
Zeiss, microcell	110	0.130	0.138	0.666
Unicam SP700	420	0.079	0.085	0.650

area of the beam impinging on the film the greater the amount of light scattered.

3.3.2 Dye/DNA-PVA Films

The absorption spectrum of a typical dye/DNA-PVA film recorded against an empty humidity cell is represented in Fig.3.3 for the dye proflavine. It can be seen that this film scatters light extensively by the comparison of the measured absorbances obtained with the different spectrophotometers used. The spectrum has been recorded at various distances between the film and the photomultiplier

- Zeiss PMQII (standard)
- Zeiss PMQII (microcell attachment)
- △ Zeiss PMQII (wide-window photomultiplier), 4mm setting
- ▲ Zeiss PMQII (wide-window photomultiplier), 14mm setting
- Unicam SP700

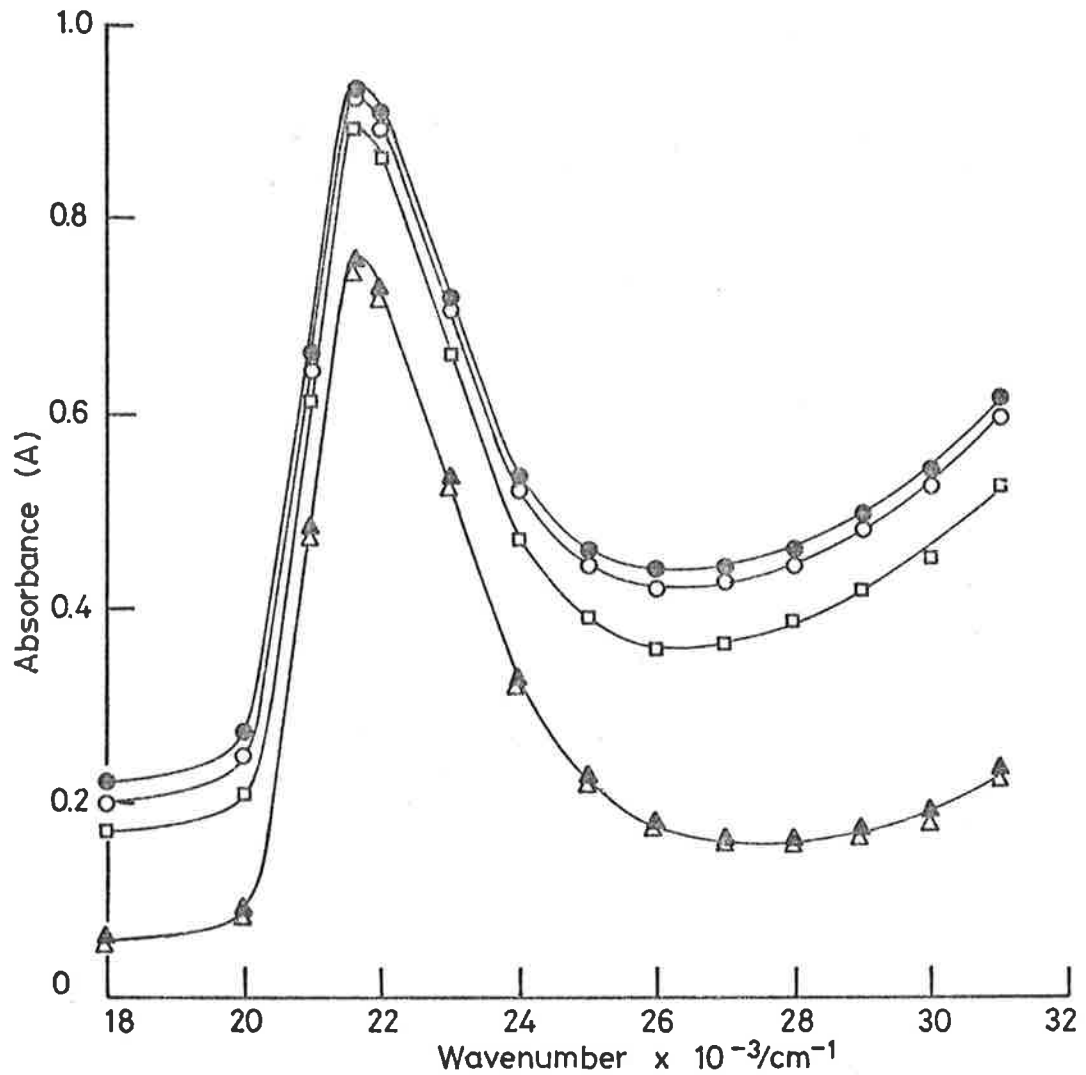


FIG 3.3 THE MEASURED ABSORPTION SPECTRUM OF A PROFLAVINE/ DNA-PVA FILM OBTAINED USING VARIOUS SPECTROPHOTOMETERS

for the Zeiss PMQII with wide-window photomultiplier attachment although only two such spectra are shown in the figure. An extrapolation to zero distance, revealed a scatter absorption component at the 4mm distance between 0.003 and 0.007 absorbance units. This was maximum at the dye maximum but random at other wavenumbers.

Preliminary absorbance measurements of proflavine/DNA-PVA films were carried out at room relative humidity using the Cary 14 spectrophotometer with Scatter Transmission Accessory in Canberra. The standard cell carriage was replaced by a modified design which was equipped with mounting positions for two polarising prisms; one prior to the sample holder, the other prior to the reference holder. The measured absorbances for two such films are recorded in Table 3.4 at the maximum proflavine absorption for both parallel (A_{11}) and perpendicular (A_{\perp}) polarised light.

In this instance, the absorption measurements have been recorded against a film prepared by exactly the same method, but without the dye. This is not the recommended method of correction as it assumes that the scatter contribution for both films is the same. However, at $21,700\text{cm}^{-1}$ (the proflavine maximum absorption), this is considered to be a reasonable assumption provided that the base-line absorbances are set equal in the non-absorption region of proflavine (prior to $19,000\text{cm}^{-1}$). These results suggest a scatter contribution between 0.008 and 0.014 at the closest approach distance of 12mm between the film and the detector. When they are compared to the measurements obtained using the Zeiss PMQII spectrophotometer with wide-window photomultiplier

Table 3.4

Absorbance of Proflavine/DNA-PVA Films at $21,700\text{cm}^{-1}$ using a Cary 14 Spectrophotometer with Scatter Transmission Accessory

Distance between Film and PM (mm)	Film 1		Film 2	
	A_{11}	A_{\perp}	A_{11}	A_{\perp}
12	0.673	0.769	0.671	0.889
20	0.687	0.781	0.675	0.904
28	0.709	0.802	0.690	0.927
38	0.728	0.819	0.708	0.954
48	0.733	0.829	0.712	0.956
58	0.731	0.826	0.718	0.965

attachment, the scatter absorbances at the 4mm equivalent position (obtained by extrapolation) lie between 0.003 and 0.005, thus supporting the previous conclusion.

3.4 Measurement and Correction of Film Spectra

Both DNA-PVA and dye/DNA-PVA film spectra were measured using the Zeiss PMQII Spectrophotometer with wide-window photomultiplier attachment. An initial correction due to the measured absorption of the complete humidity cell without film was carried out.

3.4.1 DNA-PVA Films

The distance between the DNA-PVA film and the detector was set at 4mm. At this distance no scatter correction was

necessary. The true absorbance of the DNA was taken to be the measured absorbance of the DNA-PVA film minus the measured absorbance of a PVA film (reflection correction) at the same wavenumber. In the DNA non-absorption region (below $31,600\text{cm}^{-1}$), a small but constant absorbance resulted because of the slight mismatch of the films. This constant absorbance was subtracted (or added) as a base-line correction at all wavenumbers.

This method was accurate in the spectral region up to $44,000\text{cm}^{-1}$ where the apparent absorption of the PVA film is due almost entirely to reflection with slight absorption (Tanizaki and Kubodera, 1967). Above $44,000\text{cm}^{-1}$, the apparent absorption of the PVA film is found to increase due to the rapidly increasing absorption of the PVA itself. This region was not investigated because a sizable error could be introduced into the corrected absorption spectrum of the DNA unless the DNA-PVA and PVA films were very closely matched (Zdysiewicz, 1969).

3.4.2 Dye/DNA-PVA Films

In the wavenumber range investigated ($16,600\text{cm}^{-1}$ to $31,600\text{cm}^{-1}$), both the PVA (Tanizaki and Kubodera, 1967) and DNA true electronic absorbances are negligible. The measured absorbance, A_M , may be given by

$$A_M = A_{\text{dye}} + A_S + A_R$$

where A_{dye} is the true electronic absorbance of the dye, A_S is the contribution to the measured absorbance by scattered light and A_R is that by reflected light. The DNA, dye and PVA contribute to the scatter and reflection components.

The distance between the dye/DNA-PVA film and the detector was set at 4mm. From a series of sample and reference (identical to sample but without dye) films, the amount of scattered light at this distance was found to fall between 0.003 and 0.007 absorbance units, throughout the wavenumber range investigated. The normalisation of sample and reference film absorbance base-lines in the dye non-absorption region (see Table 3.5) eliminated a further 0.004 scatter absorbance units. As the scatter contribution to the absorption spectrum was therefore minimal at a maximum of 0.003, any additional correction has been neglected. The measured absorbance may now be given by:

$$A_M = A_{\text{dye}} + A_R$$

The simplest method to eliminate the reflection contribution to the measured absorption spectrum of the dye is to subtract the measured absorbance of a reference film, prepared identically to the sample film but without dye; the spectra being normalised in the dye non-absorption region (Table 3.5). This procedure was found to be satisfactory in the lower wavenumber region of the dye spectrum but unsatisfactory at higher wavenumbers since a sizable error could be introduced into the spectrum unless the sample and reference films were very closely matched. This method requires the preparation of a reference film with every sample preparation.

In an alternative method, the measured absorption spectrum of a single reference film, prepared similarly to the dye/DNA-PVA film but without dye, is used as the basis

Table 3.5

Dye Non-Absorption Wavenumber Region Measured from 16,600cm⁻¹

Dye	Non-Absorption Region cm ⁻¹
Proflavine	16,600 - 19,200
Acriflavine	16,600 - 19,200
9-Aminoacridine	16,600 - 21,600
4-Nitro-1-naphthylamine reporter	16,600 - 19,200
2,4-Dinitroaniline reporter	16,600 - 20,200
Paranitroaniline reporter	16,600 - 20,200
Orthonitroaniline reporter	16,600 - 18,200

for the reflection correction. The procedure is as follows: The absorption spectra of the reference film (denoted 1) measured with both parallel and perpendicular linear polarised light are shown in Fig.3.4; the spectra may be subdivided into five almost linear sections. Table 3.6 lists the wavenumber range of these sections together with their absorbance gradients (calculated as the increase in absorbance units per 200cm⁻¹). This particular film was used because its reflection spectra were 1.5 - 2.5 times greater than those of any other prepared film, thus allowing the absorbance gradients shown in the table to be calculated with greater precision. Next, the absorbance

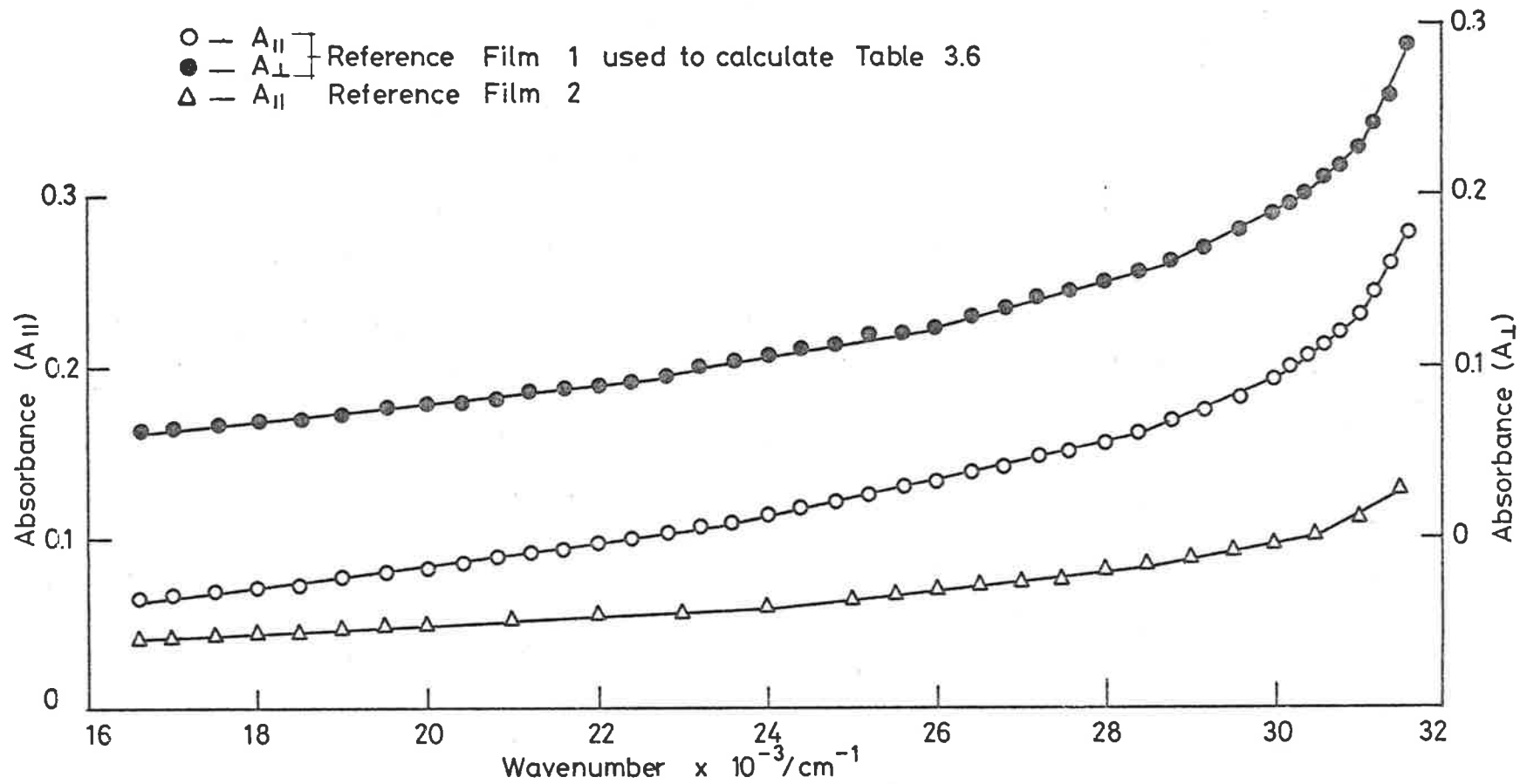


FIG 3.4 THE ABSORPTION SPECTRA OF REFERENCE DYE/DNA-PVA FILMS MEASURED WITH PARALLEL ($A_{||}$) AND PERPENDICULAR (A_{\perp}) LINEAR POLARISED LIGHT

Table 3.6

The Calculated Absorbance Gradients of Reference Film No.1

Parallel Linear Polarised Light		Perpendicular Linear Polarised Light	
Wavenumber Range (cm^{-1})	Absorbance Gradient	Wavenumber Range (cm^{-1})	Absorbance Gradient
16,600 - 23,400	0.0012 ₀	16,600 - 23,400	0.0011 ₂
23,400 - 28,600	0.0023 ₂	23,400 - 26,000	0.0017 ₅
28,600 - 30,400	0.0050 ₀	26,000 - 29,800	0.0027 ₈
30,400 - 31,000	0.0087 ₉	29,800 - 31,000	0.0076 ₅
31,000 - 31,600	0.015 ₈	31,000 - 31,600	0.023 ₁

Table 3.7

Comparison of Reflection Correction Methods

Film 1 has been used to calculate the reflection absorbance of film 2 at $31,000\text{cm}^{-1}$.

Film 1 has been normalised at $19,000\text{cm}^{-1}$ to film 2 absorbance.

	Measured Absorbance at		Calculated Absorbance at
	$19,000\text{cm}^{-1}$	$31,000\text{cm}^{-1}$	$31,000\text{cm}^{-1}$ for Film 2
Film 1	0.077	0.230	
Film 2	0.049	0.111	
Method 1			0.212
Method 2			0.106

gradient of the reference film is equalised in the first section to that of the sample film in the dye non-absorption region. The multiplication factor relating the sample and reference absorbance gradients is now used to calculate new absorbance gradients for the four other sections of the reference film. In this way, a table similar to Table 3.6 is produced. The new reflection correction spectrum may then be constructed from the adjusted absorbance gradients of the reference film after normalisation of the measured absorbances of the sample and reference films at the onset of dye absorption.

The superiority of the second method over the first is emphasized in Table 3.7 for the case where sample and reference films are not closely matched. In the example, the reference film has been used to calculate the amount of reflection of a second reference film (denoted 2 in Fig.3.4) at $31,000\text{cm}^{-1}$. Only the parallel absorption component has been employed. Whereas method 1 grossly over-estimates the reflection correction by 0.101 absorbance units, method 2 under-estimates it marginally by 0.005 absorbance units. Method 2 does not assume a parallel relationship between the reflection spectrum of sample and reference films, but assumes that such a relationship exists between their absorbance gradients. This was found to be the case within the limits of experimental error for reference films 1 and 2. Thus, method 2 has been used to eliminate the reflection contribution to the measured dye spectra for the dye/DNA-PVA films.

Finally, to stress the reliability of the correction method above, a comparison of the 9-aminoacridine/DNA spectra

Table 3.8
Comparison of Film and Solution Spectra
for the 9-Aminoacridine/DNA Complex

Solution Spectrum ¹			Film Spectrum at 93% r.h. ²		
Wavenumber	Absorbance	$\frac{A_{\max}^3}{A_{30210}}$	Wavenumber	Absorbance	$\frac{A_{\max}^3}{A_{30300}}$
Maximum (cm^{-1})			Maximum (cm^{-1})		
23,310	0.156	3.7	23,300	0.385	3.7
24,630	0.183	4.4	24,650	0.472	4.5
25,910	0.120	2.9	25,900	0.314	3.0
30,210	0.042	1.0	30,300	0.105	1.0

1. Data from Fig.5.8, Peacocke and Skerrett, 1956
2. Data from Fig.2.3, this work
3. Ratio of the absorbance at the maximum absorption relative to the absorbance at the high wavenumber maximum absorption.

recorded in aqueous solution and in the film environment at 93% relative humidity has been carried out (Table 3.8). The agreement between the number and the wavenumber of the absorption maxima and the ratio of their absorbances relative to the absorbance of the high wavenumber maximum is excellent.

3.5 Spectrophotometric Calibration

The wavenumber calibration of the monochromator of the Zeiss PMQII Spectrophotometer was checked using the mercury emission lines (Herzberg, 1944). No correction was needed

in the ultra-violet region (using the Deuterium Lamp) where the wavenumber scale was reproducible to better than 10cm^{-1} . However, the monochromator was found to be slightly in error throughout the visible region where an average over-estimate of 20cm^{-1} to the wavenumber scale occurred. No correction has been applied. The photometric accuracy of the instrument has been described elsewhere (Gianneschi and Kurucsev, 1974). The standard deviation in the transmittance scale was found to be better than 0.2%.

3.6 Conclusion

Although film samples may appear clear and homogenous, the possibility of scatter and reflection contributions to the measured spectra should not be overlooked. In this respect, the optics of the spectrophotometer are important in determining the final measured absorbance. In particular, attention should be paid to

- (i) the distance between the film sample and the detector,
- (ii) the light collecting surface area of the detector and
- (iii) the dimensions of the light beam through the film sample.

The spectrophotometer, the measurement and the method of correction that have been described above, provide true absorbances in the wavenumber range of interest with confidence limits under 0.005 of an absorbance unit.

CHAPTER FOUR

PREPARATION AND PROPERTIES OF ANISOTROPIC DNA FILM SAMPLES

4.1 Current Preparative Methods

Methods that have been reported to produce anisotropic DNA film samples may be classified into two general types; those where the DNA has been manually manipulated and those where mechanical devices have been used.

By far the most common method, has been the unidirectional stroking or shearing of a viscous concentrated DNA solution to dryness on an optically flat surface (Seeds and Wilkins, 1950; Fraser and Fraser, 1951; Sutherland and Tsuboi, 1957; Rich and Kasha, 1960; Bradbury et al, 1961; Gellert, 1961; Falk et al, 1963b; Houssier, 1964; Neville and Davies, 1966; Webb and Bhorjee, 1968; Gray and Rubenstein, 1968; Wetzel et al, 1969; Tunis-Schneider and Maestre, 1970; Pillet and Brahms, 1973). Local orientations of DNA have also been achieved around salt crystals when solutions of DNA and sodium chloride have been allowed to dry. The sodium chloride crystals were dissolved in methanol while the oriented DNA fibres remain adhered to the glass slide (White and Elmes, 1952). Further, oriented DNA fibres have been prepared by slowly withdrawing a pointed glass rod from a sticky DNA gel (Wilkins et al, 1951). The major problem with these manual methods is that non homogenous and non reproducible oriented film samples have been obtained.

Mechanical devices employed in orientation of DNA film

samples would be expected to overcome these problems. There have been four such methods reported and they include:

- (i) the orientation of DNA by the Wet Spinning Method (Rupprecht, 1963 and 1966; Zdysiewicz, 1969),
- (ii) the orientation of DNA by the mechanical stretching of a pure DNA film (Kurucsev and Zdysiewicz, 1971),
- (iii) the orientation of DNA by the mechanical stretching of a mixed DNA-PVA film (Kurucsev and Zdysiewicz, 1971), and
- (iv) the orientation of DNA by the mechanical stretching of a pure DNA film supported on the surface of a PVA film (Kurucsev and Zdysiewicz, 1971).

4.2 The Selected Preparative Method

The wet spinning method has not been investigated because of the difficulties associated with the attainment of optimum conditions for the orientation and further, because some DNA samples, in particular calf thymus DNA, appear to be unsuitable for this process (Zdysiewicz, 1969). As there are handling problems connected with the pure DNA films in the stretching process (sticky at high humidity and brittle at low humidity) and as there is good evidence for interaction between the DNA and the PVA in the mixed DNA-PVA films (Kurucsev and Zdysiewicz, 1971), it was decided to prepare anisotropic DNA film samples by the mechanical stretching of a pure DNA film supported on the surface of a PVA film. There are two ways to achieve this. The DNA film can be cast directly on the PVA film surface from a DNA solution (Kurucsev and Zdysiewicz, 1971) or alternatively, the DNA and the PVA films can be prepared independently and then

combined under high relative humidity conditions. Here, the DNA films were prepared by both methods.

4.3 The Stretching Process

High relative humidity conditions are required to orient DNA-PVA films. Therefore, the stretching device (Fig.4.1) consisted of two basic parts; the humidity controlling unit and the mechanically driven stretcher. The humidity controlling unit was built up from the brass water bath (1) (base, 37cm x 21cm; height, 11cm) with V-shaped perspex lid (2), the heating element (3) and the temperature regulator (4). The heating element (length, 76cm; 500 watt), bent into a U-shape, was placed 2cm from the bottom and near to the sides of the bath. The bath in turn, was bolted to a wooden platform (5) of convenient size to support the motor (6) and the control switch box (7) that housed the on/off and micro-switch circuits for the motor and heating element. The bath was filled to a depth of 5.5cm with water, maintained at 45°C by a thermistor probe (8) connected to the temperature regulator.

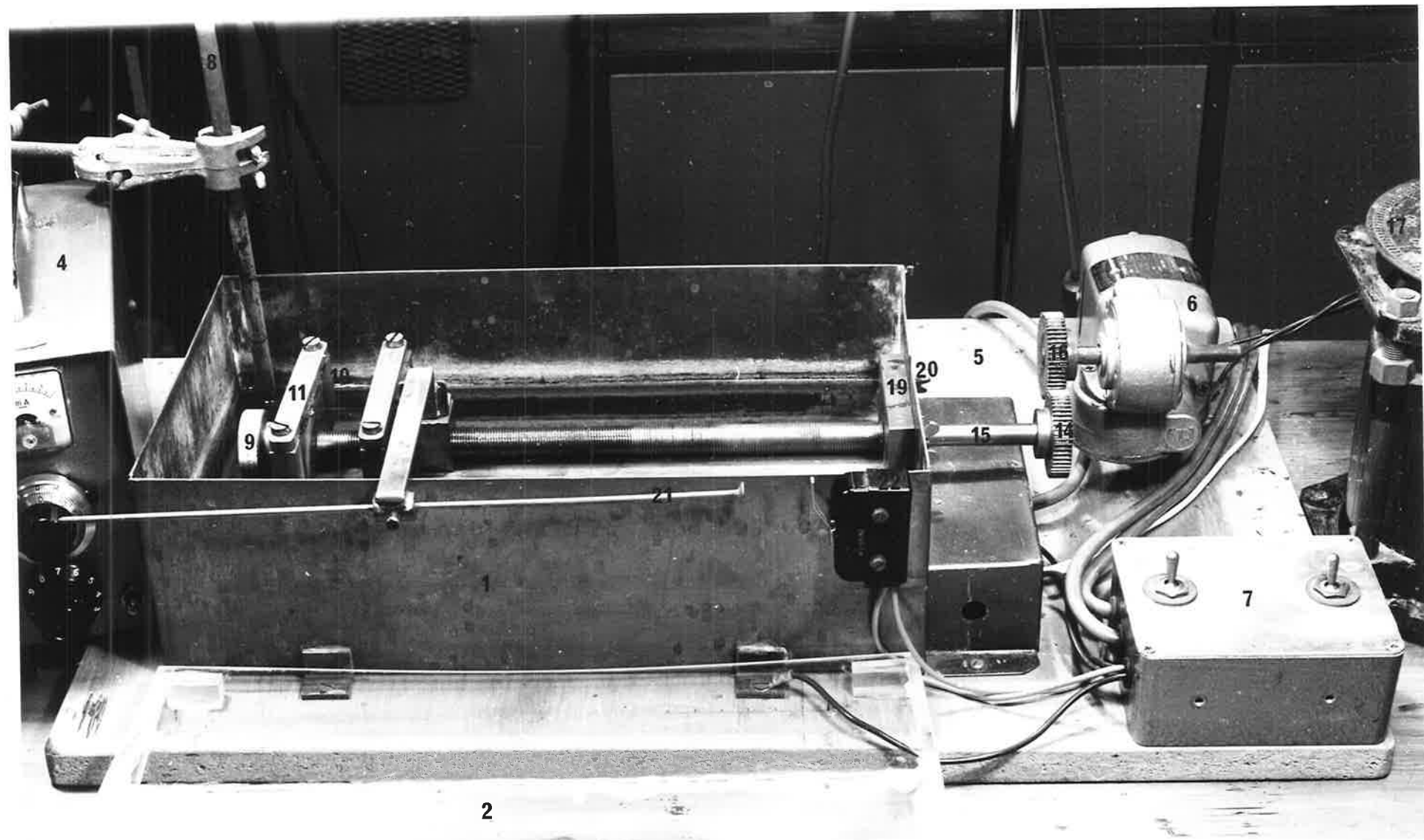
The mechanically driven stretcher (9) was developed from the manual stretcher originally reported elsewhere (Tsunoda and Yamaoka, 1965). One end of the film (10) was clamped by means of a brass plate (11) and gasket to the fixed arm (12) of the stretcher. The other end was similarly attached to the movable arm (13). The stretcher, with a spur gear (14) fastened to the protruding end of its screw thread (15), was placed in the water bath and slid into position such that its spur gear and a similar spur gear (16) fastened to the variable speed motor (SD-1SS Parvalux

Fig 4.1

The Stretching Device

Key to Figures

- | | |
|--------------------------------|--|
| 1. Brass water bath | 12. Fixed arm of stretcher |
| 2. V-shaped perspex lid | 13. Movable arm of stretcher |
| 3. Heating element (not shown) | 14. Spur Gear (connected to stretcher) |
| 4. Temperature regulator | 15. Protruding screw thread |
| 5. Wooden platform | 16. Spur Gear (connected to motor) |
| 6. Motor | 17. Variac (variable voltage supply) |
| 7. Control switch box | 18. Brass threads (not shown) |
| 8. Thermistor probe | 19. End face of stretcher |
| 9. Stretcher | 20. Wing nuts |
| 10. Film | 21. Metal rod |
| 11. Brass plate | 22. Micro-switch |



motor, A.C. series wound universal 230-250 Volt with double reduction gear box) meshed. The only requirement of the spur gears was to allow easy removal of the stretcher from the water bath. The speed of the motor was controlled by a Variac (17), a variable voltage supply. Two brass threads (18), connected to the end face (19) of the stretcher, passed through one side of the bath and with the aid of the two wing nuts (20) held the stretcher rigidly in place. A metal rod (21) which moved with the movable arm of the stretcher controlled the amount of stretch. The end of the rod was pre-set the required extension distance from the micro-switch (22) which when activated on the completion of the stretching process, automatically switched off the motor and heating element. A stretching rate of 15cm/hr. was found to be most suitable for the films.

4.4 Preparation of the Isotropic Films Required for the Preparative Method

4.4.1 PVA Films

A 5% solution of PVA (J.T. Baker Chemical Co., 99 - 100% hydrolysed, Baker Grade) was prepared in boiling 1:5 ethanol-water mixture. The cooled solution (25cc), free from air bubbles, was poured into a glass tray (base, 11cm x 9cm; height, 2cm) which was floated on a pool of mercury and left loosely covered in an air draught over three days. The resultant film was removed from the tray, and with edges trimmed, was cut into six approximately equal sections (4cm x 3cm). As these films had a tendency to curl, they were stored between filter papers under a light weight.

4.4.2 DNA Films

The DNA films were cast in perspex trays that were constructed from two pieces of perspex (9cm x 9cm x 1.3cm). Nine evenly spaced cylindrical holes (1.9cm diameter) were drilled through the top plate and both plates were cleaned prior to use by wiping with ethanol and rinsing with distilled water. The base plate was wiped unidirectionally with tissue paper to avoid possible scouring. These plates were held firmly together by four corner screws which passed through the top plate and which penetrated the base plate to a depth of 0.6cm. An appropriately shaped thin rubber gasket was placed between the plates to ensure a water tight seal. The very thin DNA films were formed from a DNA solution (0.25% DNA in 0.1mM EDTA) poured to a height of 3mm in each of the nine holes. The tray was floated on a pool of mercury inside a blackened desiccator. Phosphorus pentoxide was used as drying agent and was renewed daily until the films had formed. A period of three days was normally required. The fragile films were then removed from the dismantled tray, trimmed to 1.5cm diameter (an approximate circular shape) and stored away from the light.

4.4.3 DNA Film Cast on the PVA Film Surface

- A Cast DNA-PVA Film

A PVA film was swollen in distilled water and rolled flat with the aid of a glass rod on a glass plate (15cm x 8cm) which had two symmetrically placed glass handles useful for carrying purposes. The excess water was removed from, and the film corners were taped to, the glass plate. An area (2.5cm²) was outlined on the central portion of the film using a fine brush and hexane-wax solution. A

degassed DNA solution (0.5cc of a 0.12% DNA solution in 0.1mM EDTA) was poured onto, and then evenly distributed in, the marked area. The glass plate was placed on a bed of mercury, covered (but not air tight) to protect the PVA film with DNA solution from light and dust, and left overnight in an air draught. By the next day, a very thin DNA film had dried on the surface of the PVA film. With the size of the glass plate indicated here, two cast DNA-PVA films could be conveniently prepared at one time.

4.5 Preparation of the Anisotropic DNA Films

A Rotring rapidograph pen was used to mark two small dots (1.5cm apart) on the DNA film in the projected direction of orientation. The extension ratio was defined as the final distance between the dots divided by the initial distance. This ratio was considerably less than that obtained from the film's total dimensions, as the PVA outside that section covered by the DNA had a greater tendency to stretch.

4.5.1 From a Cast DNA-PVA Film

A cast DNA-PVA film, of the appropriate DNA thickness to record a suitable absorbance, was oriented by the mechanical stretching device to the required extension ratio.

4.5.2 From a Combined DNA-PVA Film

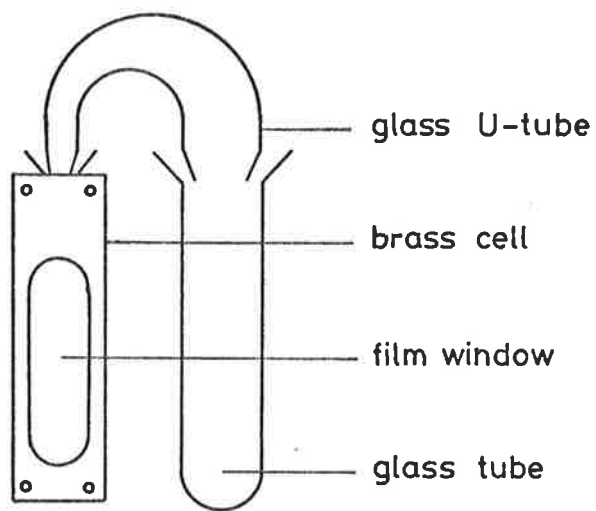
A PVA film that had been pre-swollen in distilled water and then air-dried was clamped in the mechanical stretcher. The stretcher was then placed in high relative humidity conditions for a few minutes until the PVA film became pliable. This play was taken up by a few turns of the stretcher's thread. The stretcher was quickly removed from the high relative humidity conditions and the very thin DNA

film was attached. This is most conveniently achieved by wrapping the DNA film (1.5cm diameter) around a teflon rod (diameter, 1.0cm; width, 2.5cm) and then carefully rolling it off the rod onto the moist PVA film, to which it will adhere under these conditions. The combined DNA-PVA film was oriented by the mechanical stretching device to the required extension ratio.

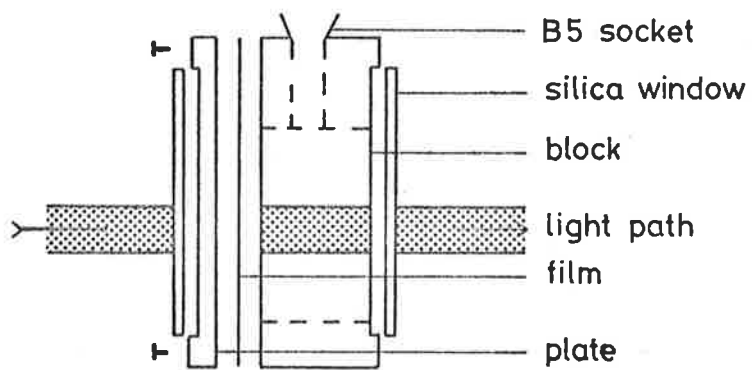
4.6 Mounting of the Anisotropic DNA-PVA Film for Spectroscopy

The film was mounted in the humidity cell (Fig.4.2) which was a modification of that previously described (Zdysiewicz, 1969), where for this design, the film and the silica windows did not touch. The dimensions of the humidity cell were such, that they allowed the humidity cell to fit conveniently into the holder of the Spectrophotometer and furthermore, allowed the incident light to pass centrally through the film for absorption spectroscopy (Chapter Three; Section 3.2.1 (b)).

The following mounting procedure was used. The stretcher was removed from the water bath and the film was immediately mounted in the humidity cell between its blackened brass block (4.3cm x 1.2cm x 1.5cm) and blackened brass plate (4.3cm x 1.2cm x 0.3cm) by four blackened countersunk screws. The film which had its direction of stretching aligned parallel to the 4.3cm side of the brass formed a window (15cm x 8cm, rounded edges) in the brass (6cm from the base, 2.5cm from each side) through which the light could pass (Fig.4.2, Side View). A thin gasket, cut to shape from black "Electrician's" tape, was used between



Front View



Side View

FIG 4.2 HUMIDITY CELL

the film and the plate. The silica windows which were countersunk into the outside sections of the block and plate were cemented in place with Apiezon grease. Next, the relative humidity inside the cell was maintained by a saturated salt solution contained in a small glass tube, connected via a glass U-tube, to a glass B5 socket araldited into the top of the block. All connections were made by quickfit joints. The saturated salt solutions used, together with their relative humidities at 20°C, are shown in Table 4.1; in addition, phosphorus pentoxide was used to obtain 0% relative humidity. Finally, the mounted films were stored away from light, in a blackened desiccator containing the appropriate saturated salt solution, until required for spectral measurements.

Table 4.1

Relative Humidity Control

Room Temperature = (20 ± 1)°C

Saturated Salt Solution	Percentage Relative Humidity	(Lange, 1961)
Potassium acetate	20	
Zinc nitrate	42	
Sodium bisulphate	52	
Sodium bromide	58	
Magnesium acetate	65	
Sodium chloride	76	
Potassium chromate	88	
Sodium sulphate	93	

4.7 Comparison of the Two DNA-PVA Film Preparations

The cast DNA-PVA film was easier to handle than the combined DNA-PVA film (due to the fragile nature of the very thin pure DNA film in the preparation). Furthermore, as a reasonable absorbance for the combined film was much more difficult to obtain (the DNA absorbance is proportional to the thickness of the DNA film), the properties of the DNA were investigated solely from cast DNA-PVA films. However, this presented the problem of checking for possible DNA-PVA interaction in the cast DNA-PVA film because DNA and PVA have been found to interact in mixed DNA-PVA films (Kurucsev and Zdysiewicz, 1971). Thus, the properties of the cast DNA-PVA film were compared with those of the combined DNA-PVA film where the interaction of the DNA with the PVA would be expected to be negligible, for it is restricted to their interface.

The isotropic absorption spectra for a cast DNA-PVA film and that for a combined DNA-PVA film are shown at 0% and 93% relative humidity in Fig.4.3. The relative humidity was attained in each case after a 24 hour equilibration period. There are no apparent differences in the shapes of the absorption spectra for the portions that may be compared. Likewise, the percentage hyperchromicity, also shown for both films in the figure, did not reveal any differences in the region where the absorbance of the combined DNA-PVA film could be measured accurately. Finally, the parallel and perpendicular polarised absorption spectra and the dichroic spectra at 93% relative humidity are recorded in Fig.4.4 for the two DNA-PVA film preparations stretched to the same extension ratio. Here again, the film preparations have

filled symbols – combined DNA-PVA film
 open symbols – cast DNA-PVA film
 ■, □ A(93% r.h.)
 ▲, △ A(0% r.h.)

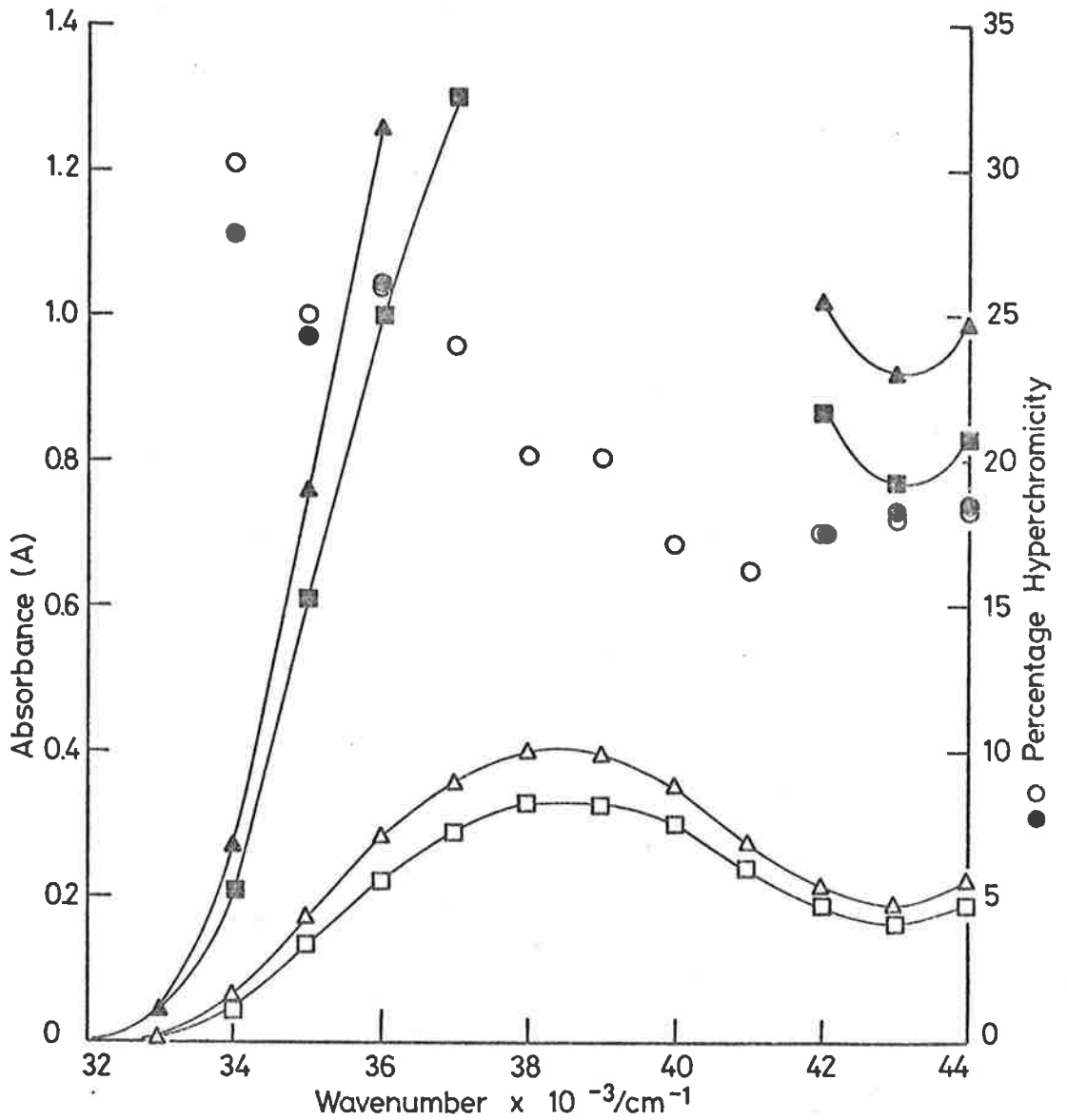


FIG 4.3 ISOTROPIC ABSORPTION SPECTRA AND PERCENTAGE HYPERCHROMICITY FOR THE TWO DNA-PVA FILM PREPARATIONS

filled symbols — combined DNA-PVA film
 open symbols — cast DNA-PVA film
 Δ, \triangle A (with parallel polarised light)
 \bullet, \circ A (with perpendicular polarised light)

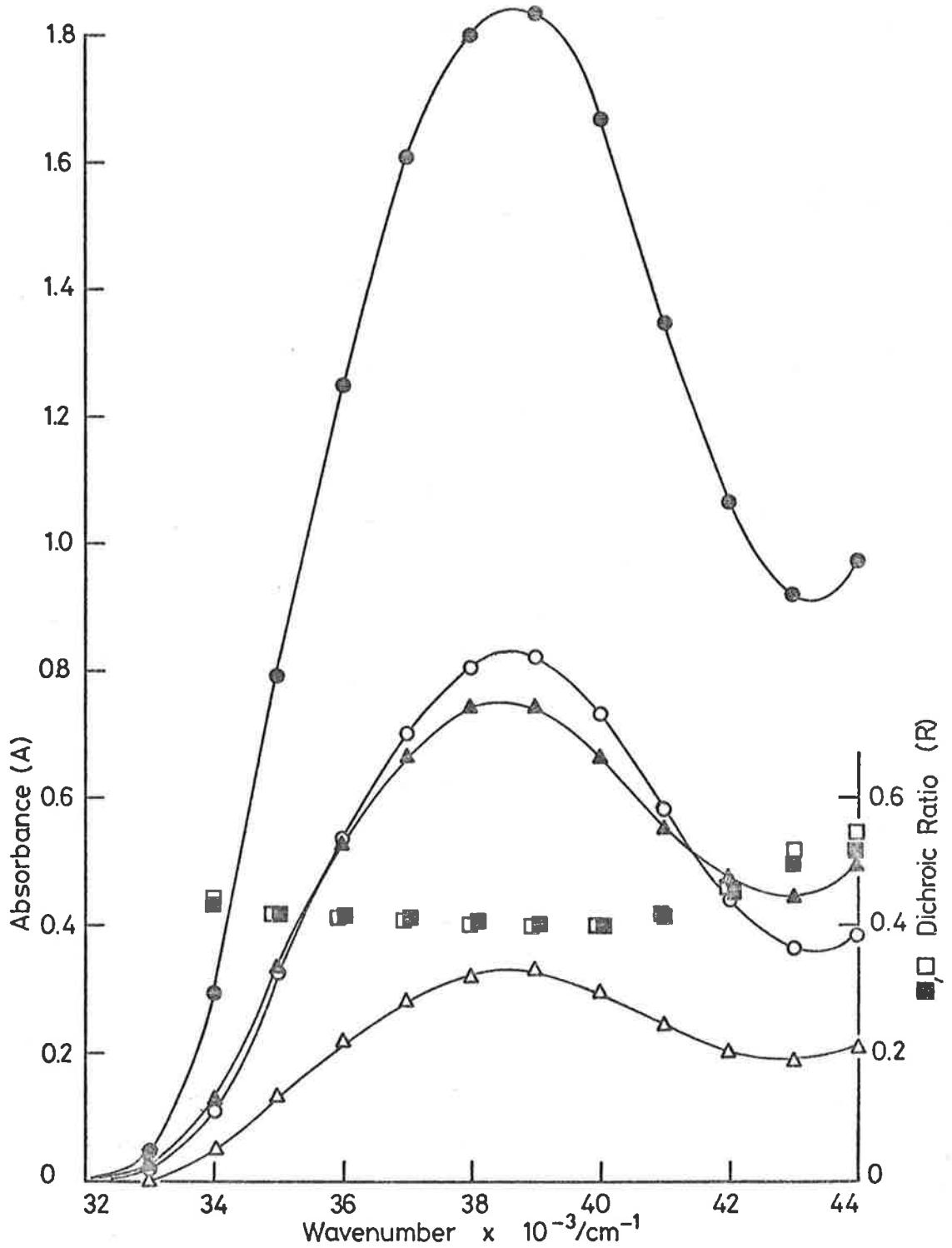


FIG 4.4 POLARISED ABSORPTION AND DICHOIC SPECTRA AT 93% RELATIVE HUMIDITY FOR THE TWO DNA-PVA FILM PREPARATIONS WITH THE SAME EXTENSION RATIO

similar behaviour. Their dichroic ratios are identical and the shapes of their polarised absorption spectra are alike for the same degree of DNA orientation. Therefore, it appears most likely that the DNA in the cast DNA-PVA film has not interacted with the PVA and so has not penetrated the PVA surface to any measurable extent.

4.8 Relative Humidity Equilibration Time

The variation of the dichroic ratio with equilibration time at 93% relative humidity is shown in Fig.4.5 for a cast DNA-PVA film at the maximum DNA absorptivity ($38,600\text{cm}^{-1}$). Zero time was taken immediately the newly oriented film was placed in the atmosphere of 93% relative humidity. A time of 15 hours was sufficient for the film to attain a constant dichroic ratio. For the melting profiles of DNA (Section, 4.9), measured over a range of relative humidities, it was convenient to take two measurements per day at twelve hourly intervals. This was considered to be sufficient equilibration time since the change in the relative humidity from one reading to the next was small. In any case, the dichroic ratio after this time was within the experimental reproducibility from film to film.

4.9 Properties of the Cast DNA-PVA Film

The properties of the DNA film preparations were found to be independent of the salt content (up to an extra 8% weight NaCl to dry weight DNA was added to some of the initial DNA film samples) for both the Calf Thymus and the Herring Sperm DNA used throughout this work. Therefore, as the salt content of the films was above the minimum requirement

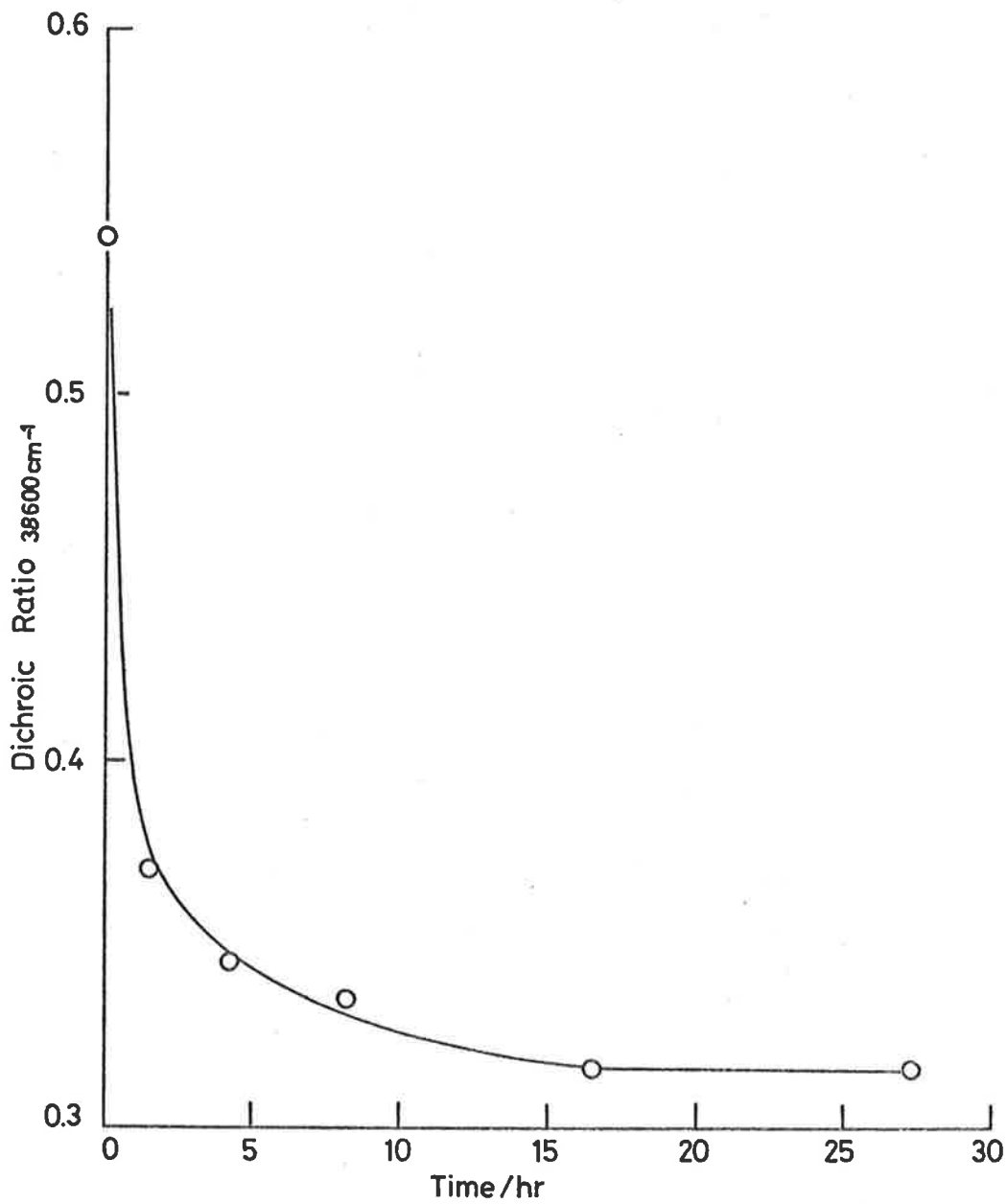


FIG 4.5 EFFECT OF RELATIVE HUMIDITY EQUILIBRATION TIME AT 93% R.H. ON THE DICHROIC RATIO OF A CAST DNA-PVA FILM MEASURED AT DNA MAXIMUM ABSORPTIVITY

(without any addition) to maintain the DNA in its native B configuration at 93% relative humidity (refer to relevant portion of Chapter One, Section 1.3), it was not added to the DNA film samples presented here, nor to the dye/DNA film samples presented in the following chapters.

4.9.1 Absorption and Dichroic Spectra

Typical absorption and dichroic spectra for the Calf Thymus DNA film, prepared by the cast DNA-PVA film method, are presented for the native structure (high, 93% relative humidity) in Fig.4.6(a) and for the denatured structure (low, 20% relative humidity) in Fig.4.6(b). Next, the absorption spectra are compared with those obtained from two other differently prepared Calf Thymus DNA film samples in Table 4.2. The shapes of the absorption spectra for the native and denatured structures, as indicated by the wavenumber positions of the maximum, minimum and shoulder, were the same for the three samples within the experimental accuracy.

The ratio of maximum to minimum absorbance is listed for the three DNA film preparations at the two relative humidities in Table 4.3. The highest ratio was found for this work. The difference is most likely due to a light scattering contribution to the absorbance in the other two film preparations where no light scattering corrections were made. The necessity for such a correction for this work has been eliminated (Chapter 3, Section 3.4.1). In the case of the mixed DNA-PVA film, the much lower ratio might also be the result of interaction between the DNA and the PVA. This ratio is furthermore a measure of the DNA purity, but it seems unlikely that the difference could be attributed to this

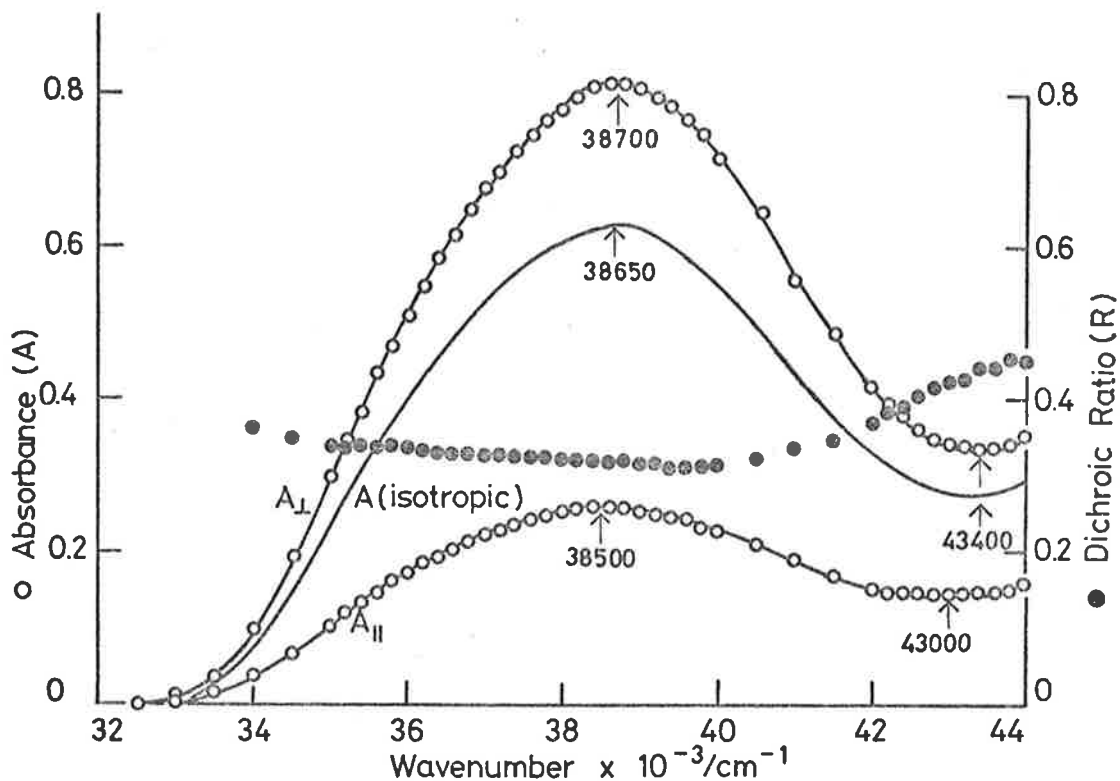


FIG 4.6a ABSORPTION AND DICHROIC SPECTRA AT 93% RELATIVE HUMIDITY FOR THE CALF THYMUS DNA FILM PREPARED BY THE CAST DNA-PVA FILM METHOD

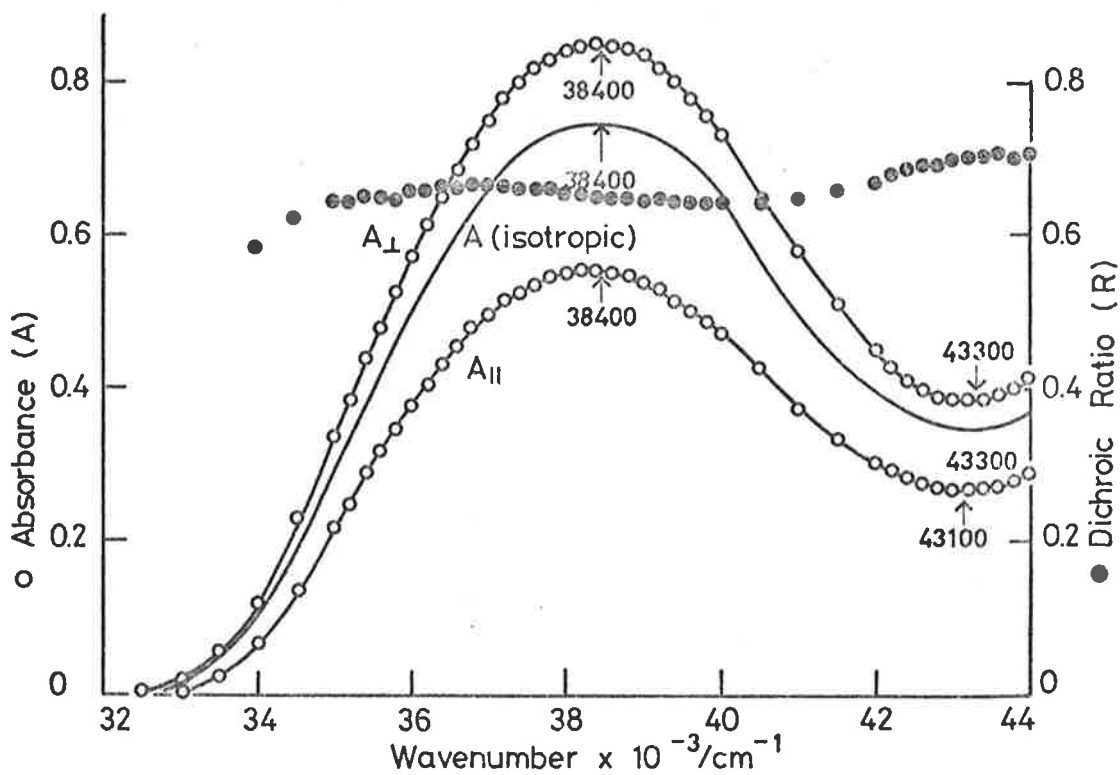


FIG 4.6b ABSORPTION AND DICHROIC SPECTRA AT 20% RELATIVE HUMIDITY FOR THE CALF THYMUS DNA FILM PREPARED BY THE CAST DNA-PVA FILM METHOD

Table 4.2

Absorption Spectra of Three Differently Prepared Calf Thymus DNA Film Samples

Film Type	Relative Humidity	$\bar{\nu}_{\max} \text{cm}^{-1}$	$\bar{\nu}_{\min} \text{cm}^{-1}$	$\bar{\nu}_{\text{sh}} \text{cm}^{-1}$	Reference
cast DNA-PVA	93%	38,650 ± 50	43,400 ± 100	35,600 ± 300	this work
pure DNA	93%	38,630 ± 30	43,290 ± 90	35,500 ± 300	Falk, 1964
mixed DNA-PVA	93%	38,620 ± 50	43,420 ± 100	35,800 ± 110	Zdysiewicz, 1969
cast DNA-PVA	20%	38,400 ± 50	43,300 ± 100	35,500 ± 300	this work
pure DNA	0%	38,390 ± 30	43,290 ± 90	35,500 ± 300	Falk, 1964
mixed DNA-PVA	0%	38,400 ± 50	43,370 ± 70	35,800 ± 140	Zdysiewicz, 1969

$\bar{\nu}_{\max}$ = wavenumber at maximum absorption

$\bar{\nu}_{\min}$ = wavenumber at minimum absorption

$\bar{\nu}_{\text{sh}}$ = wavenumber at point of inflection of shoulder

Table 4.3
Ratio of Maximum to Minimum Absorbance for Three
Differently Prepared DNA Films

Film Type	A_{\max}/A_{\min} 93% r.h.	A_{\max}/A_{\min} 0 or 20% r.h.	Reference
cast DNA-PVA	2.3	2.2	this work
pure DNA	2.1	2.1	Falk, 1964
mixed DNA-PVA	1.8 ₅	2.0 ₅	Zdysiewicz, 1969

factor.

At high relative humidity, the dichroic spectrum for the cast DNA-PVA film consisted of a plateau region extending from $36,000\text{cm}^{-1}$ to $40,000\text{cm}^{-1}$. At greater and lower wavenumbers the dichroic ratio increased. A similar spectrum was obtained at low relative humidity, with the exception that the dichroic ratio decreased on the low wavenumber side of the plateau region. The shapes of the dichroic spectra are in agreement with those for T2 and T5 bacteriophage DNA at both high and low relative humidities (Gray and Rubenstein, 1968) and for Calf Thymus DNA at high relative humidity (Zdysiewicz, 1969).

4.9.2 Hyperchromicity and Dichroic Ratio as a Function of the Relative Humidity

The similarity of the spectral changes which occur in the dehydration denaturation of a solid DNA film and the heat denaturation of a DNA solution has shown that both

processes involve loss of base-stacking to about the same extent. This was demonstrated for Calf Thymus DNA where the hyperchromicities for both processes were found to be very similar (Falk, 1964; Wetzel et al, 1969). Similarly, it would be expected that the 37% hyperchromicity measured for the heat denaturation of a Calf Thymus DNA solution in 0.1M NaCl, should compare to that obtained for the dehydration denaturation of a cast Calf Thymus DNA-PVA film at the maximum DNA absorptivity ($38,600\text{cm}^{-1}$). This was not so, as a consistent hyperchromicity of 20% was found for many such films. Thus, if the DNA does not interact with the PVA and if it is native at 93% relative humidity and denatured at low (0% or 20%) relative humidity, then the question arises why the amount of hyperchromicity does not conform to expectation. In order to answer this question, the hyperchromicity and dichroic ratio were investigated as a function of the relative humidity at the maximum DNA absorptivity ($38,600\text{cm}^{-1}$).

The hydration-dehydration cycle is shown in Fig.4.7 for a cast Calf Thymus DNA-PVA film which was equilibrated at 93% relative humidity immediately after stretching and mounting. The relative humidity was decreased to 0% and finally returned to 93%, with the process taking eight days to complete. The DNA in this time had shown complete reversibility to the original values of absorbance and dichroic ratio.

The variation of the isotropic absorbance, A , where $A = (A_{11} + 2A_{\perp})/3$ (Fraser, 1960) is shown as a function of the relative humidity in Fig.4.7(a). A similar variation of the dichroic ratio as a function of relative humidity is

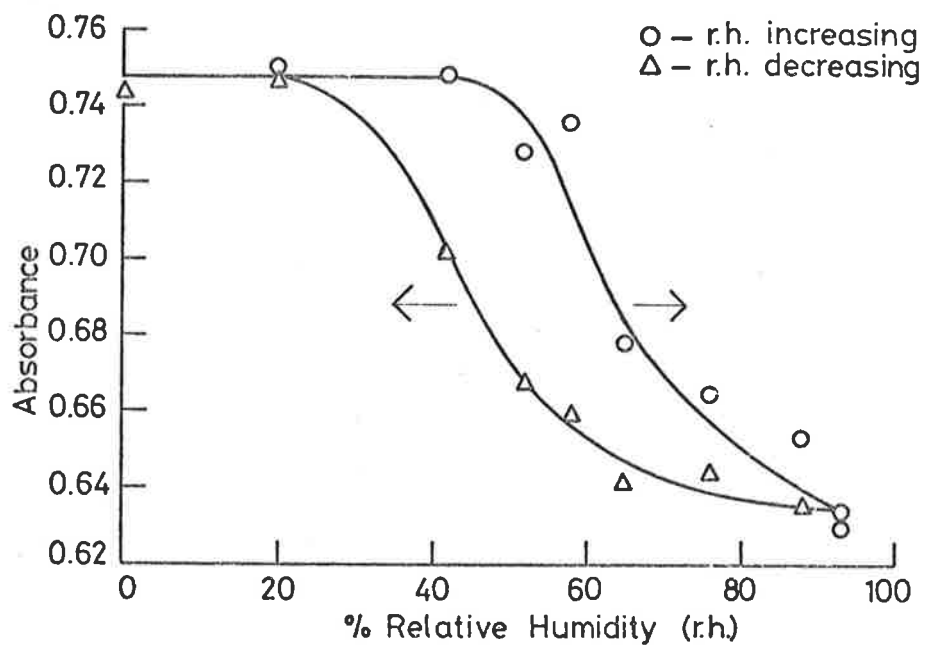


FIG 4.7a THE HYDRATION-DEHYDRATION CYCLE: ABSORBANCE AT $38,600\text{cm}^{-1}$ FOR A CAST CALF THYMUS DNA-PVA FILM

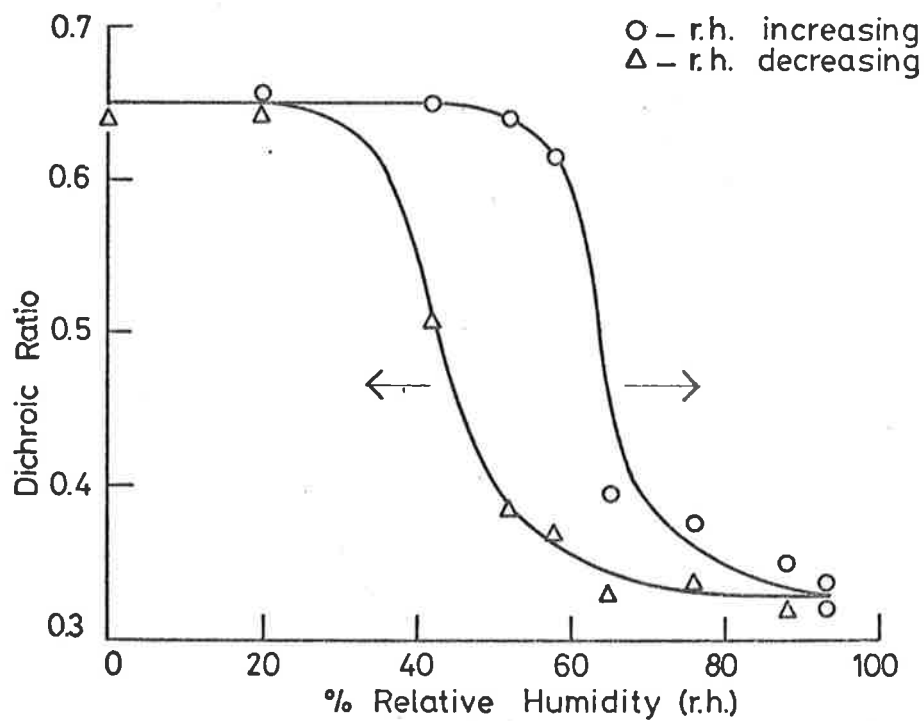


FIG 4.7b THE HYDRATION-DEHYDRATION CYCLE: DICHOIC RATIO AT $38,600\text{cm}^{-1}$ FOR A CAST CALF THYMUS DNA-PVA FILM

shown in Fig.4.7(b). Two plateau regions were observed; one below 50%, the other above 75% relative humidity. Between these relative humidities, a sharp transition region was observed. This was accompanied by hysteresis. The transition, the range over which it occurred and the noted hysteresis are in agreement with earlier reported work on pure Calf Thymus DNA films (Falk et al, 1962; Falk et al, 1963b). In the case of the mixed DNA-PVA films, however, the relative humidity range over which this transition occurred has been broadened and lowered relative to both pure DNA and cast DNA-PVA films (Kurucsev and Zdysiewicz, 1971). When the relative humidity was decreased, the transition was not observed until 0% relative humidity was attained (Zdysiewicz, 1969). In the case of the mixed DNA-PVA films, this was taken to be good evidence for the interaction of the DNA with the PVA. Conversely, the sharpness of the transition, the relative humidity range over which it occurred and the noted hysteresis are taken to indicate that the DNA in the cast DNA-PVA film is native at 93% relative humidity and is denatured at low relative humidity. It is thus concluded that "full" hyperchromicity is not a necessary criterion for the complete "melting" of DNA in films. It is relevant in this context that with T2 and T5 Bacteriophage DNA, a comparable hyperchromicity between the heat denatured solution and the dehydrated denatured film was not found (Gray and Rubenstein, 1968).

One may conjecture that the lack of observed hyperchromicity may be accounted for as follows. When a PVA film absorbs moisture it expands while oriented DNA fibres shorten at the same time. This size change is quite marked

and may be seen as a macroscopic effect to the naked eye for both types of films. Thus, when the two films are joined through a common surface two opposing forces appear during any change in the relative humidity and although the originally mounted film is flat, with a change in the relative humidity (either an increase or a decrease), lengthwise corrugations appear. These corrugations do not affect the amount of scattering and produce only slight alterations in the baseline reflection correction. At the same time, however, as a result of the corrugations, the same portion or cross-sectional area of DNA may not be in the light path of the spectrophotometer at different relative humidities. Moreover, the contraction of the DNA at high relative humidity could affect the amount or thickness of DNA viewed by the spectrophotometer relative to low relative humidity. Either of these two effects, corrugations and DNA volume changes may affect significantly the comparison of absorbance measurements obtained at high and low relative humidities (the hyperchromicity). The latter effect may also invalidate a comparison of the dichroic ratios at different relative humidities since it may change the degree of orientation in the film.

4.9.3 Dichroic Ratio as a Function of Extension Ratio

The dichroic ratio, at the maximum DNA absorptivity ($38,600\text{cm}^{-1}$), is shown in Fig.4.8 as a function of the extension ratio for two different film samples of DNA, prepared by the cast DNA-PVA film method. Calf Thymus DNA showed a slightly greater tendency to orient than Herring Sperm DNA. For a particular extension ratio, both DNA film samples exhibited dichroic ratios that were reproducible

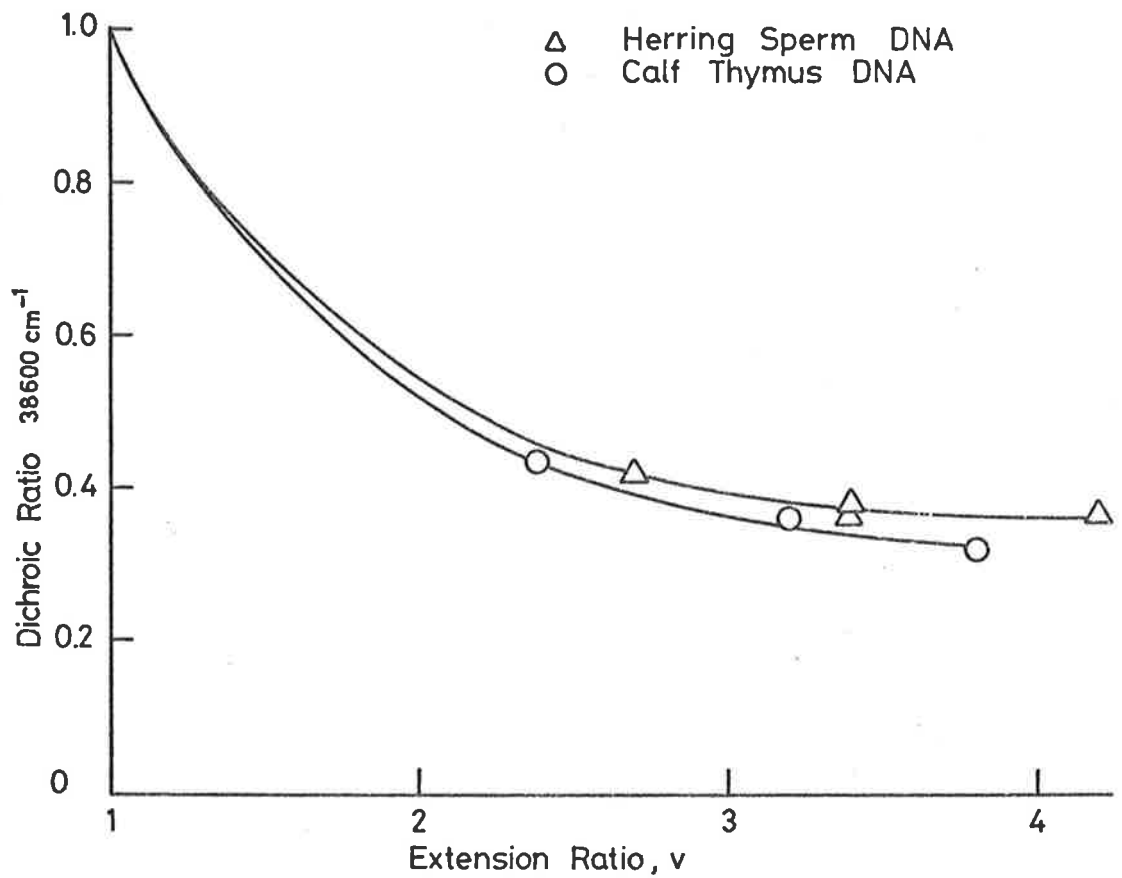


FIG 4.8 THE EFFECT OF EXTENSION RATIO ON THE DICHOIC RATIO OF CAST DNA-PVA FILMS MEASURED AT DNA MAXIMUM ABSORPTIVITY AT 93% RELATIVE HUMIDITY

to ± 0.02 units.

4.10 Conclusion

The absorption and dichroic spectra are characteristic of the DNA native structure at high (93%) relative humidity and of the denatured structure at low (0 or 20%) relative humidity. However, the mechanical properties of the films are altered by the type of interaction of the PVA with the DNA in the cast DNA-PVA film that is physical rather than chemical. The properties so affected cause interference with the magnitude of the changes in absorbance (hyperchromicity) and dichroic ratio with relative humidity that are characteristic of the structural changes in DNA with relative humidity. Thus, for example, a pure DNA film stretched 1.8 times its original length exhibited a dichroic ratio of 0.45 (Kurucsev and Zdysiewicz, 1971) while for an equivalent extension ratio, a dichroic ratio of 0.6 was obtained for the cast DNA-PVA films (see Fig.4.8); thus providing evidence that the PVA support has physically interacted with the DNA by hindering its alignment. Finally, the experimentally uniform low dichroic ratios obtained for cast DNA-PVA films with equivalent extension ratios has shown that this method, indeed, produces reproducible highly oriented DNA film samples; the "physical" interactions between DNA and PVA do not prevent either the high extent or reproducibility of DNA orientation.

CHAPTER FIVE

PREPARATION AND PROPERTIES OF ANISOTROPIC DYE/DNA FILMS

5.1 The Preparation in Principle

An anisotropic dye/DNA film and an anisotropic DNA film are prepared independently but with the same extension ratio, by the orientation of the respective isotropic film on the surface of a PVA film. The fraction of oriented DNA chains in both samples are subsequently assumed to be the same and may be evaluated from the dichroism of the DNA film by the method of Fraser (1960), with the assumption that the purine and pyrimidine bases are perpendicular to the helix axis in the uncomplexed native DNA B form at high relative humidity (Chapter One, Section 1.3).

5.2 The Initial Preparative Method

Although it is an advantage to use cast DNA-PVA films in preference to combined DNA-PVA films for the investigation of the properties of the anisotropic DNA films, this is not necessarily so when the properties of the anisotropic dye/DNA films are studied. For the latter case, a low dye to DNA phosphate ratio, D/P, is required (Chapter One, Section 1.3) and this implies that a greater amount of DNA is needed to constitute a film of measurable dye absorbance. The excessive DNA absorbance thus produced in the ultra-violet region is of no consequence, since it is the dye spectrum (visible and near ultra-violet) that is of interest. Thus, isotropic dye/DNA films could be prepared

of a thickness that enabled them to be easily handled and convenient to use, as in the preparation of anisotropic dye/DNA films by the combined DNA-PVA film method (Chapter Four, Section 4.5.2). Furthermore, this method of orientation was preferred to the cast DNA-PVA film method because it was felt, that the long drying period (at least 24 hours) of the dye/DNA solution on the PVA surface in the latter method, would enable an appreciable quantity of the dye to diffuse into the PVA matrix.

5.2.1 Preparation of the Isotropic Dye/DNA Films

The dye/DNA solutions, from which the isotropic dye/DNA films were cast, were prepared by the gradual addition of the dye solution (5cc) (appropriate concentrations listed in Table 5.1) to the 1% DNA solution (15cc) (Chapter Two, Section 2.2.1) with constant stirring. The slow addition of the dye solution with constant stirring eliminated the possibility of DNA precipitation and produced an homogeneous dye/DNA solution. The construction of the perspex tray and the method of preparation of the films are described in Chapter Four, Section 4.4.2. For the dye/DNA films, each hole in the perspex tray was completely filled with the dye/DNA solution. The films took approximately one week to form and measured $(3.5 \pm 0.5) \times 10^{-4}$ cm in thickness.

5.2.2 Preparation of the Anisotropic Dye/DNA Film

The anisotropic dye/DNA film was prepared by the combined DNA-PVA film method outlined in Chapter Four, Section 4.5.2, with one exception. The dye/DNA film was attached to the PVA film by supporting it at one edge with the aid of a pair of pliers so that its opposite edge touched the PVA film surface. It was then progressively adhered to

Table 5.1Concentration of the Aqueous Dye Solutions

The dyes were dissolved in water with no added buffer,
pH = 5.0 ± 0.3

Dye	Approximate Concentration (g/100cc)	D/P
Proflavine	0.007	0.002 - 0.003
Acriflavine	0.006	0.002 - 0.003
9-Aminoacridine	0.018	0.004 - 0.008
Paranitroaniline reporter	0.027	0.007
Orthonitroaniline reporter	0.070	0.018 - 0.019
2,4-Dinitroaniline reporter	0.030	0.007 - 0.010
4-Nitro-1-naphthylamine reporter	0.030	0.007

the PVA film by removing the support and by rolling flat with a small teflon rod.

5.2.3 Dye Penetration into the PVA matrix

The study of dye penetration into the PVA matrix has been based on the optical properties of the acridine dye, proflavine. The shape of the monomer spectrum of the dye in both PVA and DNA is similar, with only a slight red shift in PVA relative to DNA for dried films (Strauss et al, 1971). Further, there are minimal changes between the absorption spectra of the dye/DNA film at low and high relative

humidity (Neville and Davies, 1966). Therefore, little if any observable change to the isotropic absorption spectrum of the dye in the combined dye/DNA-PVA film would be expected to arise from dye penetration into the PVA matrix.

In an oriented polymer film, it may be assumed that the major axis of the (dye) molecule aligns parallel to the direction of stretching (Dorr, 1966). For proflavine, the transition moment direction of the first absorption band is polarised parallel to the major (z molecular) axis (Wittwer and Zanker, 1959; Zanker and Thies, 1962; also refer to Chapter Two, Section 2.5) and so, it is not unexpected that proflavine exhibits a dichroic ratio much greater than one in the oriented PVA film (Figure 5.1). However, in the DNA film, the major axis of the proflavine molecule must lie in, or be at a small angle to, the plane normal to the helix axis (approximately perpendicular to the direction of stretching) since a dichroic ratio of 0.32 has been reported for an oriented wet spun proflavine/DNA film at its maximum absorption (Rupprecht et al, 1969). The large difference between the linear dichroism of the dye in the two anisotropic films may therefore be used to determine the amount of dye penetration.

For any partially oriented sample, the dichroic ratio, R , fixes the angle, ω , which is defined as the angle between the transition moment vector of the dye and the orientation axis:

- (i) for a positive dichroism where $R > 1$, $0^\circ \leq \omega < 55^\circ$ and
- (ii) for a negative dichroism where $R < 1$, $55^\circ < \omega \leq 90^\circ$

(Fraser, 1960).

○ Δ Proflavine / PVA Film ($\nu = 3.6$)
 ● Combined Proflavine / DNA - PVA Film

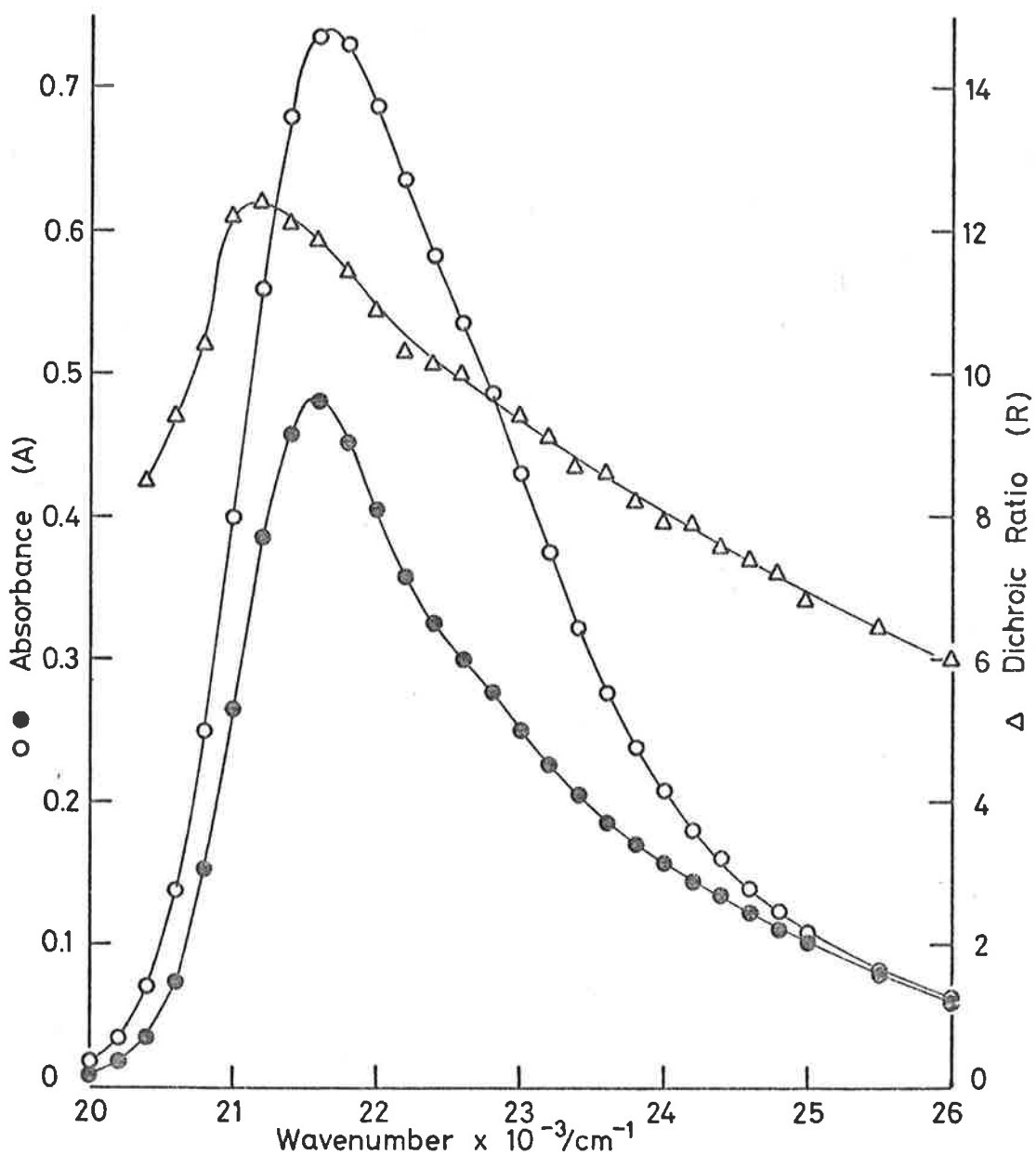


FIG 5.1 ISOTROPIC ABSORPTION SPECTRA OF PROFLAVINE/PVA AND PROFLAVINE/DNA FILMS AND DICHROIC SPECTRUM OF PROFLAVINE/PVA FILM

Thus, for any two partially oriented film samples, a change in the dichroic ratio at a fixed wavelength from less than to greater than one (or visa versa) indicates a contribution to the dichroic ratio from at least two orientations of the dye molecule. This effect was observed for the combined proflavine/DNA-PVA films, and so suggested that the dye had penetrated into the PVA matrix.

5.3 The Preparative Method

In an attempt to eliminate dye penetration into the polymer support, the initial method was modified by placing a layer of DNA between the PVA film and the dye/DNA film. The intermediate DNA layer was cast on the PVA film surface (Chapter Four, Section 4.4.3) and the thickness of the layer was varied by altering the volume and concentration of the DNA solution spread in the outlined area. The DNA solutions varied in concentration from 0.12% to 1.0% and the volumes applied varied from 0.4cc to 1.5cc. It was necessary to use viscous DNA solutions in the preparation of the intermediate DNA layer, especially when large volumes were applied in the outlined area. The thickness of the DNA layer was not measured directly on the PVA film surface but was determined indirectly as the thickness parameter, the product of the volume and the concentration of the DNA solution used. The cast DNA-PVA film was subsequently treated in the same manner as the PVA film was treated in the Initial Preparative Method.

5.3.1 The Elimination of Dye Penetration into the PVA Matrix

The effect of the thickness of the DNA layer on the

extent of dye penetration into the PVA film has been evaluated by examining the measured parallel and perpendicular polarised absorption spectra and the wavenumber where the dichroic ratio changes from less than to greater than one. The parallel and perpendicular polarised absorption spectra are shown in Fig.5.2, for two combined proflavine/DNA-PVA films; one with a DNA thickness parameter of 0.3 (0.4cc of 0.75% DNA solution), the other with a DNA thickness parameter of 1.5 (1.5cc of 1.0% DNA solution). Although the shapes of the perpendicular polarised absorption spectra for the two samples are very similar, their parallel polarised spectra are not. It is apparent therefore, that the high wavenumber side of the anisotropic absorption band is sensitive to, and so can be used as a measure of, dye penetration. Likewise the dichroic spectrum is sensitive to dye penetration, with a change being the direct result of a change to the parallel absorption component.

It was found most convenient to describe the amount of dye penetration in terms of a related quantity, namely, the wavenumber where the dichroic ratio changes from less than to greater than one (a dichroic ratio of one is invariant to the amount of sample alignment). Thus, an increasing red-shift for this measured wavenumber would indicate a greater proportion of the dye in the PVA matrix. The effect of the thickness parameter of the intermediate DNA layer on the wavenumber where the dichroic ratio changes from less than to greater than one for a series of proflavine/DNA-PVA films is shown in Fig.5.3. The degree of alignment of the samples represented in the figure may not necessarily be the same. At zero dye penetration, such a

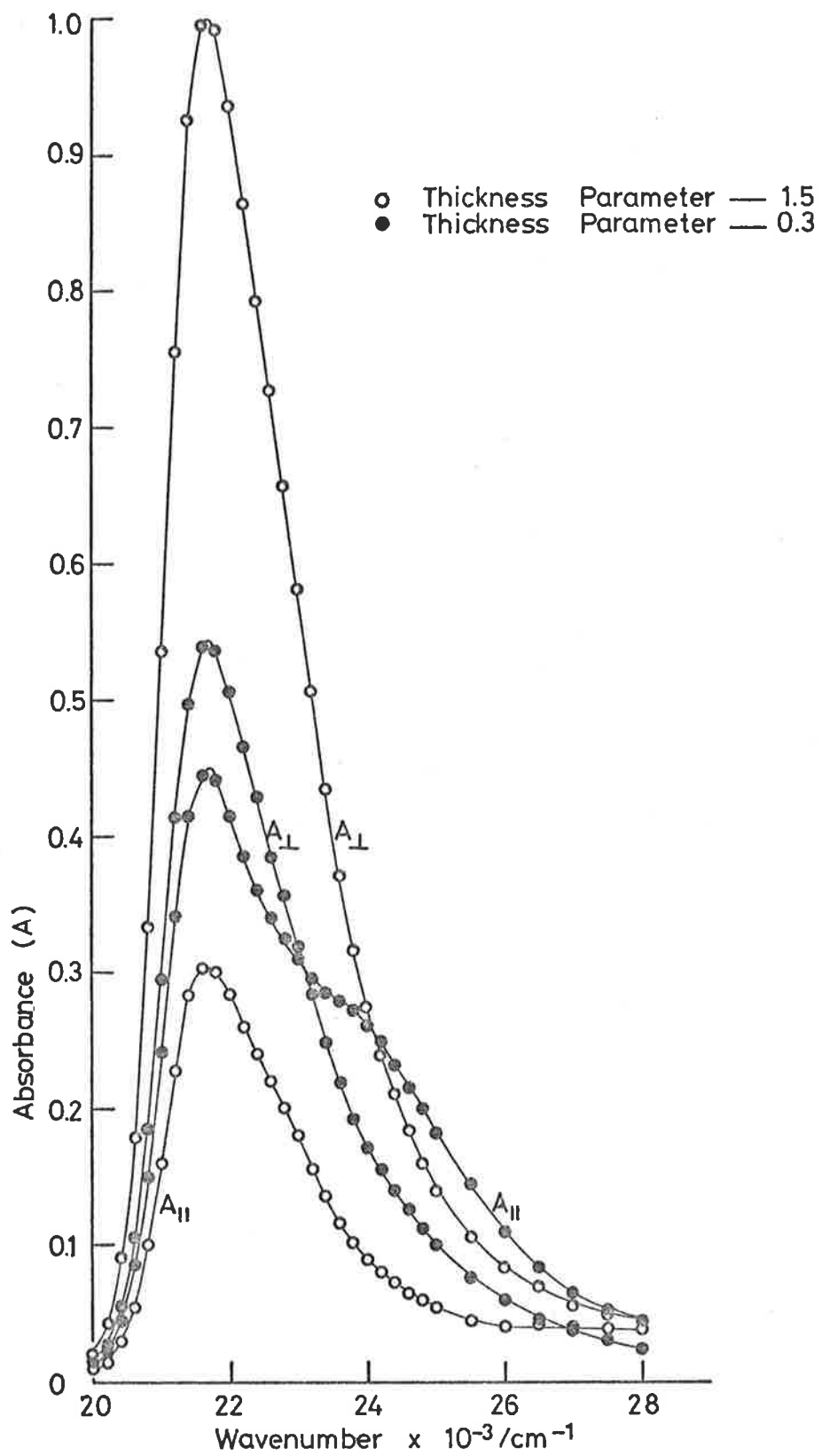


FIG 5.2 POLARISED ABSORPTION SPECTRA OF TWO COMBINED PROFLAVINE/DNA-PVA FILMS WITH DIFFERENT DNA THICKNESS PARAMETERS

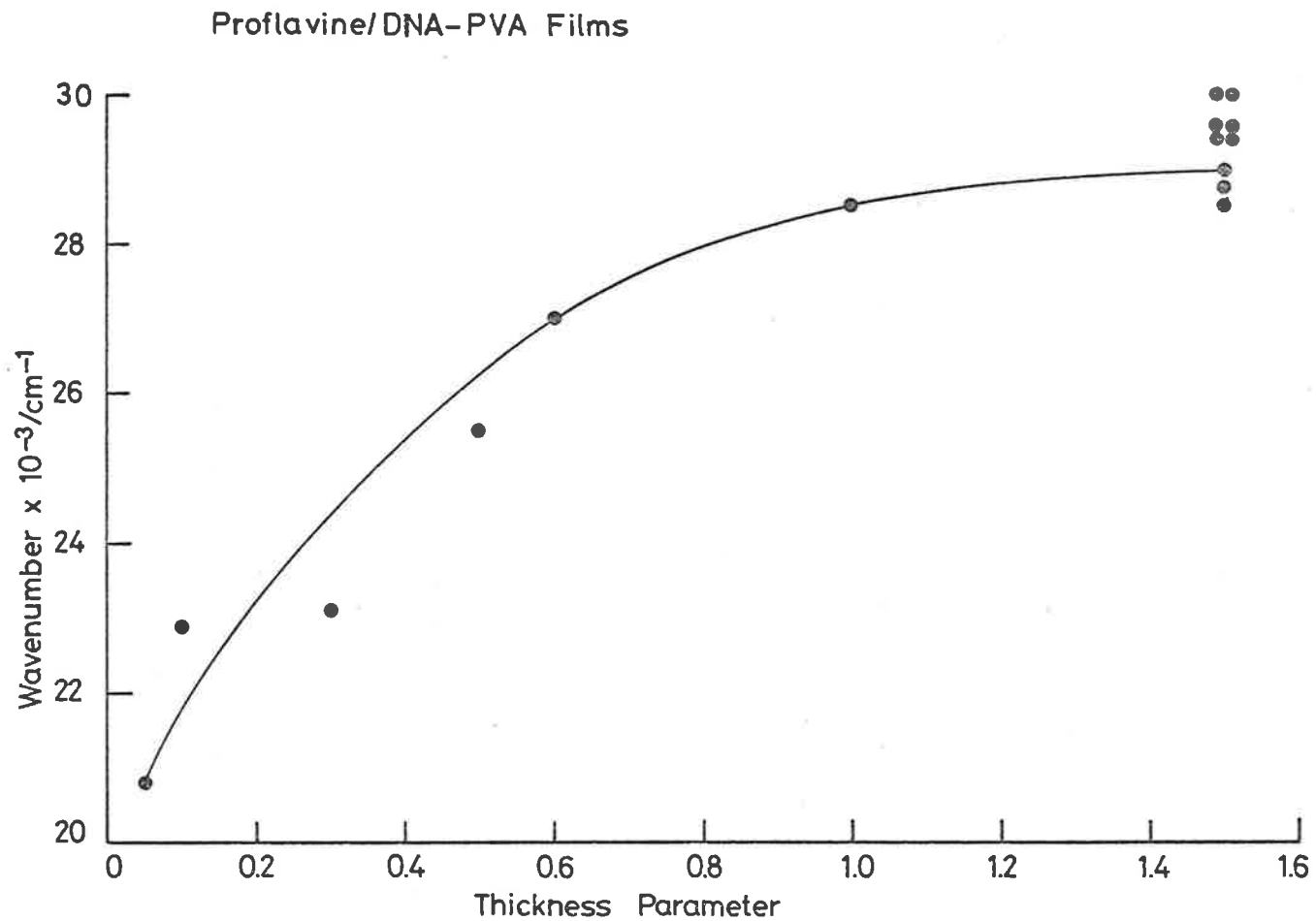


FIG 5.3 THE EFFECT OF THE THICKNESS PARAMETER OF THE INTERMEDIATE DNA LAYER ON THE WAVENUMBER WHERE THE DICHOIC RATIO CHANGES FROM LESS THAN ONE TO GREATER THAN ONE

plot assumes that there is a wavenumber where the dichroic ratio of the dye in the DNA is unity. The experimental results indicate that this may not necessarily be so at the greatest thickness parameter of the intermediate DNA layer employed, since such a wavenumber would occur where the dye absorptivity was comparatively very low and the difference therefore, between the parallel and perpendicular absorption components, would be reduced to the precision of the measurement. In some cases therefore, the wavenumber at which the dichroic ratio made its closest approach to unity has been used. Similarly, the plotted wavenumber at which the dichroic ratio changes from less than to greater than one, measured at wavenumbers greater than $28,000\text{cm}^{-1}$ was subject to experimental error, so that any wavenumber up to $31,000\text{cm}^{-1}$ was equally likely. Thus, Fig.5.3 indicates that a DNA thickness parameter of one (1cc of a 1.0% DNA solution) is required to eliminate dye penetration. For all further preparative film work, 1.5cc of a 1.0% DNA solution was used to prepare the intermediate DNA layer as an added precaution against possible dye penetration. Throughout the preparative work, the high molecular weight Calf Thymus DNA preparation was used in preference to the "highly polymerised" Herring Sperm DNA preparation for the casting of the intermediate DNA layer because of the much greater viscosity of the 1% solution. Conversely, it was more convenient to use the less viscous 1% Herring Sperm DNA solution in the preparation of the isotropic dye/DNA films.

The practice of combining two different sources of DNA in the one film was not intended. The Herring Sperm DNA was originally supplied as Calf Thymus DNA and it was not

until six months after the initial "Calf Thymus" DNA sample had been received (the work being well under way), that notification of the error was received from the Sigma Chemical Co. It would be expected that little if any alteration to the properties of the dye/DNA-PVA films would result, since the GC content for both Herring Sperm DNA and Calf Thymus DNA are almost identical at 45% and 43% respectively (Mahler and Cordes, 1966). This indeed was found to be so for the properties of the two 4-nitro-1-naphthylamine reporter/DNA-PVA films prepared (see later in this Chapter). In one case, the isotropic dye/DNA film was prepared from the Calf Thymus DNA (the only example in this work) and in the other case, from the Herring Sperm DNA.

5.3.2 Fraction of Oriented DNA Chains

As the layer structure of the combined dye/DNA-PVA film is different from that of the cast DNA-PVA film, it is important to check that the fraction of oriented DNA chains, that may be derived for the single layer of DNA in the cast DNA-PVA film, may be equated to that for the top layer of DNA in the combined dye/DNA-PVA film, under identical conditions. It became apparent that this was not possible, since the dichroic ratio measured for proflavine/DNA-PVA films at the proflavine visible absorption maximum was much smaller than that measured for cast DNA-PVA films, at the ultra-violet absorption maximum of the DNA bases under identical conditions of stretch and relative humidity. Thus, the fraction of oriented DNA chains in the cast DNA-PVA film, obtained from the dichroic ratio of the DNA bases, by assuming an orientation for them of 90° to the DNA helix axis (from equation 1.20), was less than that obtained from

the dichroic ratio of proflavine in the combined dye/DNA-PVA film, by assuming that its transition moment vector is oriented at 90° to the DNA helix axis (any smaller orientation angle would clearly increase the calculated fraction of oriented DNA chains).

The orientation process was investigated further by orienting both the sample combined dye/DNA-PVA film and a cast DNA-PVA film side by side on the same PVA film support. The total length of the clamped film was stretched approximately four-fold and the extension ratio of the central portion of each film was measured. In all cases, the cast DNA-PVA film revealed a much higher extension ratio than the combined dye/DNA-PVA film (Table 5.2). It appeared therefore, that as the DNA film became thicker, the mechanical contact between the PVA film and progressive layers of the DNA film was reduced, such that the orientation of the DNA, most distant from the DNA-PVA interface, was least. It was therefore, not possible to determine the fraction of oriented DNA chains in the dye/DNA-PVA film by a straight forward extrapolation from the cast DNA-PVA film. The choice of alternative orientation standards is discussed in Chapter Six, Section 6.1.

5.4 The Polarised Absorption and Dichroic Spectra of the Dye/DNA Complexes

For aromatic molecules in solution, the totally symmetric modes of vibration appear as the most dominant in the absorption spectra (McCoy and Ross, 1962). Thus, under these conditions, not only is constancy of the dichroism across the absorption band well approximated, but the

Table 5.2

Extension Ratios for the Central Portion of Cast
and Combined DNA-PVA Films, Oriented on the Same PVA Film

Film	Extension Ratio	
	Combined Proflavine/DNA-PVA	Cast DNA-PVA
1	2.5	3.3
2	2.8	3.7

dichroism is directly related to the electronic transition moment direction. Breakdown of the above approximation, that is contribution from non totally symmetric vibrational modes to the overall absorption region, generally occurs at higher wavenumbers within the vibronic envelope. For this reason, the most reliable dichroism that relates to the purely electronic transition is obtained experimentally from the red-end of an absorption band. Conversely, the vibronic transition involving many different types of non totally symmetric vibrational modes tends to produce a dichroic ratio approaching unity at the blue end of the absorption band.

5.4.1 The Acridine/DNA Complex

Typical polarised absorption and dichroic spectra for the anisotropic proflavine, acriflavine and 9-aminoacridine/DNA film complexes are shown in Figures 5.4, 5.5 and 5.6 respectively. All samples have an extension ratio of 2.8 and have been equilibrated at 93% relative

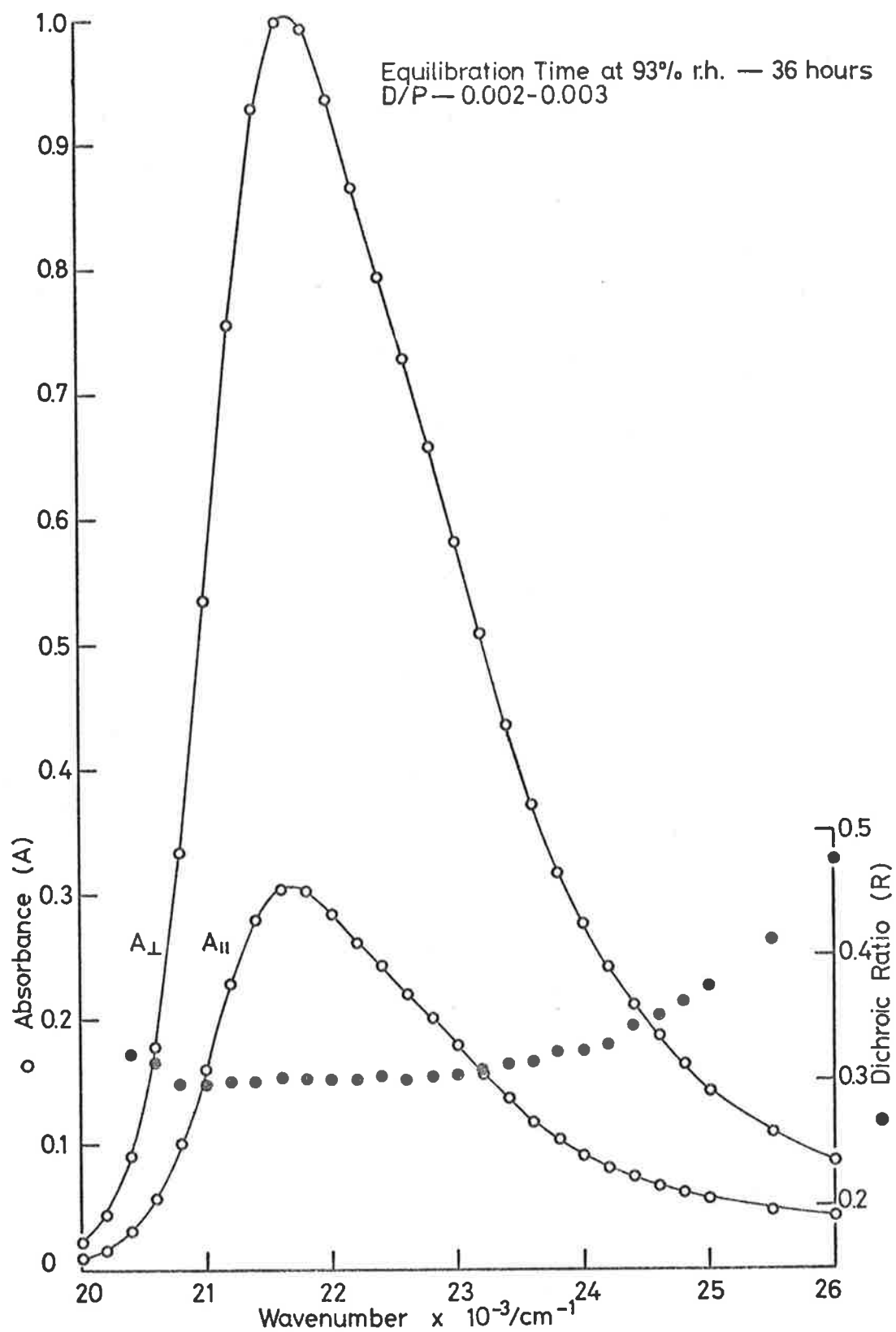


FIG 5.4 THE POLARISED ABSORPTION AND DICHROIC SPECTRA OF A COMBINED PROFLAVINE/DNA FILM

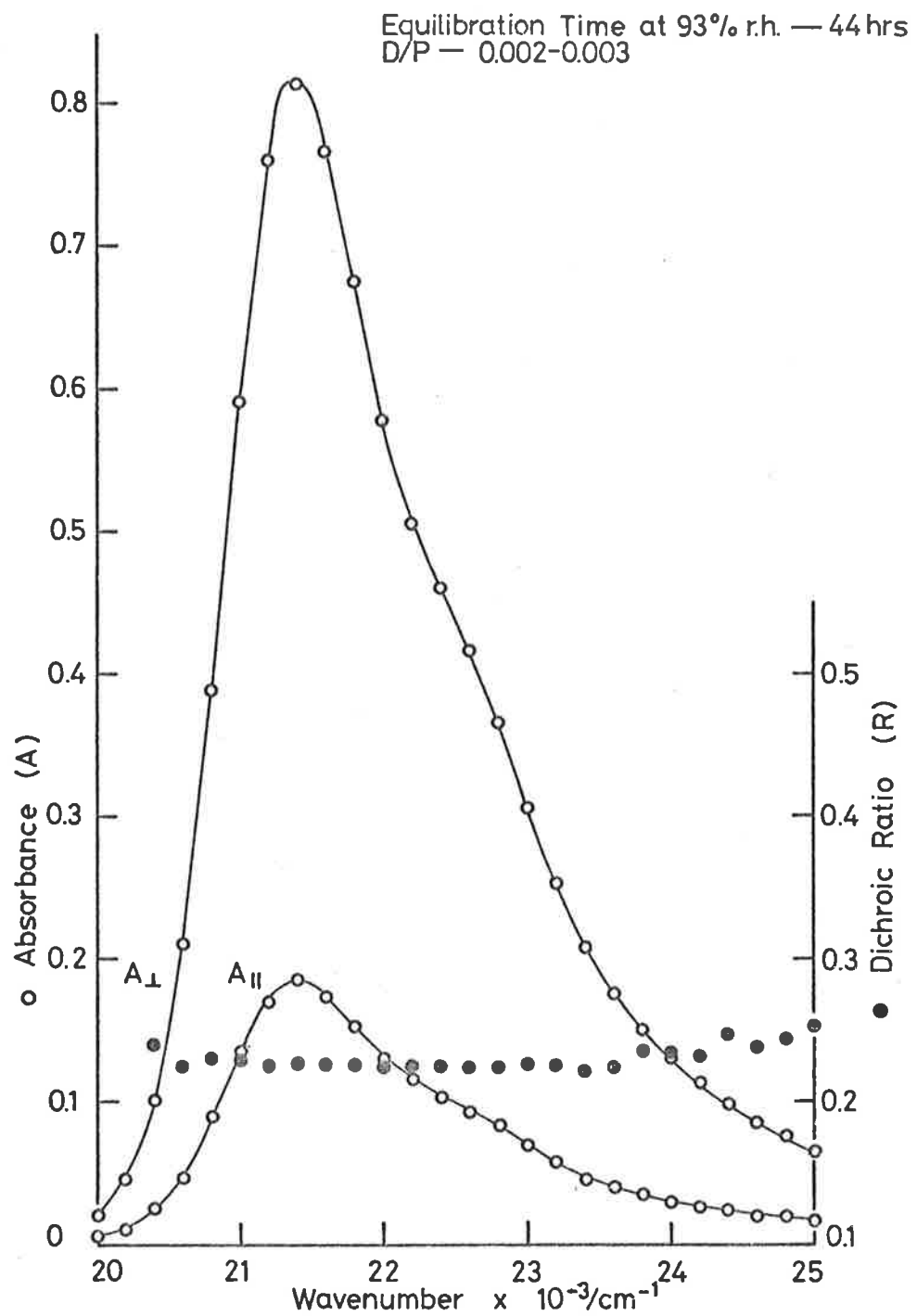


FIG 5.5 THE POLARISED ABSORPTION AND DICHOIC SPECTRA OF A COMBINED ACRIFLAVINE/DNA FILM

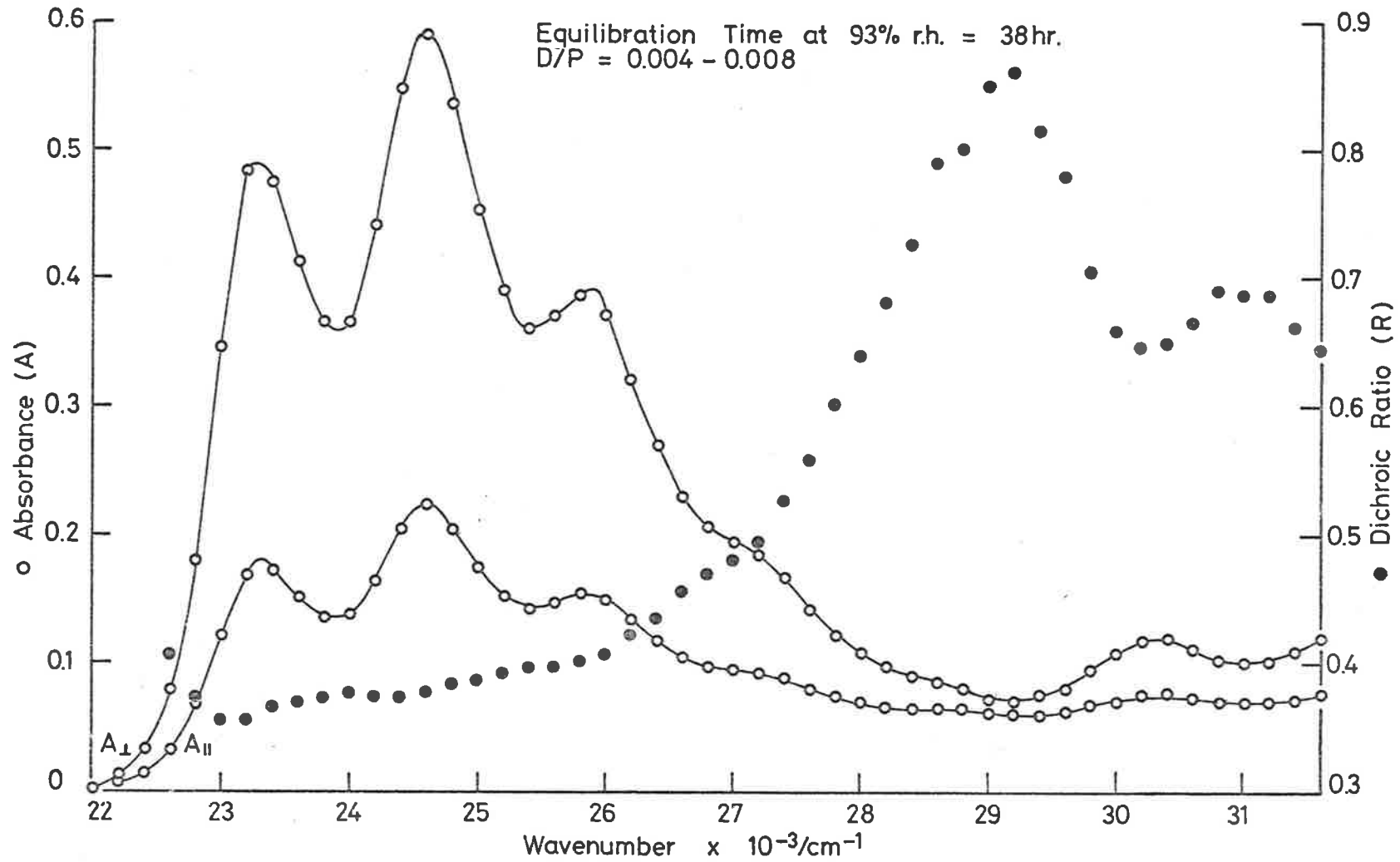


FIG 5.6 THE POLARISED ABSORPTION AND DICHOIC SPECTRA OF A COMBINED 9-AMINOACRIDINE/DNA FILM

humidity over $1\frac{1}{2}$ - 2 days. The dye to DNA phosphate ratio is 0.002 - 0.003 for proflavine and acriflavine and 0.004 - 0.008 for 9-aminoacridine.

The polarised absorption spectra for the proflavine and acriflavine/DNA complexes (shown between $20,000\text{cm}^{-1}$ and $26,000\text{cm}^{-1}$) are very similar, except for the red shift of the acriflavine spectrum relative to that of proflavine. The shapes of the dichroic spectra are likewise very similar and approximate most closely to a constant dichroic ratio in the vicinity of their absorption maxima. The plateau dichroic ratio region extends approximately $3,000\text{cm}^{-1}$ for acriflavine and $2,400\text{cm}^{-1}$ for proflavine; on either side of the plateau region, the dichroic ratio is seen to increase.

The shapes of the polarised absorption and dichroic spectra for the 9-aminoacridine/DNA complex are quite different. In particular, the dichroic spectrum does not display a genuine plateau region; there is a noticeable but gradual increase in the dichroic ratio throughout the wavenumber range spanned by the three visible absorption maxima which comprise the major portion of the first electronic transition. Beyond this region (at higher wavenumbers), there is a rapid increase in the dichroic ratio similar to that observed for the proflavine and acriflavine/DNA complexes. This is in agreement with the expected effect of non symmetric modes of vibration on the measured dichroic ratio. The spectrum of the 9-aminoacridine/DNA complex has been extended to the onset of DNA absorption where a further absorption band (maximum at $30,300\text{cm}^{-1}$) appears. The presence of this electronic transition has caused a sudden fall in the measured

dichroic ratio.

5.4.2 The Reporter/DNA Complex

Figures 5.7, 5.8, 5.9 and 5.10 are representative of the polarised absorption and dichroic spectra for the anisotropic 2,4-dinitroaniline, paranitroaniline, orthonitroaniline and 4-nitro-1-naphthylamine reporter/DNA film complexes respectively. The extension ratios and equilibration times at 93% relative humidity are the same as those for the acridine/DNA complexes. The dye to DNA phosphate ratios are 0.007 - 0.010, 0.007, 0.018 - 0.019, and 0.007 respectively.

The polarised absorption spectra of the orthonitroaniline, paranitroaniline and 4-nitro-1-naphthylamine reporter/DNA complexes exhibit one absorption band in the visible region. In addition, a further absorption band is discernible preceding the onset of DNA absorption for the 4-nitro-1-naphthylamine reporter/DNA complex. The 2,4-dinitroaniline reporter/DNA complex is composed of two absorption bands in the visible region with the first appearing as a shoulder on the low wavenumber side of the second.

The shapes of the dichroic spectra for the ortho- and paranitroaniline reporter/DNA complexes are very similar as can be seen by the gradual increase in their dichroic ratios towards higher wavenumbers. This increase is more abrupt in the case of the 4-nitro-1-naphthylamine reporter/DNA complex (which has a correspondingly smaller band-width). The next absorption band for this dye measured prior to DNA absorption is well demonstrated by the approximately constant dichroic ratio. The dichroic spectrum between these two absorption bands is not shown since it is experimentally

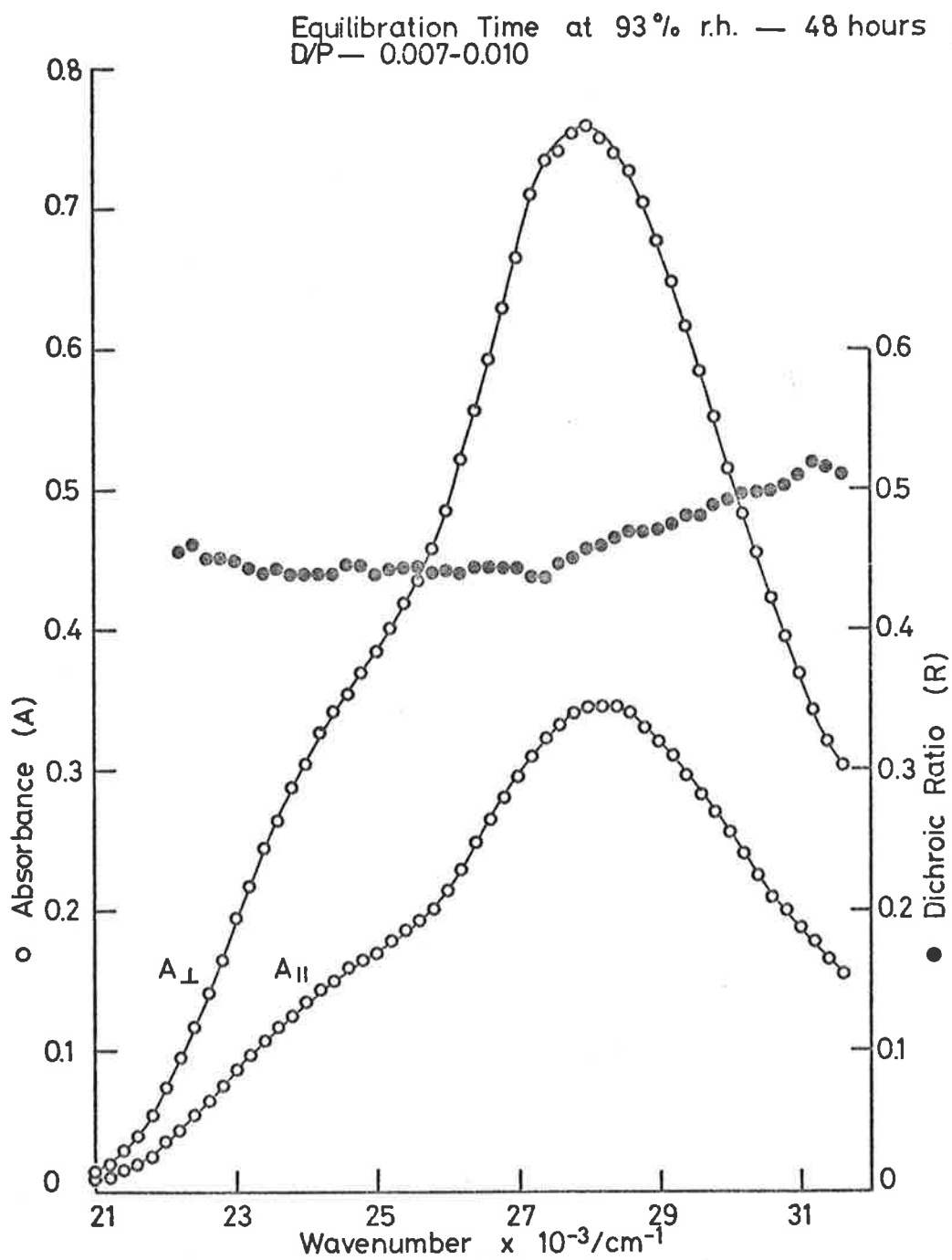


FIG 5.7 THE POLARISED ABSORPTION AND DICHOIC SPECTRA OF A COMBINED 2,4-DINITROANILINE REPORTER/DNA FILM

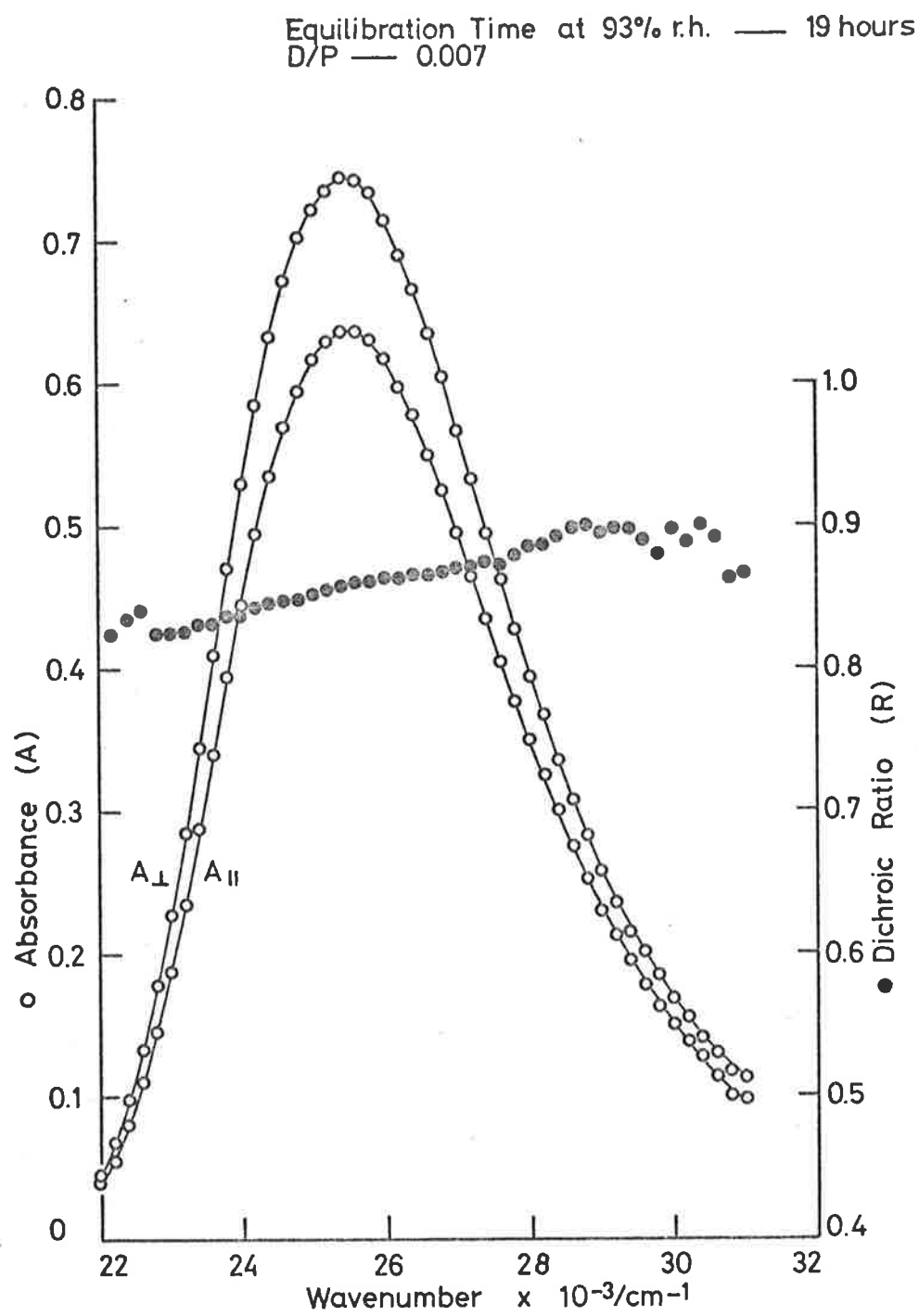


FIG 5.8 THE POLARISED ABSORPTION AND DICHOIC SPECTRA OF A COMBINED PARANITROANILINE REPORTER/DNA FILM

Equilibration Time at 93% r.h. — 22 hours
D/P — 0.018-0.019

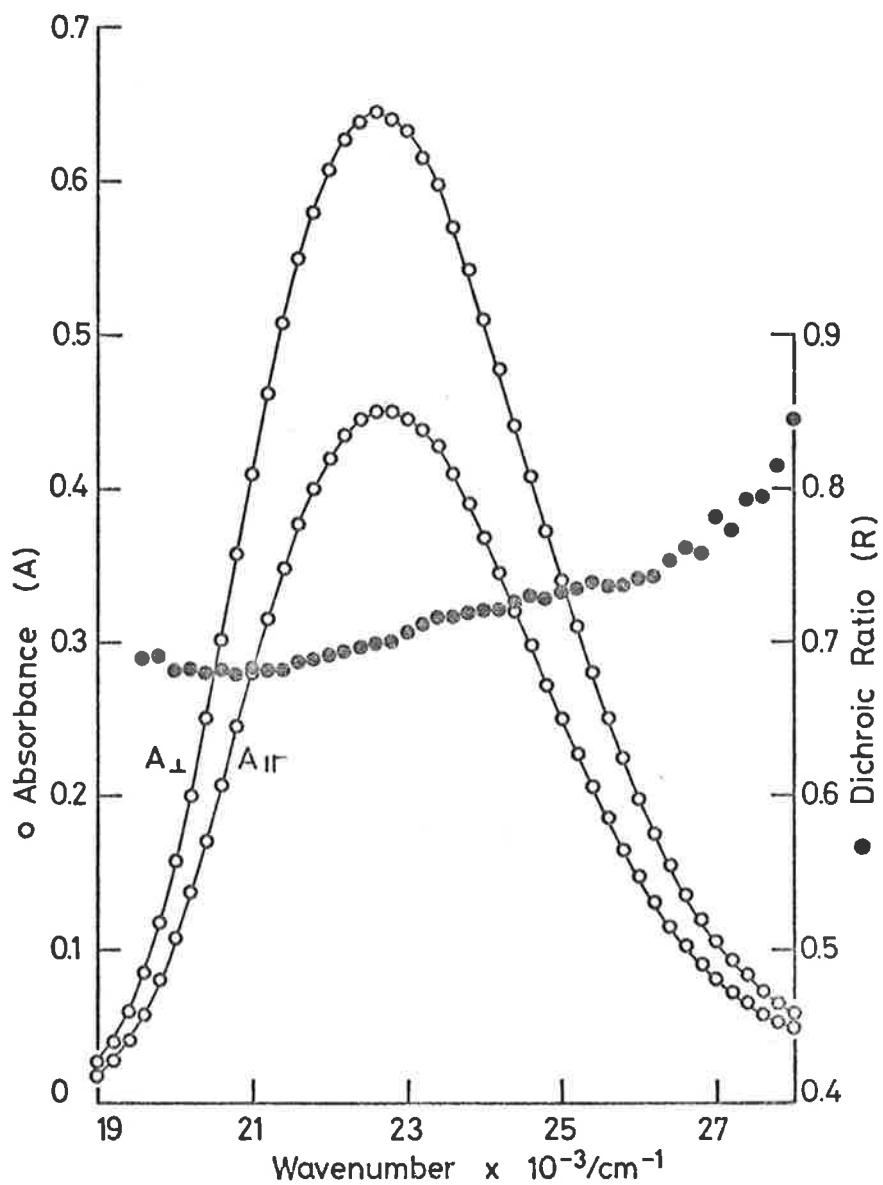


FIG 5.9 THE POLARISED ABSORPTION AND DICHOIC SPECTRA OF A COMBINED ORTHONITROANILINE REPORTER/DNA FILM

Equilibration Time at 93% r.h. — 23 hours
D/P — 0.007

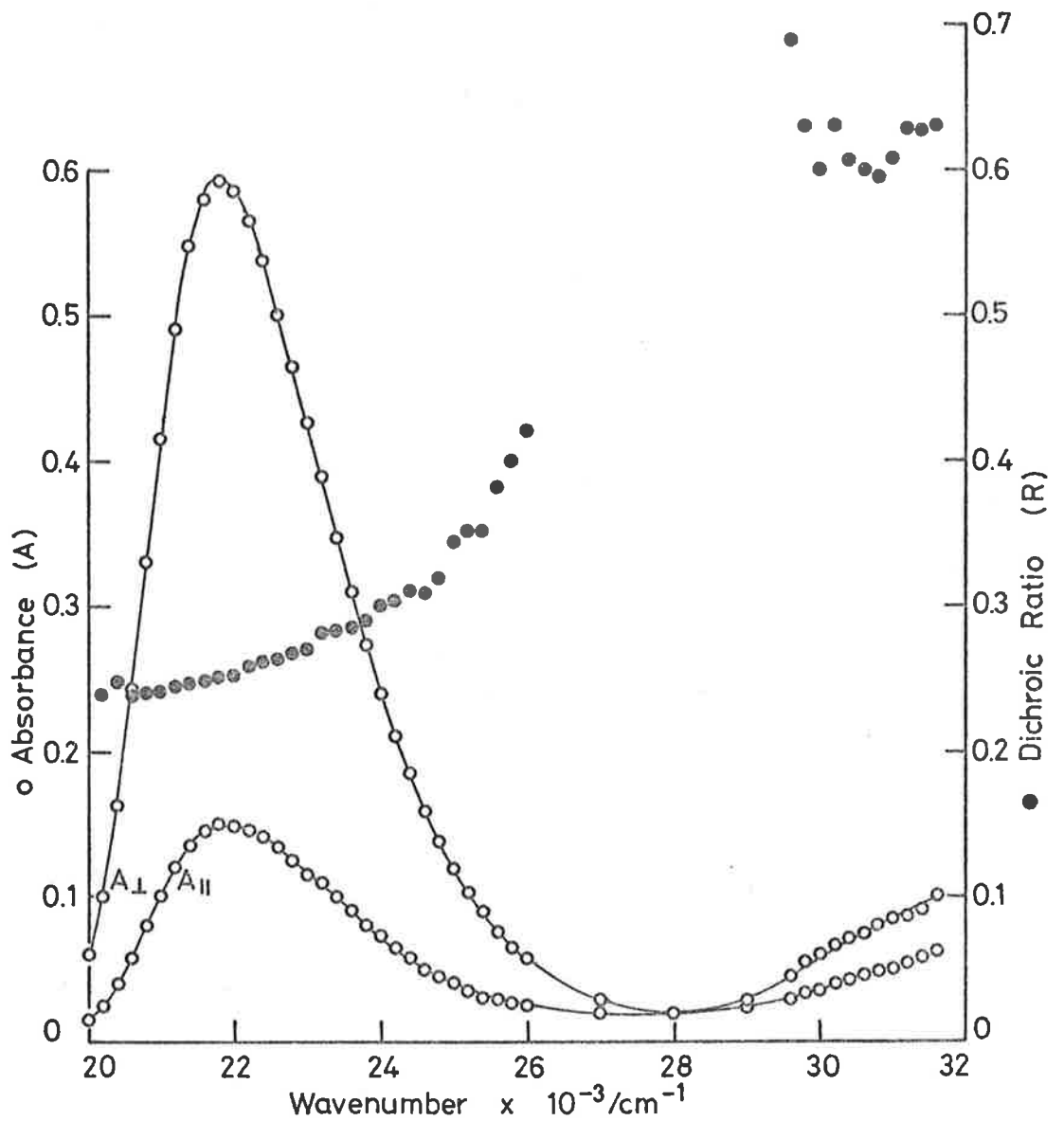


FIG 5.10 THE POLARISED ABSORPTION AND DICHROIC SPECTRA OF A COMBINED 4-NITRO-1-NAPHTHYLAMINE REPORTER/DNA FILM

uncertain at the low recorded absorbances. The dichroic spectrum of the 2,4-dinitroaniline reporter/DNA complex is represented by a plateau region spanning the low wavenumber absorption band (shoulder) and extending almost to the maximum absorption of the high wavenumber absorption band. At further increasing wavenumbers, there is a steady increase in the measured dichroic ratio.

For all dye/DNA complexes, the continual increase in the dichroic ratio across an absorption band is well accounted for by the increased contribution from non symmetric vibrational modes at higher wavenumbers. This effect is not observable for the first electronic transition of the 2,4-dinitroaniline reporter/DNA complex. Here, the following electronic transition has completely overwhelmed any effect that may have appeared from the non symmetric vibrational modes of the previous absorption band.

5.5 Relative Humidity Equilibration Time

The effect of the relative humidity equilibration time on the measured dichroic ratio has been investigated at selected wavenumbers for each of the dyes' observable electronic transitions in the wavenumber region prior to DNA absorption. The selected wavenumbers have been chosen from that portion of the absorption band where the dichroic ratio may be conveniently related to the pure electronic transition, i.e., the red end of the appropriate absorption band. This presented no difficulties when the dichroic ratio was constant throughout this region. However, when it was found to steadily increase (as was the case for most of the dyes studied), it was considered necessary to choose one or

even two further wavenumbers. This enabled any difference in the calculated geometry of the respective dye transition moment vector to be assessed in terms of the reliability of the overall dye/DNA geometry (Chapter Six, Section 6.2).

5.5.1 The Acridine/DNA Complex

The effect of the equilibration period at 93% relative humidity on the measured dichroic ratio of the acriflavine and the proflavine/DNA complexes (D/P, 0.002 - 0.003) is shown in Fig.5.11. The plotted dichroic ratios have been drawn from the plateau region of the dichroic spectra. Both dyes are represented by six film samples that have been measured over different equilibration times. For some of the samples, the dichroic ratio has not been plotted to its limiting equilibration value (approximately attained after 40 hours) because of the greater tendency of the films to fracture with increasing equilibration time. Both dye/DNA complexes behaved identically, with the dichroic ratio falling to a constant minimum value.

Fig.5.12 shows the effect of equilibration time at 93% relative humidity on the dichroic ratio of the 9-aminoacridine/DNA complex (five film samples; D/P, 0.004 - 0.008). The dichroic ratios have been studied at the three visible wavenumber maxima (the first absorption band) and at the plateau region prior to DNA interference (the second absorption band). The dye/DNA complex reached a constant dichroic ratio at the above wavenumbers, prior to a twenty hour equilibration period. No measurements were recorded under this time.

5.5.2 The Reporter/DNA Complex

The effect of the equilibration period at 93% relative

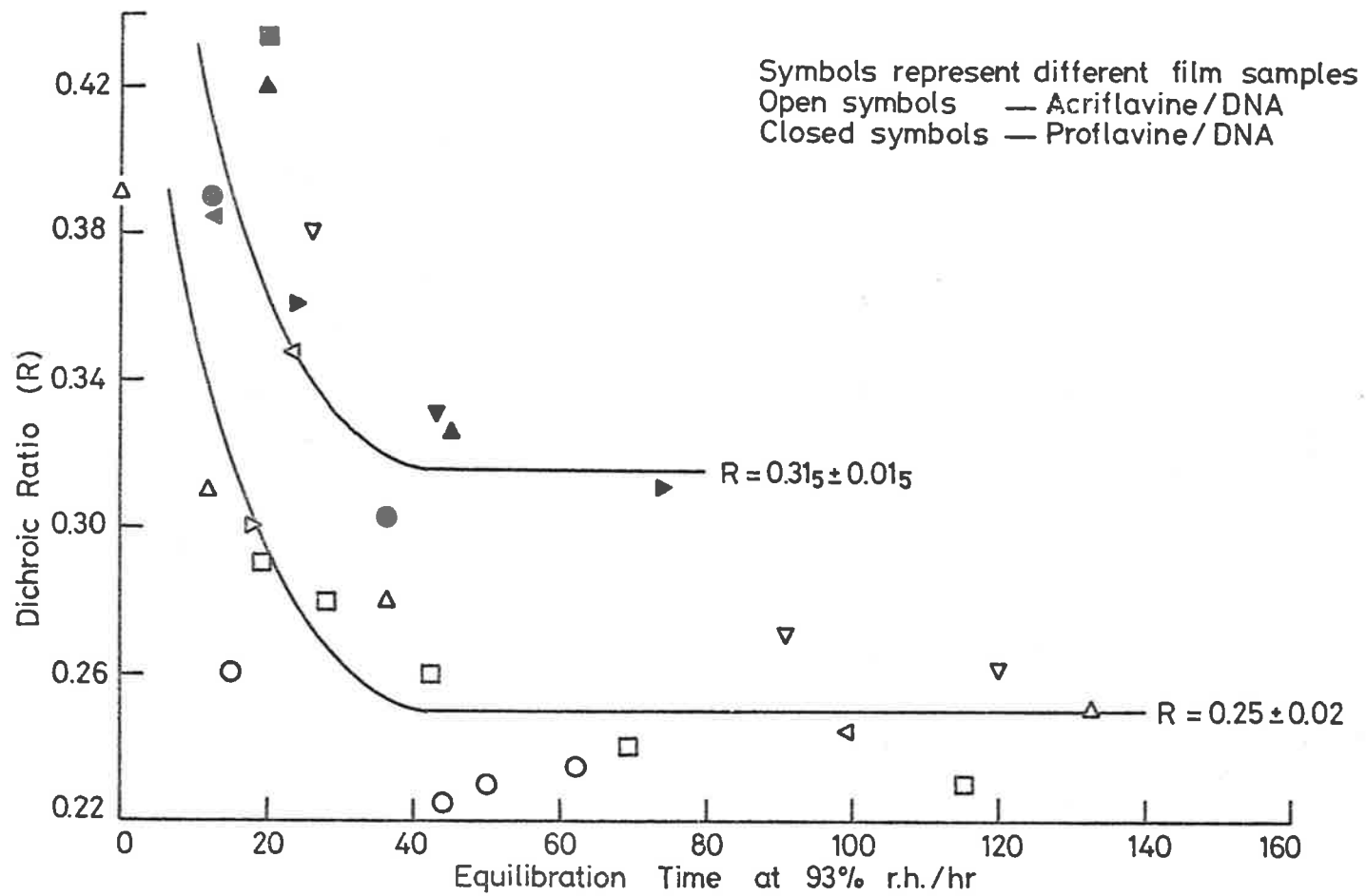


FIG 5.11 THE EFFECT OF EQUILIBRATION TIME ON THE DICHOIC RATIO MEASURED AT THE PLATEAU OF THE DICHOIC SPECTRUM FOR ACRIFLAVINE/DNA FILMS (SIX SAMPLES) AND PROFLAVINE/DNA FILMS (SIX SAMPLES) WITH D/P = 0.002-0.003

Symbols represent different film samples

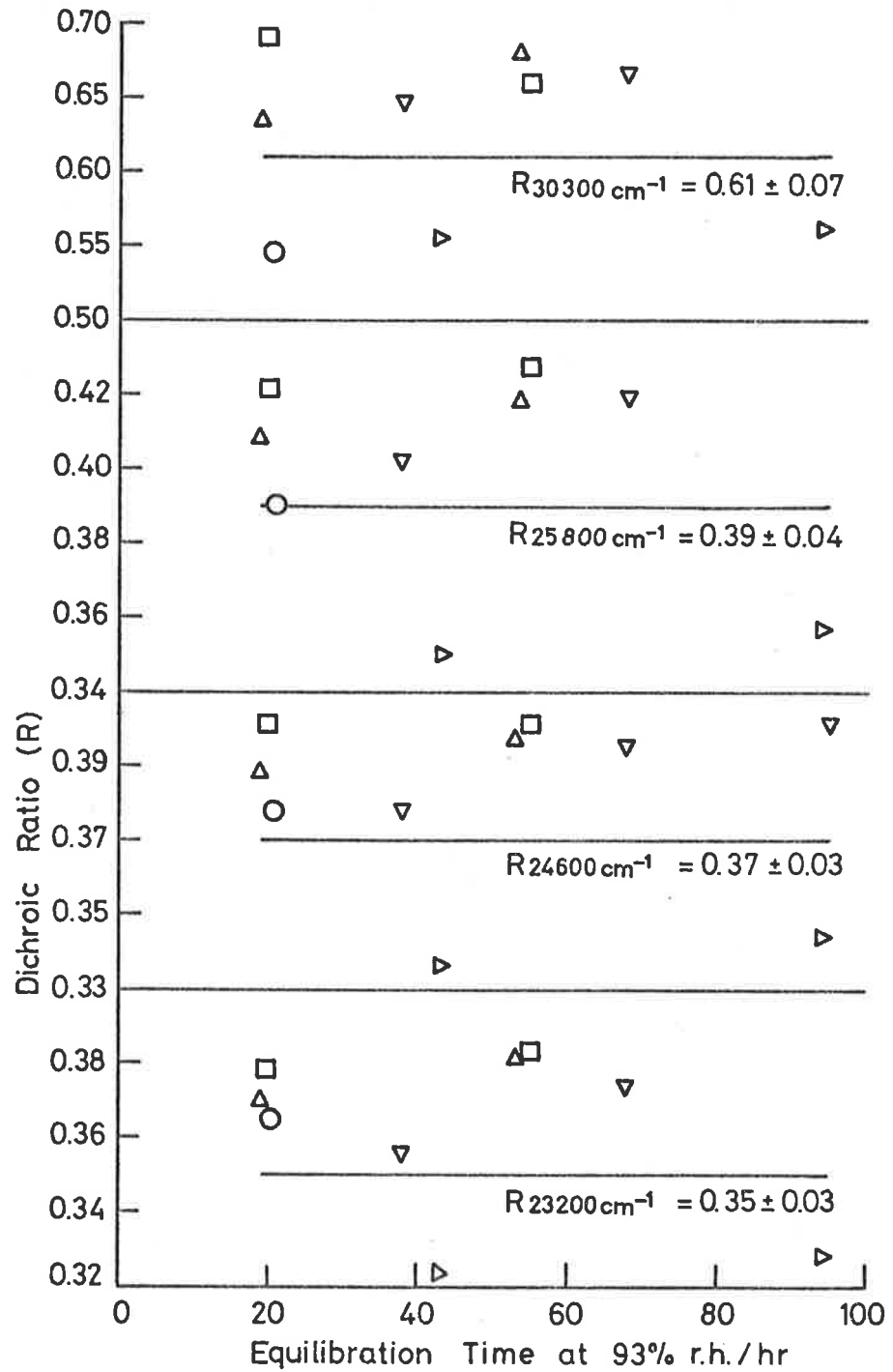


FIG 5.12 THE EFFECT OF EQUILIBRATION TIME ON THE DICHOIC RATIO AT THE INDICATED WAVENUMBERS FOR 9-AMINOACRIDINE/DNA FILMS (FIVE SAMPLES) WITH D/P = 0.004-0.008

humidity on the dichroic ratio of the reporter/DNA complex is shown in Fig.5.13 for the paranitroaniline (3 samples; D/P, 0.007) and orthonitroaniline (4 samples; D/P, 0.018 - 0.019) reporters and in Fig.5.14 for the 2,4-dinitroaniline (5 samples; D/P, 0.007 - 0.010) and 4-nitro-1-naphthylamine (2 samples; D/P, 0.007) reporters. At wavenumbers preceding the absorption maximum of the 2,4-dinitroaniline reporter/DNA complex, the dichroic ratio was constant (Fig.5.7). Thus, the dichroic ratio in this wavenumber region together with that at the maximum absorption were investigated. For the other reporter/DNA complexes, the dichroic ratio was studied at two wavenumbers, selected at the limits of the half band width of the visible absorption band. In addition, a further dichroic ratio representative of the low intensity near ultra-violet absorption band of the 4-nitro-1-naphthylamine reporter/DNA complex was studied.

An equilibration period of twenty hours was sufficient for all reporter/DNA complexes to reach a steady dichroic ratio (Figs.5.13 and 5.14). The 2,4-dinitroaniline reporter/DNA complex was investigated more fully, from which it was observed that the dichroic ratio fell to a constant value over the initial twenty hour equilibration period (Fig.5.14). The same behaviour was also apparent for the 4-nitro-1-naphthylamine reporter/DNA complex (Fig.5.14).

5.6 Quality of the Anisotropic Dye/DNA Films

The quality of the anisotropic dye/DNA films may be judged in terms of their appearance, their amount of orientation and the reproducibility of their measured

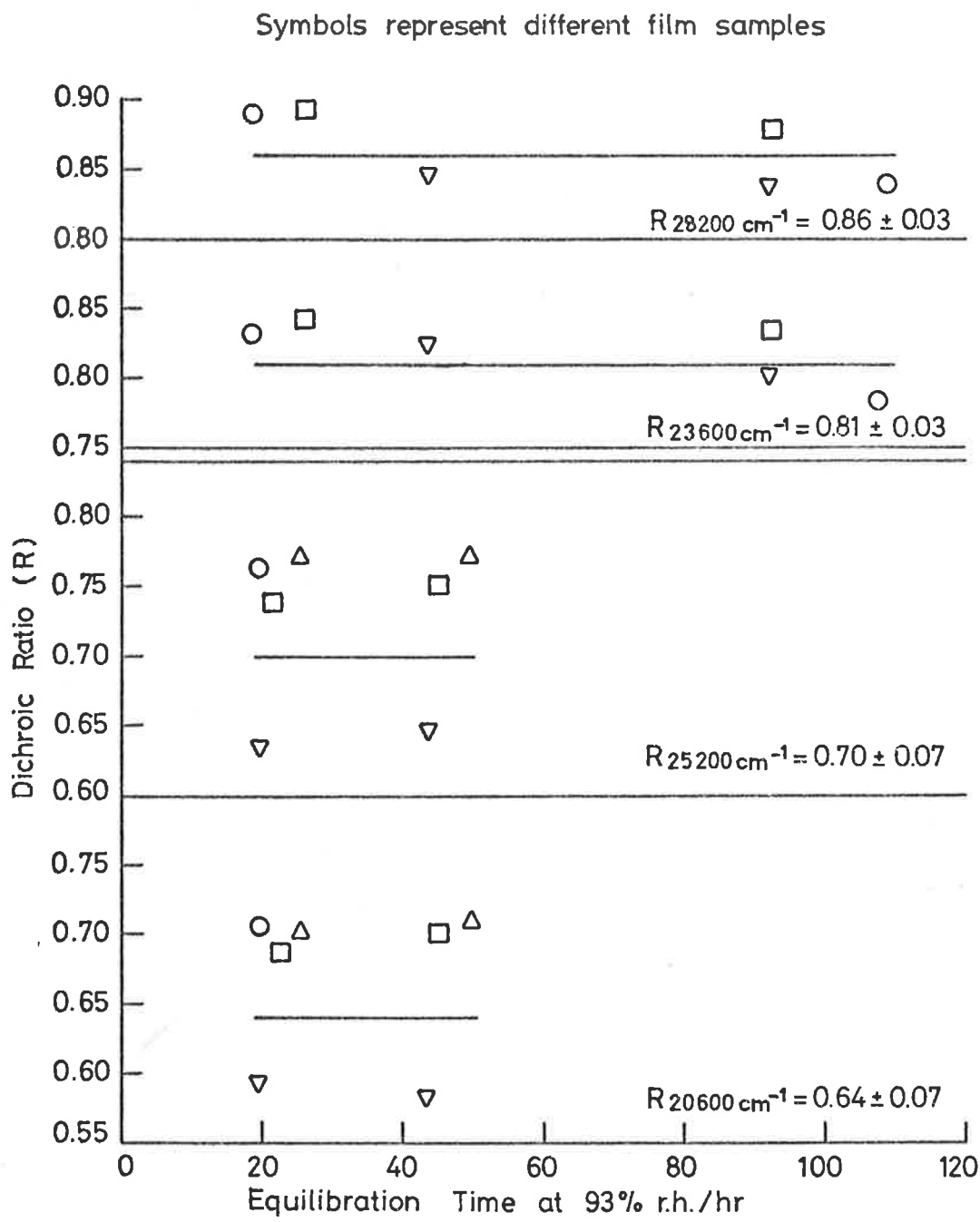


FIG 5.13 THE EFFECT OF EQUILIBRATION TIME ON THE DICHROIC RATIO AT THE INDICATED WAVENUMBERS FOR PARANITROANILINE REPORTER/DNA FILMS (THREE SAMPLES - UPPER TWO PLOTS) WITH D/P = 0.007 AND FOR ORTHONITROANILINE REPORTER/DNA FILMS (FOUR SAMPLES LOWER TWO PLOTS) WITH D/P = 0.018 - 0.019

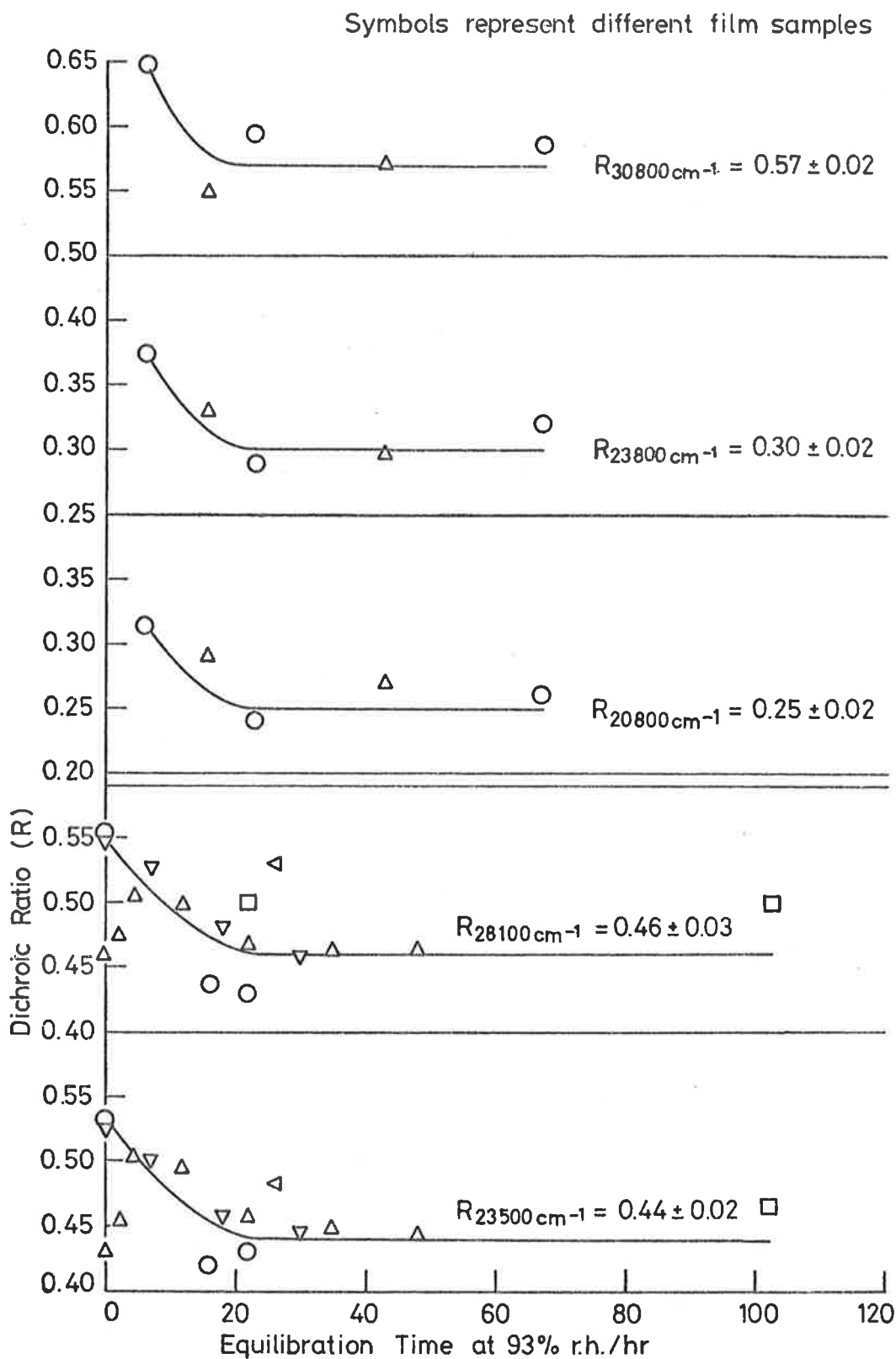


FIG 5.14 THE EFFECT OF EQUILIBRATION TIME ON THE DICHOIC RATIO AT THE INDICATED WAVENUMBERS FOR 4-NITRO-1-NAPHTHYLAMINE REPORTER/DNA FILMS (TWO SAMPLES — UPPER THREE PLOTS) WITH D/P = 0.007 AND FOR 2,4-DINITROANILINE REPORTER/DNA FILMS (FIVE SAMPLES — LOWER TWO PLOTS) WITH D/P = 0.007-0.010

dichroic ratios. The appearance of the film mounted in the humidity cell is somewhat dependent on the initial attachment process in the preparative method. It must be remembered that the unattached dye/DNA film is at low relative humidity while the DNA-PVA film is at high relative humidity (the DNA-PVA surface must be moist prior to attachment). On attachment, the subsequent contraction of the dye/DNA film, causes slightly less than total adherence between the two films. This is further enhanced by any surface irregularities on either of the films. At various points in the combined film, minute air bubbles may appear and although they do affect the overall recorded spectrum, they do not influence the final corrected spectrum (refer to spectra corrections in Chapter Three, Section 3.4.2).

The amount of orientation of the dye/DNA films is discussed in Chapter Six, Section 6.1, in terms of the fraction of oriented DNA chains. It is very high. If a dichroic ratio comparison is used, this method is at least as good as the previously reported best orientation method (Rupprecht et al, 1969). The reproducibility of that method was not quoted. For the method used here, the dichroic ratio associated with each major absorption band is reproducible to ± 0.03 units for all but one dye/DNA complex.

Throughout the preparation of the anisotropic dye/DNA films, an extension ratio of 2.8 has been used. This was found to be the best compromise between degree of orientation, reproducibility and breakage. At higher extension ratios, the upper dye/DNA film invariably

fractured or formed small holes during the stretching process. This allowed the film to partially relax, with a consequent decrease in the measured dichroism. Even if the films that fractured or formed holes were not included, the reproducibility at higher extension ratios was less and this was probably due to small undetected faults (fractures or holes) in the films.

CHAPTER SIX

INTERPRETATION OF LINEAR DICHROISM FOR THE DYE/DNA COMPLEX

The model, suggested by Fraser (1953, 1956) and outlined in Chapter One, Section 1.2 in which a certain fraction, f , of the polymer chains is assumed to be perfectly oriented parallel to the fibre axis while the remaining fraction, $(1 - f)$, is perfectly random, has been used here to interpret the linear dichroism. For the dye/DNA complex, the fibre or orientation axis is taken to be the DNA helix axis.

6.1 Estimation of the Fraction of Oriented DNA Chains

The ideal way to obtain f is to compare the fraction of oriented DNA chains in the combined double layer dye/DNA-PVA film to that in the cast DNA-PVA film. However, such a direct comparison is not possible because of the different physical (mechanical) properties of the two films (Chapter Five, Section 5.3.2).

Alternatively, Fraser (1958) has derived a general equation for evaluating the relation between the dichroic ratio and a parameter describing a model distribution. He concluded that the most plausible model described the distribution of crystallite orientations in a stretched polymer containing rod-like crystallites in an isotropic matrix (Kratky, 1933). The use of this model, in conjunction with the general equation, has led to the relationship between f and the extension ratio, v (defined in Chapter Four, Section 4.5), as follows:

$$f = \frac{3v^3}{2(v^3 - 1)} \left[\frac{2v^3 + 1}{3v^3} - \frac{\tan^{-1}(v^3 - 1)^{\frac{1}{2}}}{(v^3 - 1)^{\frac{1}{2}}} \right] \quad (6.1)$$

and this function is plotted in Fig.6.1. Provided that the relationship between f and v holds, R_0 can be evaluated by substituting the value of f and the measured dichroic ratio, R , in equation 1.20. For an extension ratio of 2.8 which has been used throughout all preparations of the anisotropic dye/DNA film samples, f is 0.60 (Fig.6.1). The measured dichroic ratios of the acriflavine/DNA and 4-nitro-1-naphthylamine reporter/DNA films may be used to demonstrate that under the current experimental conditions this is a considerable under-estimate. For $R = 0.25$ (Chapter Five, Figs.5.11 and 5.14), an f value of 0.67 is obtained when it is assumed that for perfect alignment of the films the dichroic ratio, R_0 , will approach zero. It is therefore more appropriate to select the dichroic ratio of the acriflavine/DNA or the 4-nitro-1-naphthylamine reporter/DNA films as the reference basis to estimate f . In this way, the lower limit for f is set at 0.67 under the current experimental conditions. (If R_0 were to approach a non-zero value for the perfect alignment of the dye/DNA complex, a higher value for f would be found.) The difference between f obtained from Fig.6.1 at $v = 2.8$ and that obtained using either the dichroic ratio of the acriflavine/DNA or the 4-nitro-1-naphthylamine reporter/DNA complex films may indicate that the orientation of the complex increases after the initial stretching process in the confines of the humidity cell.

An upper limit for f may be estimated from an

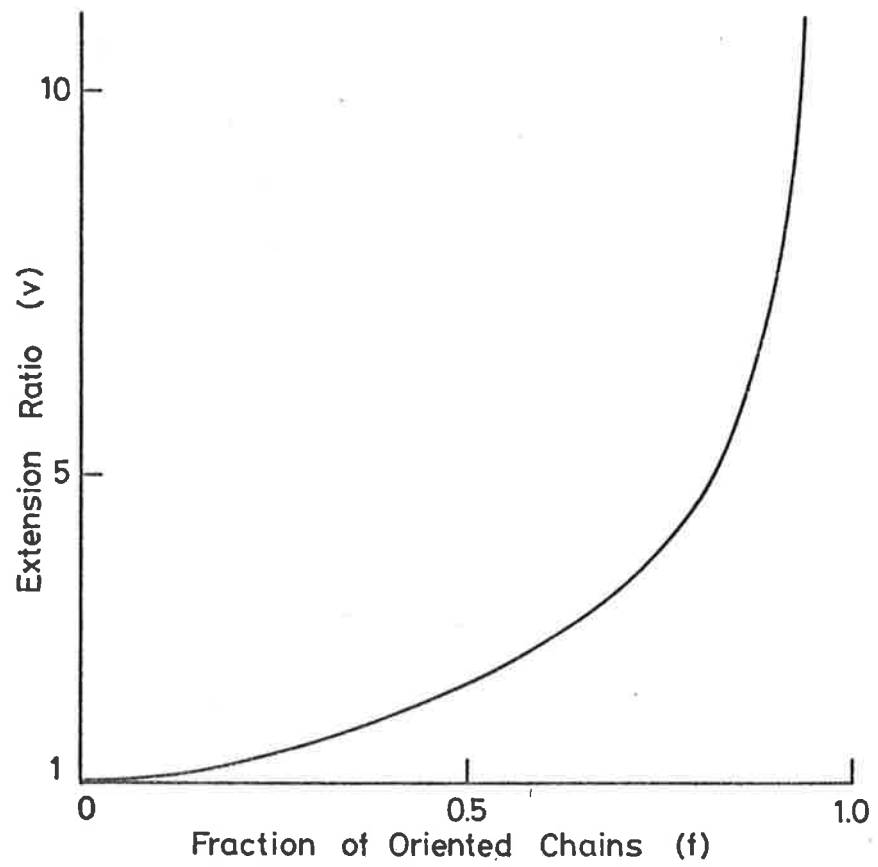


FIG 6.1 THE RELATION BETWEEN THE FRACTION OF ORIENTED CHAINS AND THE EXTENSION RATIO

examination of the many reported dichroic ratios for anisotropic DNA film samples (Table 6.1). The tabulated dichroic ratios refer to the 260nm maximum absorption band which is a composite band due to $\pi^* \leftarrow \pi$ transitions in the plane of the purine and pyrimidine bases (Falk et al, 1963b; Kasha, 1961; Wilkinson et al, 1959). For perfect alignment of the DNA film sample, R_0 would approach zero for an angle of 90° between the helix axis and the plane of the bases (Chapter One, Section 1.3). The lowest ever reported dichroic ratio of $R = 0.16$ leads to $f = 0.78$ (Table 6.1). However, this value was discarded as the upper limit for the fraction of oriented DNA chains for the following reason.

The dichroic ratio of proflavine/DNA complex films (measured at maximum absorption) prepared here and prepared by the "wet spinning method" are very similar (Table 6.2). Consequently, the fraction of oriented DNA chains in both samples would be expected to be approximately the same. If f is evaluated for the wet spun proflavine/DNA film from the dichroic ratio of the wet spun DNA film (where R_0 approaches zero), a value of 0.63, slightly smaller than the lower limit of 0.67 set here, is found (Table 6.2). Thus, a comparison between f , estimated for the dye/DNA complex for the current experimental conditions (0.67 to 0.78), and a value that may be calculated for the "wet spinning method" (0.63), suggest that the lower limit of $f = 0.67$ is the more reliable value, whilst the upper limit of $f = 0.78$ is most likely a considerable over-estimate. Therefore, for this work, f has been confined to the range 0.67 - 0.72, with the new upper limit being calculated from

Table 6.1
Orientation of DNA Films

Method of Alignment	DNA Origin	%r.h.	Wavenumber cm ⁻¹	R	f	Reference
Shearing gel between coverslip and slide	Thymus	90	37,040	0.21	0.72	Seeds, 1953
Stroking gel on quartz disc	Calf Thymus	-	38,460	0.16	0.78	Rich and Kasha, 1960
Stroking gel with spatula on fluorite disc	Calf Thymus	93	37,040	0.31	0.60	Falk et al, 1963b
Wet spinning	Thymus	93	37,040	0.28	0.63	Rupprecht, 1963 and 1966
Drawing out gel between two quartz plates	-	98	-	0.36	0.54	Houssier, 1964
Stroking gel with quartz slide on another slide	T5st - 0 4 samples T2H 2 samples	92	38,460	0.21- 0.35	0.72- 0.55	Gray and Rubenstein, 1968
Stroking gel on quartz slide	Calf Thymus	94	38,460	0.3- 0.5	0.61- 0.40	Wetzel et al, 1969
Stretching gel into microscopic fibres	-	-	38,460	0.31	0.60	Thorell and Ruch, 1951

Table 6.2
Calculation and Comparison of f

Film Sample	R, at Maximum Absorption	f	Reference ¹
Acridine/DNA	0.25	0.67 ²	This work, Fig.5.11
DNA	0.16	0.78 ²	Rich and Kasha, 1960
Proflavine/DNA	0.31 ₅ ± 0.02	0.67 - 0.78 ³	This work, Fig.5.11
Wet Spun DNA	0.28	0.63 ²	Rupprecht, 1963 and 1966
Wet Spun Proflavine/DNA	0.317 - 0.331	0.63 ⁴	Rupprecht et al, 1969

1. Reference refers to R, at Maximum Absorption
2. f has been calculated from equation 1.20, assuming
 $R_0 = 0$
3. The limits of f have been set by the first two entries
of the table (see text)
4. f is assumed to be the same as that for the wet spun
DNA film

a dichroic ratio of 0.21. This value represents the second best degree of alignment of DNA chains achieved by any previous method (Table 6.1), and seems to be more in keeping with the distribution of the lowest dichroic ratios listed in Table 6.1.

6.2 Determination of the Angle between the Transition Moment Vector of the Dye and the DNA Helix Axis

Tables 6.3 and 6.4 present the angle between the dyes' transition moment vector(s) at selected wavenumber(s) and the DNA helix axis for the acridine and reporter molecules respectively. The dichroic ratio, R (Figs.5.11 - 5.14), and the limits of f (set in the previous section) have been substituted in turn, into equations 1.20 and 1.16 to calculate R_0 and ω , the angle between the transition moment of the dye and the DNA helix axis. The last column of Tables 6.3 and 6.4 lists the total determined angle range. This angle range has made allowance for both the experimental variation in R (the measured dichroic ratio) and the calculated variation in f (the fraction of oriented DNA chains).

The dichroic ratio, measured throughout the plateau region of the dichroic spectra for the proflavine and acriflavine/DNA complexes, is representative of the totally symmetric mode of vibration for the electronic transition and so has been used in the calculations. For the first electronic transition of the 9-aminoacridine/DNA complex, the dichroic ratios, measured at the three vibronic absorption maxima, have been used to calculate ω . Although the dichroic ratio is slightly greater at the two higher wavenumber vibronic maxima, the difference in the determined angle range is minimal (Table 6.3). Moreover, as the dichroic ratio measured at the wavenumber corresponding to the first vibronic maximum is most representative for the symmetric mode of vibration of this electronic transition, the angle range determined at this wavenumber only, will be

Table 6.3

The Angle between the Transition Moment Vector of the Dye and the DNA Helix Axis
for the Acridine Molecules

Dye	$\bar{\nu}$ cm ⁻¹	R	f = 0.67		f = 0.72		
			R ₀	Angle (Degrees)	R ₀	Angle (Degrees)	Angle Range (Degrees)
Acriflavine	20,600- 23,600	0.25 ± 0.02	0 - .024	90 - 84	.023 - .069	84 - 80	85 ± 5
Proflavine	20,800- 23,200	0.31 ₅ ± 0.01 ₅	.060 - .096	80 - 78	0.10 - 0.14	77 - 75	77½ ± 2½
9-Aminoacridine	23,200	0.35 ± 0.03	.084 - 0.16	78 - 74	0.13 - 0.20	76 - 72	75 ± 3
	24,600	0.37 ± 0.03	0.11 - 0.18	77 - 73	0.15 - 0.22	75 - 72	74½ ± 2½
	25,800	0.39 ± 0.04	0.12 - 0.22	76 - 72	0.16 - 0.26	74 - 70	73 ± 3
	30,300	0.61 ± 0.07	0.36 - 0.55	67 - 62	0.39 - 0.57	66 - 62	64½ ± 2½
	30,300	0.54 ± 0.07 ^a	0.27 - 0.45	70 - 64	0.31 - 0.48	69 - 64	67 ± 3

(a) Calculated, non-experimental value.

Table 6.4

The Angle between the Transition Moment Vector of the Dye and the DNA Helix Axis
for the Reporter Molecules

Dye	$\bar{\nu}_{-1}$ cm ⁻¹	R	f = 0.67		f = 0.72		
			R ₀	Angle (Degrees)	R ₀	Angle (Degrees)	Angle Range (Degrees)
4-Nitro-1-	20,800	0.25 ± 0.02	0 - .024	90 - 84	.023 - .069	84 - 80	85 ± 5
naphthylamine	23,800	0.30 ± 0.02	.036 - .084	82 - 78	.081 - 0.13	79 - 76	79 ± 3
reporter	30,800	0.57 ± 0.02	0.37 - 0.43	67 - 65	0.41 - 0.46	66 - 64	65½ ± 1½
2,4-Dinitroaniline	23,200-						
	27,900	0.44 ± 0.02	0.21 - 0.26	72 - 70	0.25 - 0.30	71 - 69	70½ ± 1½
reporter	28,100	0.46 ± 0.03	0.22 - 0.30	72 - 69	0.26 - 0.33	70 - 68	70 ± 2
Orthonitroaniline	20,600	0.64 ± 0.07	0.40 - 0.59	66 - 62	0.43 - 0.61	65 - 61	63½ ± 2½
reporter	25,200	0.70 ± 0.07	0.48 - 0.67	64 - 60	0.51 - 0.69	63 - 60	62 ± 2
Paranitroaniline	23,600	0.81 ± 0.03	0.68 - 0.77	60 - 58	0.70 - 0.78	58 - 58	59 ± 1
reporter	28,200	0.86 ± 0.03	0.75 - 0.84	59 - 57	0.77 - 0.85	58 - 57	58 ± 1

used in further discussion. The small difference in the angle range, determined at the following two vibronic maxima, emphasizes the negligible effect that small but noticeable increases in the dichroic ratio have on this calculation.

The dichroic ratio listed in Table 6.3 for the second electronic transition of the 9-aminoacridine/DNA complex has been measured at the $30,300\text{cm}^{-1}$ maximum (see Fig.5.6). At this wavenumber, the dichroic ratio would be representative of the electronic transition provided that there is no interference from the preceding electronic transition. However, a visual extrapolation of the first absorption band would suggest a probable 20% contribution to the isotropic absorbance at this wavenumber (refer Fig.5.6). Table 6.5 shows the effect of such a contribution to the experimental absorbance at $30,300\text{cm}^{-1}$.

It has been assumed that the dichroic ratio of the first electronic transition at $30,300\text{cm}^{-1}$ will be composed of many non symmetric modes of vibration, so that the overall dichroic ratio would approach unity. This approximation allows the calculation of the minimum dichroic ratio that would be obtained at $30,300\text{cm}^{-1}$ for transition two, without interference from transition one. The dichroic ratio thus calculated is 0.07 units lower than the experimental value. Such an overall lowering of the experimental dichroic ratio is shown in the final entry of Table 6.3, where the range of ω has been altered by 3° . For further discussions involving this electronic transition, ω has been confined to the range that covers both determinations.

For the first electronic transition of the orthonitro-aniline, paranitroaniline and 4-nitro-1-naphthylamine

Table 6.5

Effect of a 20% Absorbance Contribution from Transition One to the Dichroic Ratio of Transition Two at $30,300\text{cm}^{-1}$ for the 9-Aminoacridine/DNA Complex

	A_{11}	A_{\perp}	A^2	R
Experimental Measurement ¹	0.078	0.121	0.107	0.64 ₅
Estimated Contribution from Transition One	0.020	0.020	0.020	1.00
Remaining Contribution from Transition Two	0.058	0.101	0.087	0.57 ₄

1. The experimental measurement has been taken from Fig.5.6
2. The isotropic absorbance, $A = (A_{11} + 2A_{\perp})/3$ (Fraser,1960)

reporter/DNA complexes where ω has been determined from the dichroic ratios measured at two different wavenumbers (representing the low and high wavenumber side of the absorption band respectively), it is found that the difference in the calculated angle range is small (Table 6.4). Since ω is more reliably evaluated at the lower wavenumber dichroic ratio, this value alone has been used in latter discussions. The determination of ω for the second electronic transition of the 4-nitro-1-naphthylamine reporter/DNA complex has been carried out at $30,800\text{cm}^{-1}$ (Table 6.4). At this wavenumber, there is no overlap from the previous absorption band (see Fig.5.10). For the 2,4-dinitroaniline reporter/DNA complex, there is no dichroic ratio change in the region

where the two absorption bands initially overlap. This is good evidence that ω is the same for both electronic transitions. Thus, ω has been conveniently calculated for both visible electronic transitions from the constant dichroic ratio recorded across the first absorption band (Fig.5.7) as shown by the fourth entry of Table 6.4. The fifth entry of the table shows just how small the angle range would be changed if it were calculated from the dichroic ratio at the maximum absorption of the second electronic transition. The one degree increase in the determined angle range has not been included in latter discussions.

A summary of the relevant information is presented in Table 6.6. The quantities, R_0 , the dichroic ratio for perfect alignment and ω , the angle between the transition moment vector and the DNA helix axis (both determined from the experimental data), have been grouped with ϕ , the theoretical transition moment vector (calculated relative to the dye z molecular axis) for each of the dyes' observable electronic transitions.

6.3 Geometry of the Dye Molecule in the Dye/DNA Complex

The dyes may be placed into two general categories; those that fully intercalate and those that do not. The geometry of the latter group of dye/DNA complexes, which includes the orthonitroaniline and paranitroaniline reporters, may not be interpreted uniquely since either a fraction of the dye molecules fully intercalate with the remaining fraction externally bound or alternatively, all the dye molecules equally, but only partially intercalate. Both models are consistent with the viscosity data.

Table 6.6

The Quantities R_0 , ω and ϕ for each of the Dyes' Observable Electronic Transitions

Dye	R_0	Angle of Moment with DNA Helix Axis (Degrees)	Angle of Moment with Dye z Molecular Axis (Degrees)
Acriflavine	0 - 0.069	80 - 90	0
Proflavine	0.060 - 0.14	75 - 80	0
9-Aminoacridine	0.084 - 0.20	72 - 78	90
	0.27 - 0.57	62 - 70	0
4-Nitro-1-naphthylamine reporter	0 - 0.069	80 - 90	84
	0.37 - 0.46	64 - 67	56 - 69
2,4-Dinitroaniline reporter	0.21 - 0.30	69 - 72	13 - 20
	0.21 - 0.30	69 - 72	88 - 90
Orthonitroaniline reporter	0.40 - 0.61	61 - 66	7 - 8
Paranitroaniline reporter	0.68 - 0.78	58 - 60	90

For the first model, the geometry of the intercalated dye molecule may not be solved because of the unknown contribution to the overall measured dichroic ratio from the externally bound dye. Although the relative proportions of the externally bound to the fully intercalated dye may be estimated from the ratio of the viscosity of the dye/DNA complex relative to some other fully intercalated dye/DNA complex, the dichroic ratio of the externally bound dye species remains an unknown. If the second model is assumed, then the geometry of the partially intercalated dye molecule may be treated in exactly the same manner as that for the fully intercalated dye molecule and may be evaluated in terms of the tilt and twist angles defined previously in Chapter One, Section 1.2.3, with the aid of equations 1.22 and 1.26. Moreover, because of the symmetry of the dye/DNA complex, all unique combinations of the tilt and twist angles, to be represented here by $f(\beta, \gamma)$, may be conveniently determined in the range $\beta = 0 - 90^\circ$ with $\gamma = 0 - 180^\circ$ since

$$f(\beta, \gamma) = f(\pi + \beta, \gamma) = f(\pi - \beta, \pi + \gamma) = f(\pi - \beta, \pi - \gamma).$$

In Figures 6.2-6.7, the shaded areas represent the total permissible range of $f(\beta, \gamma)$ and include both the uncertainty in f and R_0 and cover the total variation in the theoretically determined transition moment vectors (see Chapter Two, Section 2.5). The shaded areas in Figures 6.2 and 6.3 represent the allowed combinations of the tilt and twist angles for the orthonitroaniline and paranitroaniline reporter/DNA complexes respectively. It should be emphasized that for these materials the full intercalation

 $f(\beta, \gamma)$; transition moment vector = 8°

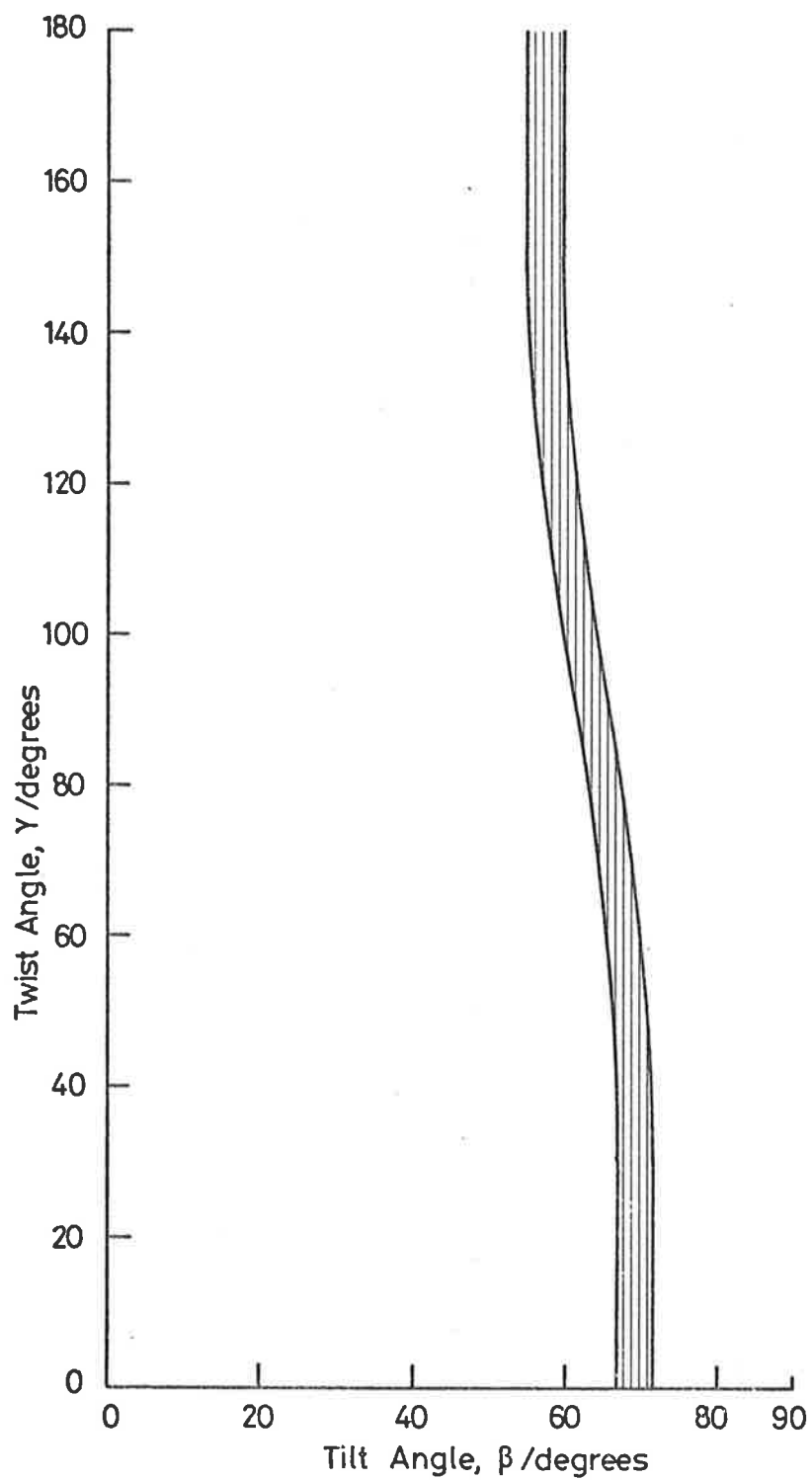
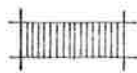


FIG 6.2 TILT AND TWIST ANGLES FOR THE ORTHONITROANILINE REPORTER IN THE DNA COMPLEX



$f(\beta, \gamma)$; transition moment vector = 90°

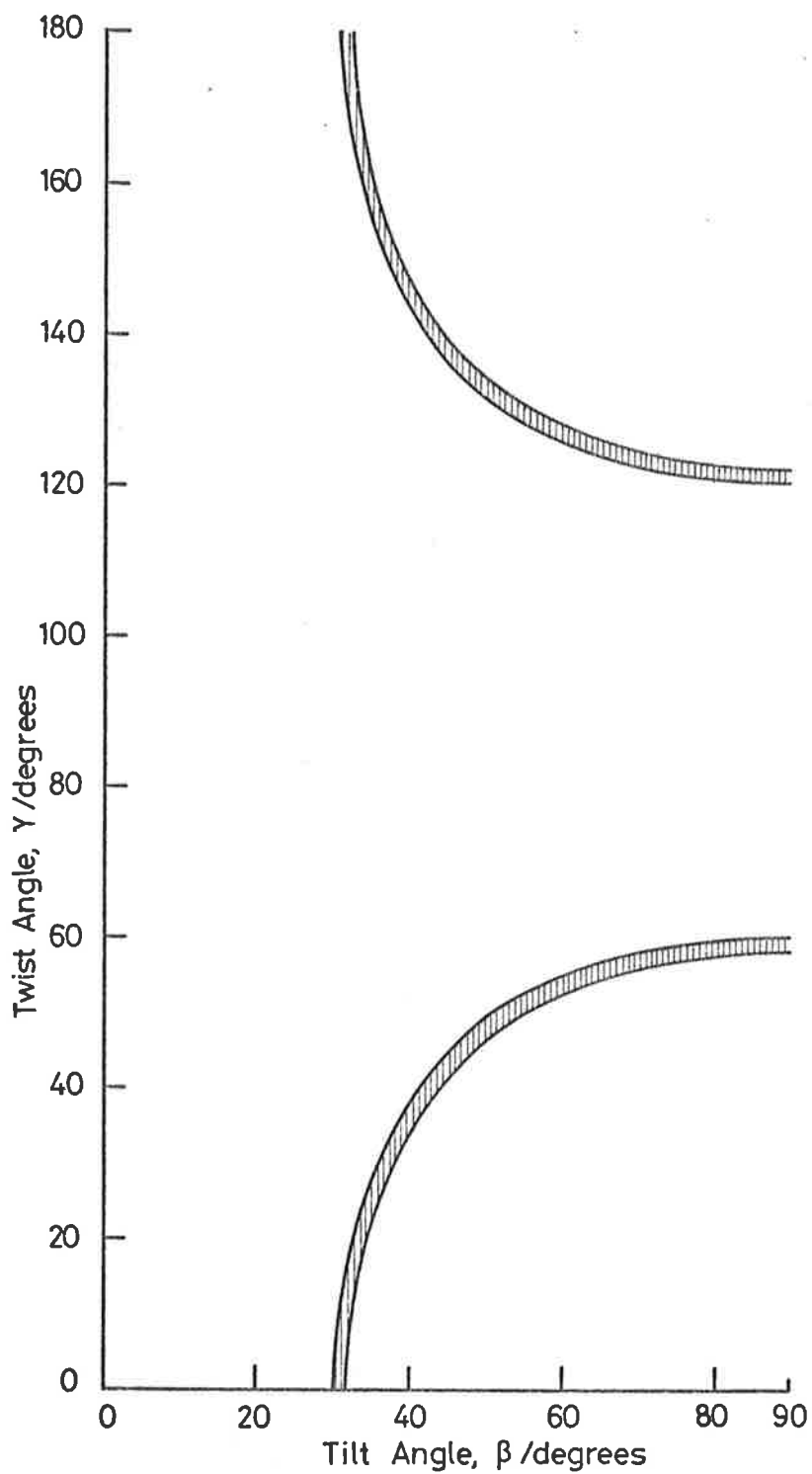

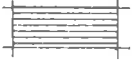


FIG 6.3 TILT AND TWIST ANGLES FOR THE PARANITROANILINE REPORTER IN THE DNA COMPLEX

Proflavine  $f(\beta, \gamma)$; transition moment vector = 0°
 Acriflavine  $f(\beta, \gamma)$; transition moment vector = 0°

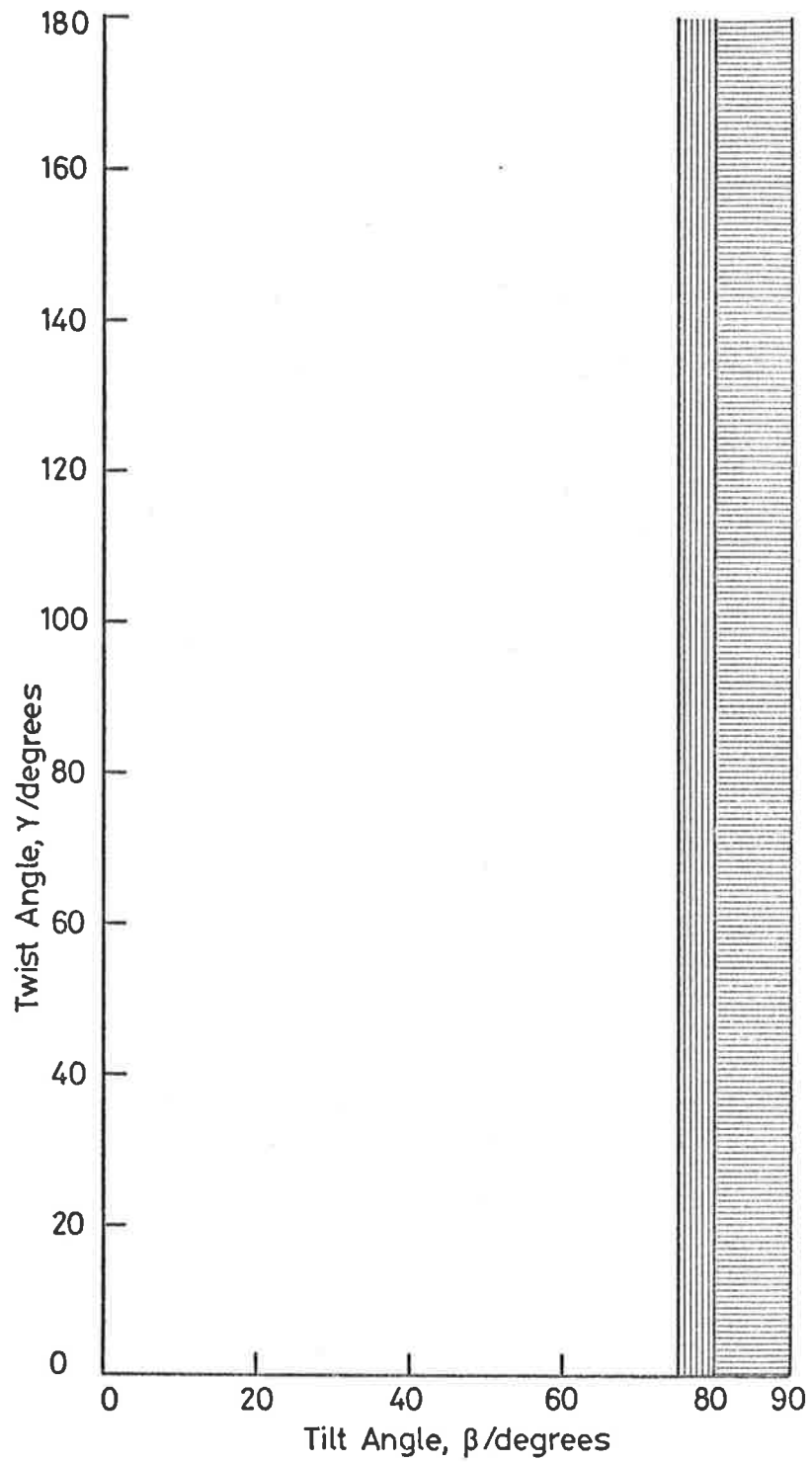


FIG 6.4 TILT AND TWIST ANGLES FOR ACRIFLAVINE IN THE DNA COMPLEX, AND FOR PROFLAVINE IN THE DNA COMPLEX

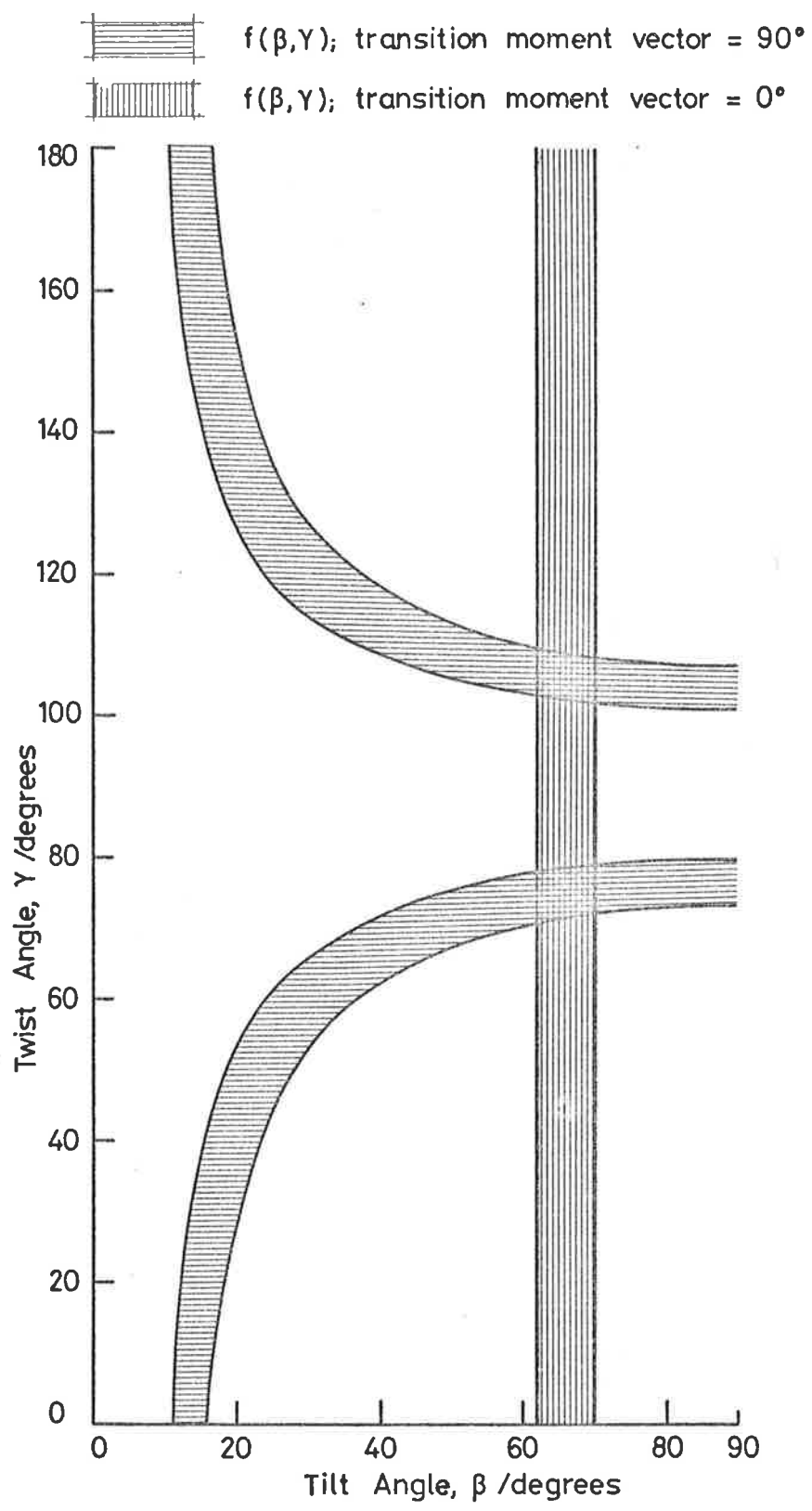


FIG 6.5 TILT AND TWIST ANGLES FOR 9-AMINOACRIDINE IN THE DNA COMPLEX

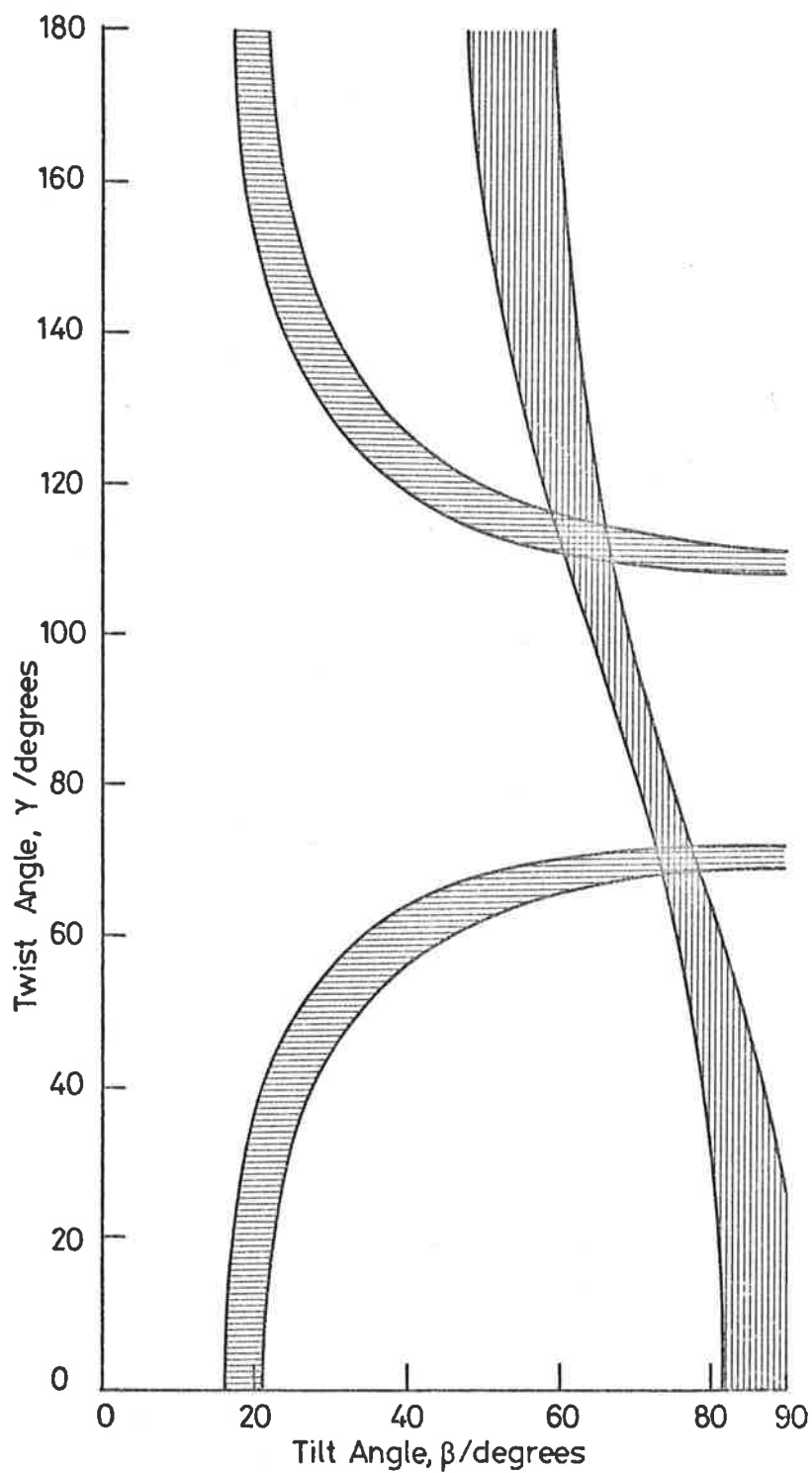
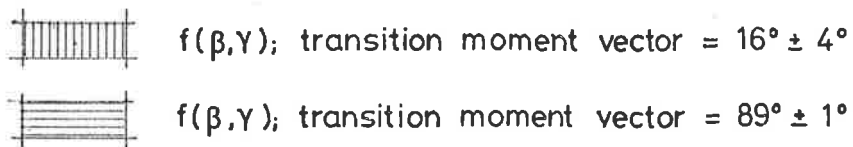
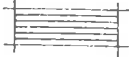



FIG 6.6 TILT AND TWIST ANGLES FOR THE 2,4-DINITROANILINE REPORTER IN THE DNA COMPLEX

 $f(\beta, \gamma)$; transition moment vector = 84°
 $f(\beta, \gamma)$; transition moment vector = $63^\circ \pm 7^\circ$

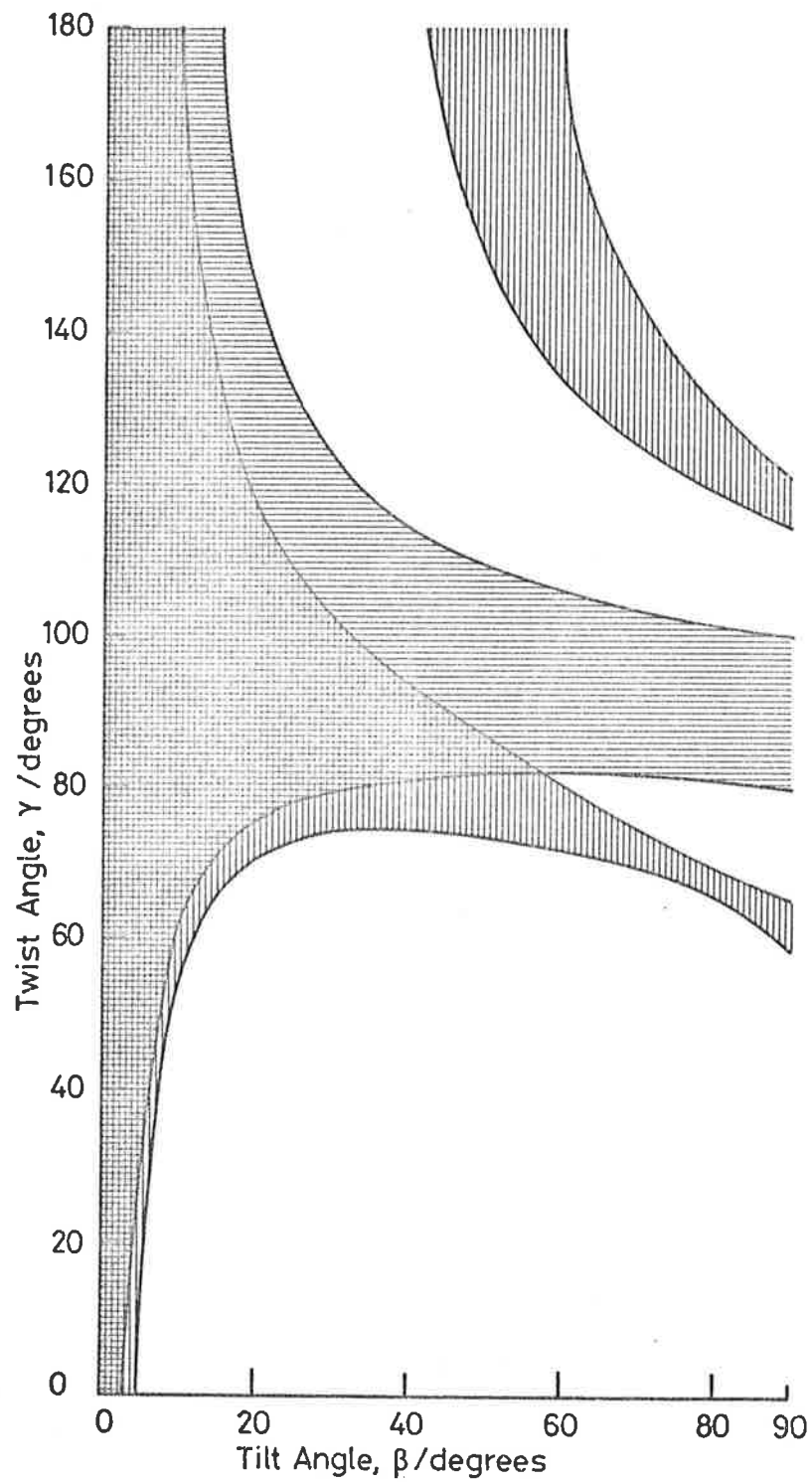


FIG 6.7 TILT AND TWIST ANGLES FOR THE 4-NITRO-1-NAPHTHYLAMINE REPORTER IN THE DNA COMPLEX

model was assumed. For the orthonitroaniline reporter, the tilt angle has been restricted to a small range between 55° and 75° , while the twist angle remains unrestricted. The geometric range of $f(\beta, \gamma)$, shown in Fig.6.3 for the paranitroaniline reporter, is best considered in conjunction with plausible hand-constructed molecular models. Thus, tilt and twist angles between 0° and 40° appeared prohibitive. A similar plot is represented in Fig.6.4 for the dyes proflavine and acriflavine. Here, the tilt angles were determined at $75^\circ - 80^\circ$ and $80^\circ - 90^\circ$ for each dye respectively. However, no restriction may be calculated for the twist angles, although an examination of possible molecular models of the intercalated dye/DNA complex revealed that twist angles between 0° and 40° were prohibitive.

For the molecules discussed so far, limited geometrical information has been obtained for the intercalated dye/DNA complex since dichroic ratio measurements, representative of only one transition moment vector were obtained and so used to interpret the geometry; subsequent refinement being possible only after inspection of molecular models. A totally different situation occurs when dichroic ratio measurements arising from two different transition moment vectors are used to elucidate the tilt and twist angle geometry of the dye in the intercalated DNA complex. In this case, a considerable restriction is imposed on $f(\beta, \gamma)$ as can be seen in Figs.6.5 and 6.6 for the molecules 9-aminoacridine and 2,4-dinitroaniline reporter respectively. The intersection of the shaded areas now represents the only two allowed combinations of β and γ that solve the relevant

Table 6.7

Tilt and Twist Angle Geometry, $f(\beta, \gamma)$

Dye	Tilt Angle, β (degrees)	Twist Angle, γ (degrees)
9-Aminoacridine	62 - 70	70 - 75 and 105 - 110
2,4-Dinitroaniline reporter	60 - 68 73 - 79	109 - 116 68 - 72

equations. The results are also shown in Table 6.7. The possible geometry, $f(\beta, \gamma)$, of the 4-nitro-1-naphthylamine reporter is presented in Fig.6.7, as the intersection of the shaded areas. For this particular molecule, the overlap area, representing the allowed combinations of $f(\beta, \gamma)$ for each transition moment vector, is considerably greater than that for the 9-aminoacridine or 2,4-dinitroaniline reporter molecules. This is partly because of the uncertainty in the direction of one of the transition moment vectors ($56^\circ - 69^\circ$) and partly because of the small difference in the orientation between it and the other transition moment vector (84°). However, the major portion of this overlap may be discounted, as only tilt angles greater than 40° are sterically possible for full intercalation. Thus, the range of $f(\beta, \gamma)$ can be considered to form a triangle with the apices represented by $f(40, 81)$, $(40, 94)$ and $(57, 82)$.

6.4 Conclusion

Overall, the method that has been used here to study

the geometry of the intercalated dye/DNA complex, is suitable to define the plane of the dye molecule with respect to the DNA helix axis by the tilt and twist angles, when measurements based on two of the molecule's transition moment vectors may be carried out. This method has overcome the associated experimental difficulties in defining R_0 , and to a lesser extent f , so that provided the transition moment vectors of the molecule are known, then the tilt and twist angles may be accurately determined within a small range (e.g. 9-aminoacridine). When the transition moment vectors are known with less certainty (e.g. 2,4-dinitroaniline reporter), the precision of the resulting measurement is somewhat reduced until finally, when the transition moment vectors are more uncertain and both are oriented at a small angle to each other, considerable imprecision in the final measurement results (e.g. 4-nitro-1-naphthylamine reporter). However, with the aid of hand-constructed molecular intercalation models, some of the latter difficulties may be overcome.

A refinement of the molecular structure of DNA has shown that there is a very slight departure of the plane of the base pairs from the perpendicular to the DNA helix axis. The tilt of the base planes about the diad axis (relating the two glycosidic links in each base pair) is -2.1° while the angle by which the base pairs are twisted about an axis perpendicular to both the helix axis and the diad axis is 4.0° (Arnott et al, 1969). This minor refinement does not alter the fact that for some of the intercalated dye molecules studied, the plane of the dye molecule does not lie parallel to the plane of the DNA base

Table 6.8Tilt Angles for the Acridine Dyes

Dye	Tilt Angle (Degrees)
9-Aminoacridine	62 - 70
Proflavine	75 - 80
Acridine	80 - 90

pairs (as has been implied many times previously), but is instead, inclined at a small angle to it.

According to the intercalation model proposed by Dalglish et al. (1969 and 1971), ^{the binding of} 9-aminoacridine would ~~bind~~ ^{from that of} differently ~~to~~ proflavine and acridine, since these latter two acridines possess a common sub-structure, namely the 7-aminoquinoline moiety, not possessed by 9-aminoacridine. Thus, it would be expected that their intercalation geometries would be different. Although the twist angles for these acridines have not been determined, their tilt angles do reveal a marked difference (Table 6.8). This result is in excellent agreement with the above model in that the geometries of proflavine and acridine are different from that of 9-aminoacridine; although it is inconclusive as to whether or not the geometries of proflavine and acridine are the same.

The non-fully intercalated reporter molecules have not been included in any discussion of possible intercalation models because of the difficulties associated with the

interpretation. The geometries of the two reporter molecules that fully intercalate are different (Table 6.7). Whether this is caused by the difference in the length of the positively charged alkyl "tails" that bind to the DNA phosphate group, or whether it is a property of the aromatic moiety is open to question. What is relevant, is that the geometries, when grouped with those of the acridine molecules, present a series of different relative intercalation geometries. Thus the work presented here, supports the current hypothesis that the geometry of the intercalated dye/DNA complex is not determined solely by the conformation of the binding site but is also determined by the properties of the intercalated dye.

APPENDIX

Exciton Interactions in Molecular Aggregates in Solution

It is being increasingly recognised that exciton interactions are important in biological processes as well as in the technological applications of dyes.

Two types of studies have been carried out. Firstly, the exciton interaction has been studied quantitatively between dimer molecules of the important wool dye Rhodamine B. This work has led to the novel conclusion that light fastness of dyes has a dependence on the magnitude of the exciton coupling in their aggregates. Secondly, the two purine derivatives, caffeine and 6-methylpurine have been studied in aqueous solution and the existence of energy transfer by the exciton mechanism in their aggregates has been established unequivocally.

All results and conclusions relating to the above work have been published previously. The copies of the relevant articles are included in this thesis.

BIBLIOGRAPHY

- A. Albert, in "The Acridines", published by Edward Arnold Ltd., London, 2nd edition (1966)
- R.W. Armstrong, T. Kurucsev and U.P. Strauss, J. Am. Chem. Soc., 92, 3174-3181 (1970)
- S. Arnott, S.D. Dover and A.J. Wonacott, Acta Cryst., B25, 2192-2206 (1969)
- M.L. Bailey, Theoret. Chim. Acta, 13, 56-64 (1969)
- M.L. Bailey, Theoret. Chim. Acta, 16, 309-315 (1970)
- A. Blake and A.R. Peacocke, Biopolymers, 6, 1225-1253 (1968)
- C.C. Bott and T. Kurucsev, J. Chem. Soc., Faraday II, accepted for publication.
- E.M. Bradbury, W.C. Price and G.R. Wilkinson, J. Mol. Biol., 3, 301-317 (1961)
- S. Bram, Nature New Biology, 232, 174-176 (1971)
- S. Brenner, L. Barnett, F.H.C. Crick and A. Orgel, J. Mol. Biol., 3, 121-124 (1961)
- W.C. Brunner and M.F. Maestre, Biopolymers, 13, 345-357 (1974)
- J. Cairns, Cold Spring Harbor Symp. Quant. Biol., 27, 311-318 (1962)
- L.M. Chan and Q. Van Winkle, J. Mol. Biol., 40, 491-495 (1969)
- I. Clementi, I.B.M. Research Paper, RJ-256 (1963)
- G. Cohen and H. Eisenberg, Biopolymers, 8, 45-55 (1969)
- P.J. Cooper and L.D. Hamilton, J. Mol. Biol., 16, 562-563 (1966)
- F.H.C. Crick, L. Barnett, S. Brenner and A. Watts-Tobin, Nature, 192, 1227-1232 (1961)
- D.G. Dalgleish, H. Fujita and A.R. Peacocke, Biopolymers, 8, 633-645 (1969)

- D.G.Dalgleish, A.R.Peacocke, G.Fey and C.Harvey, *Biopolymers*, 10, 1853-1863 (1971)
- F.Dorr, *Angew. Chem. Internat. Edit.*, 5, 478-495 (1966)
- J.Downing and J.Michl, *Int. J. Quantum Chemistry*, 6, 311-317 (1972)
- D.S.Drummond, N.J.Pritchard, V.F.W.Simpson-Gildemeister and A.R.Peacocke, *Biopolymers*, 4, 971-987 (1966)
- D.S.Drummond, V.F.W.Simpson-Gildemeister and A.R.Peacocke, *Biopolymers*, 3, 135-153 (1965)
- N.F.Ellerton and I.Isenberg, *Biopolymers*, 8, 767-786 (1969)
- S.W.Englander and H.T.Epstein, *Arch. Biochem. Biophys.*, 68, 144-149 (1957)
- M.Falk, *J. Am. Chem. Soc.*, 86, 1226-1228 (1964)
- M.Falk, K.A.Hartman Jr. and R.C.Lord, *J. Am. Chem. Soc.*, 84, 3843-3846 (1962)
- M.Falk, K.A.Hartman Jr. and R.C.Lord, *J. Am. Chem. Soc.*, 85, 387-391 (1963a)
- M.Falk, K.A.Hartman Jr. and R.C.Lord, *J. Am. Chem. Soc.*, 85, 391-394 (1963b)
- M.Feughelman, R.Langridge, W.E.Seeds, A.R.Stokes, H.R.Wilson, C.W.Hooper, M.H.F.Wilkins, R.K.Barclay and L.D.Hamilton, *Nature*, 175, 834-838 (1955)
- R.E.Franklin and R.G.Gosling, *Acta. Cryst.*, 6, 673-677 (1953)
- R.D.B.Fraser, *J. Chem. Phys.*, 21, 1511-1515 (1953)
- R.D.B.Fraser, *J. Chem. Phys.*, 24, 89-95 (1956)
- R.D.B.Fraser, *J. Chem. Phys.*, 28, 1113-1115 (1958)
- R.D.B.Fraser, in "A Laboratory Manual of Analytical Methods of Protein Chemistry", editors P.Alexander and R.J.Block, Pergamon Press Ltd., London, Vol.2, p318-325 (1960)
- M.J.Fraser and R.D.B.Fraser, *Nature*, 167, 761-762 (1951)

- E.J.Gabbay, J. Am. Chem. Soc., 90, 6574-6575 (1968)
- E.J.Gabbay, J. Am. Chem. Soc., 91, 5136-5150 (1969)
- E.J.Gabbay and A.DePaolis, J. Am. Chem. Soc., 93,
562-564 (1971)
- E.J.Gabbay, R.DeStefano and K.Sanford, Biochem. Biophys.
Res. Com., 46, 155-161 (1972)
- E.J.Gabbay and B.Gaffney, J. Macromol. Sci.-Chem., A4,
1315-1325 (1970)
- E.J.Gabbay, R.Glasser and B.L.Gaffney, Ann. N.Y. Acad. Sci.,
171, 810-826 (1970)
- E.J.Gabbay and J.Mitschele, Biochem. Biophys. Res. Com.,
34, 53-59 (1969)
- M.Gellert, J. Am. Chem. Soc., 83, 4664-4665 (1961)
- L.P.Gianneschi and T.Kurucsev, J. Chem. Soc., Faraday II,
70, 1334-1342 (1974)
- D.M.Gray and I.Rubenstein, Biopolymers, 6, 1605-1631 (1968)
- G.V.Gurskii, Biofizika, 11, (5) 737-746 (1966)
- A.E.Hansen, Mol. Phys., 13, 425-431 (1967)
- G.R.Haugen and W.H.Melhuish, Trans. Faraday Soc., 60,
386-394 (1964)
- G.W.Haupt, J. Opt. Soc. Am., 42, 441-447 (1952)
- G.Herzberg in "Atomic Spectra and Atomic Structure",
New York Dover Publications Mercury Emission
Spectrum taken from page 6 (1944)
- C.Houssier, Indust. Chim. Belge, 29, 914-915 (1964)
- C.Houssier, Indust. Chim. Belge, 30, 235-247 (1965)
- C.Houssier and E.Fredericq, Biochim. Biophys. Acta, 120,
434-447 (1966)
- K.Jackson and S.F.Mason, Trans. Faraday Soc., 67,
966-989 (1971)

- D.O.Jordan, in "The Chemistry of Nucleic Acids", published
by Butterworth Co. Ltd., London (1960)
- M.Kasha, in "Light and Life", McElroy and Glass, Ed.,
Johns Hopkins Press, Baltimore, Md., p31 (1961)
- E.Kay, N.Simmons and A.Dounce, J. Am. Chem. Soc., 74,
1724-1726 (1952)
- H.B.Klevens and J.R.Platt, J. Chem. Phys., 17, 470-481 (1949)
- O.Kratky, Kolloid Z., 64, 213-222 (1933)
- O.Kratky and G.Porod, Rec. Trav. Chim. Phys-Bas, 68,
1106-1122 (1949)
- T.Kurucsev, Archives Biochem. Biophys., 102, 120-124 (1963)
- T.Kurucsev, unpublished results (1969)
- T.Kurucsev and J.R.Zdysiewicz, Biopolymers, 10, 593-599 (1971)
- Karl Lambrecht, Chicago, Illinois 60613, U.S.A., Technical
Bulletin C-67, entitled "Polarizing Prisms for the
Ultra-Violet".
- N.A.Lange (Ed.), "Handbook of Chemistry" (McGraw-Hill Book
Company Inc., New York), pl420-1422 (1961)
- R.Langridge, D.A.Marvin, W.E.Seeds, H.R.Wilson, C.W.Hooper,
M.H.F.Wilkins and L.D.Hamilton, J. Mol. Biol., 2,
38-64 (1960a)
- R.Langridge, W.E.Seeds, H.R.Wilson, C.W.Hooper, M.H.F.Wilkins
and L.D.Hamilton, J. Cell Biology, 3, 767-778 (1957)
- R.Langridge, H.R.Wilson, C.W.Hooper, M.H.F.Wilkins and
L.D.Hamilton, J. Mol. Biol., 2, 19-37 (1960b)
- L.S.Lerman, J. Mol. Biol., 3, 18-30 (1961)
- L.S.Lerman, Proc. Natl. Acad. Sci. (U.S.), 49, 94-102 (1963)
- L.S.Lerman, J. Cellular Comp. Physiol. Suppl. 1, 64,
1-18 (1964)

- P.H.Lloyd, R.N.Prutton and A.R.Peacocke, *Biochem. J.*, 107,
353-359 (1968)
- G.Lober, *Z. Chem.*, 9, 252-265 (1969)
- G.Lober, *Z. Chem.*, 11, 135-145 (1971)
- G.Lober and G.Achtert, *Biopolymers*, 8, 595-608 (1969)
- V.Luzzati, F.Masson and L.S.Lerman, *J. Mol. Biol.*, 3,
634-639 (1961)
- H.R.Mahler and E.H.Cordes in "Biological Chemistry",
Harper International Edition, p138, Table 4.2 (1966)
- D.A.Marvin, M.Spencer, M.H.F.Wilkins and L.D.Hamilton,
J. Mol. Biol., 3, 547-565 (1961)
- E.F. McCoy and I.G. Ross, *Aust. J. Chem.* 15, 573-590 (1962)
- S.F.Mason and A.J.McCaffery, *Nature*, 204, 468-470 (1964)
- Y.Mauss, J.Chambron, M.Daune and H.Benoit, *J. Mol. Biol.*,
27, 579-589 (1967)
- J.Michl, E.W.Thulstrup and J.H.Eggers, *J. Phys. Chem.*,
74, 3878-3884 (1970)
- W.Muller and D.M.Crothers, *J. Mol. Biol.*, 35, 251-290 (1968)
- C.Nagata, M.Kodama, Y.Tagashira and A.Imamura, *Biopolymers*,
4, 409-427 (1966)
- D.M.Neville and D.R.Davies, *J. Mol. Biol.*, 17, 57-74 (1966)
- G.Oster, in "Physical Techniques in Biological Research"
(Ed. by G.Oster and A.W.Pollister, Academic Press,
New York), Vol.1, Chapter 2, p51 (1955)
- R.G.Parr, in "Quantum Theory of Molecular Electronic
Structure", W.A.Benjamin Inc., New York (1963)
- F.Passero, E.Gabbay, B.Gaffney and T.Kurucsev, *Macromolecules*,
3, 158-162 (1970)
- A.R.Peacocke, *Studia Biophysica*, 24/25, 213-224 (1970)
- A.R.Peacocke and J.N.H.Skerrett, *Trans. Faraday Soc.*, 52,
261-279 (1956)

- J.Pillet and J.Brahms, *Biopolymers*, 12, 387-403 (1973)
- J.R.Platt, *J. Chem. Phys.*, 17, 484-495 (1949)
- N.J.Pritchard, A.Blake and A.R.Peacocke, *Nature*, 212,
1360-1361 (1966)
- A.Rich and M.Kasha, *J. Am. Chem. Soc.*, 82, 6197-6199 (1960)
- R.Rigler, *Ann. N.Y. Acad. Sci.*, 157, 211-224 (1969)
- A.Rupprecht, *Biochem. Biophys. Res. Com.*, 12, 163-168 (1963)
- A.Rupprecht, *Acta Chem. Scand.*, 20, 494-504 (1966)
- A.Rupprecht, R.Rigler, B.Forslind and G.Swanbeck, *European
J. Biochem.*, 10, 291-301 (1969)
- W.E.Seeds, in "Progress in Biophys. Biophys. Chem."
(Eds. J.A.V.Butler and J.T.Randall, Pergamon Press,
London), 3, 27-46 (1953)
- W.E.Seeds and M.H.F.Wilkins, *Discuss. Faraday Soc.*, 9,
417-423 (1950)
- K.Shikama, *Nature*, 207, 529-530 (1965)
- R.F.Steiner and R.F.Beers, in "Polynucleotides", Elsevier
Publishing Company, Appendix B, p348-349 (1961)
- G.Strauss, S.B.Broyde and T.Kurucsev, *J. Phys. Chem.*, 75,
2727-2733 (1971)
- G.B.B.M.Sutherland and M.Tsuboi, *Proc. Roy. Soc.*, A239,
446-463 (1957)
- L.E.Sutton (Ed.), in "Tables of Interatomic Distances and
Configuration in Molecules and Ions", London, The
Chemical Society, Special Publ. No.18 (1965)
- Y.Tanizaki and S.Kubodera, *J. Mol. Spectroscopy*, 24,
1-18 (1967)
- B.Thorell and F.Ruch, *Nature*, 167, 815 (1951)
- T.Tsunoda and T.Yamaoka, *J. Polymer Sci., Part A*, 3,
3691-3698 (1965)

- R.K.Tubbs, W.E.Ditmars, Q.Van Winkle, *J. Mol. Biol.*, 9,
545-557 (1964)
- M.J.B.Tunis-Schneider and M.F.Maestre, *J. Mol. Biol.*, 52,
521-541 (1970)
- S.J.Webb and J.S.Bhorjee, *Can. J. Biochem.*, 46, 691-695 (1968)
- G.Weill and M.Calvin, *Biopolymers*, 1, 401-417 (1963)
- R.Wetzel, D.Zirwer and M.Becker, *Biopolymers*, 8, 391-401 (1969)
- J.C.White and P.C.Elmes, *Nature*, 169, 151-152 (1952)
- M.H.F.Wilkins, R.G.Gosling and W.E.Seeds, *Nature*, 167,
759-760 (1951)
- G.R.Wilkinson, W.C.Price and E.M.Bradbury, *Spectrochim.
Acta*, 14, 284-307 (1959)
- A.Wittwer and V.Zanker, *Z. Physik. Chem. N.F.*, 22,
417-439 (1959)
- V.Zanker, *Z. Physik. Chem. N.F.*, 2, 52-78 (1954)
- V.Zanker and G.Schiefele, *Berichte Bunsengesellschaft
Physik. Chem.*, 62, 86-93 (1958)
- V.Zanker and J.Thies, *Z. Physik. Chem. N.F.*, 33, 46-59 (1962)
- Carl Zeiss No.1, Oberkochen/WURTT., West Germany, Pamphlet
entitled "Absorption Measurement with Large Optical
Paths for the Spectrophotometer PMQII", 50-657/MRD-e, p6.
- Carl Zeiss No.2, Oberkochen/WURTT., West Germany, Pamphlet
entitled "Sphere Attachment for the Spectrophotometer
PMQII", 50-657/KA/Erg-e, p10-22.
- J.R.Zdysiewicz, Ph.D. Thesis, The University of Adelaide,
(1969)

Gál, M. E., Kelly, M. E. & Kurucsev, M. E. (1973). Derivation and interpretation of the spectra of aggregates. Part 2. - Dimer of Rhodamine B in aqueous solutions. *Journal of the Chemical Society, Faraday Transactions 2*, 69, 395-402.

NOTE:

This publication is included in the print copy of the thesis held in the University of Adelaide Library.

It is also available online to authorised users at:

<http://dx.doi.org/10.1039/F29736900395>

Kikkert, J. N., Kelly, G. R. & Kurucsev, T. (1973). Interactions between purine derivatives: electronic spectral studies. I. Electronic transitions in caffeine monomer and exciton coupling in caffeine dimer. *Biopolymers*, 12(7), 1459-1477.

NOTE:

This publication is included in the print copy
of the thesis held in the University of Adelaide Library.

It is also available online to authorised users at:

<http://dx.doi.org/10.1002/bip.1973.360120703>

Kelly, G. R. & Kurucsev, T. (1974). Interactions between purine derivatives: electronic spectral studies. II. Excitation interactions in the dimer of 6-methylpurine in aqueous solution. *Biopolymers*, 13(4), 769-778.

NOTE:

This publication is included in the print copy of the thesis held in the University of Adelaide Library.

It is also available online to authorised users at:

<http://dx.doi.org/10.1002/bip.1974.360130412>